

1  
2     **Sustained monitoring of the Southern Ocean at Drake Passage:**  
3         **past achievements and future priorities**  
4

5  
6     Michael P. Meredith<sup>1</sup>, Philip L. Woodworth<sup>2</sup>, Teresa K. Chereskin<sup>3</sup>, David P. Marshall<sup>4</sup>,  
7     Lesley C. Allison<sup>5</sup>, Grant R. Bigg<sup>6</sup>, Kathy Donohue<sup>7</sup>, Karen J. Heywood<sup>8</sup>, Chris W. Hughes<sup>2</sup>,  
8     Angela Hibbert<sup>9</sup>, Andrew McC. Hogg<sup>10</sup>, Helen L. Johnson<sup>11</sup>, Loïc Jullion<sup>12</sup>, Brian A. King<sup>12</sup>,  
9     Harry Leach<sup>9</sup>, Yueng-Djern Lenn<sup>13</sup>, Miguel A. Morales Maqueda<sup>2</sup>, David R. Munday<sup>4</sup>,  
10    Alberto C. Naveira Garabato<sup>12</sup>, Christine Provost<sup>14</sup>, Jean-Baptiste Sallée<sup>1</sup> and Janet  
11    Sprintall<sup>3</sup>.  
12  
13  
14

15    <sup>1</sup>*British Antarctic Survey, Cambridge, U.K.*

16    <sup>2</sup>*National Oceanography Centre, Liverpool, U.K.*

17    <sup>3</sup>*Scripps Institution of Oceanography, La Jolla, California, U.S.A.*

18    <sup>4</sup>*Atmospheric, Oceanic and Planetary Physics, University of Oxford, U.K.*

19    <sup>5</sup>*Department of Meteorology, University of Reading, U.K.*

20    <sup>6</sup>*Department of Geography, University of Sheffield, U.K.*

21    <sup>7</sup>*Graduate School of Oceanography, University of Rhode Island, U.S.A.*

22    <sup>8</sup>*School of Environmental Sciences, University of East Anglia, Norwich, U.K.*

23    <sup>9</sup>*Department of Earth and Ocean Sciences, University of Liverpool, U.K.*

24    <sup>10</sup>*Research School of Earth Sciences, Australian National University, Canberra, Australia.*

25    <sup>11</sup>*Department of Earth Sciences, University of Oxford, U.K.*

26    <sup>12</sup>*National Oceanography Centre, Southampton, U.K.*

27    <sup>13</sup>*School of Ocean Sciences, Bangor University, U.K.*

28    <sup>14</sup>*LOCEAN, Université Pierre et Marie Curie, Paris, France.*

29   **Abstract**

30

31   Drake Passage is the narrowest constriction of the Antarctic Circumpolar Current (ACC)  
32   in the Southern Ocean, with implications for global ocean circulation and climate. We  
33   review the long-term sustained monitoring programmes that have been conducted at  
34   Drake Passage, dating back to the early part of the twentieth century. Attention is drawn  
35   to numerous breakthroughs that have been made from these programmes, including (a)  
36   the first determinations of the complex ACC structure and early quantifications of its  
37   transport; (b) realization that the ACC transport is remarkably steady over interannual  
38   and longer periods, and a growing understanding of the processes responsible for this;  
39   (c) recognition of the role of coupled climate modes in dictating the horizontal transport,  
40   and the role of anthropogenic processes in this; (d) understanding of mechanisms driving  
41   changes in both the upper and lower limbs of the Southern Ocean overturning circulation,  
42   and their impacts. It is argued that monitoring of this passage remains a high priority for  
43   oceanographic and climate research, but that strategic improvements could be made  
44   concerning how this is conducted. In particular, long-term programmes should  
45   concentrate on delivering quantifications of key variables of direct relevance to large-  
46   scale environmental issues: in this context, the time-varying overturning circulation is, if  
47   anything, even more compelling a target than the ACC flow. Further, there is a need for  
48   better international resource-sharing, and improved spatio-temporal coordination of the  
49   measurements. If achieved, the improvements in understanding of important climatic  
50   issues deriving from Drake Passage monitoring can be sustained into the future.

51

52   **1) The global significance of Drake Passage and the need for sustained**  
53   **observations**

54

55   **1.1) Drake Passage, global circulation and climate**

56

57   Due to its unique geography, the Southern Ocean exerts a profound influence on global  
58   ocean circulation. In particular, the presence of zonally unblocked latitudes in the  
59   Southern Ocean permits the flow of the only current to circumnavigate the globe, namely  
60   the Antarctic Circumpolar Current (ACC; Figure 1). This is the largest current system in  
61   the world, and it plays a key role in connecting the three major ocean basins (Figure 2),  
62   allowing an interbasin exchange of heat, salt, carbon and other chemical and biological  
63   properties. Associated with the strong eastward flow of the ACC, density surfaces tilt  
64   strongly upwards toward the south in the Southern Ocean, exposing dense layers of the  
65   ocean to interaction with the atmosphere and cryosphere. This acts to transfer water  
66   between density classes, and leads to the existence of a vigorous overturning circulation  
67   in the Southern Ocean. This can be viewed as two counter-rotating upper and lower cells  
68   (Figure 2) [*Lumpkin and Speer, 2007*]. Because of its strong three-dimensional  
69   circulation, the ACC is a key component of the global climate system [*Rintoul et al., 2001*].

70

71   Lying between the South American and Antarctic continents, Drake Passage (Figure 3a) is  
72   the region of narrowest constriction of the ACC and, as such, exerts a strong constraint on  
73   both its path and strength. The passage has a width of roughly 800 km, although the  
74   submerged barrier blocking circumpolar contours at depth is located further east, around  
75   the edges of the Scotia Sea. The precise timing of the opening of Drake Passage remains  
76   controversial. *Livermore et al. [2005]* date the opening of a shallow connection during the  
77   early Eocene (~50 Ma) with a deep water connection developing around the Eocene-  
78   Oligocene boundary (34-30 Ma), based on analysis of marine geophysical data. These  
79   results are broadly consistent with analysis of neodymium isotope ratios in the Atlantic  
80   sector that indicate an influx of shallow Pacific water around 41 Ma [*Scher and Martin,*  
81   2006], although other studies date the opening somewhat later [*Barker, 2001*].  
82   Associated with the uncertainty concerning the timing of the opening of Drake Passage,  
83   the initiation of the ACC remains similarly uncertain [*Barker et al., 2007*]. Nevertheless,  
84   the hypothesis that Drake Passage opened during the Eocene, allowing the onset of a  
85   form of the ACC and development of Antarctica's climatic isolation, is consistent with the

86 gradual decline in global temperature from ~50 Ma, followed by abrupt cooling and the  
87 onset of glaciation at 33-34 Ma [Zachos *et al.*, 2001].

88  
89 Dynamically, the pivotal importance of Drake Passage is due to the absence of zonal  
90 pressure gradients within the ocean there. At other (blocked) latitudes, the zonal wind  
91 stress at the surface can be balanced by zonal pressure gradients within the upper few  
92 hundred meters: any directly wind-forced transport at the surface (i.e. equatorward  
93 Ekman transport) can then be opposed by poleward geostrophic transport, leading to  
94 shallow overturning Ekman cells. However, in the absence of continental barriers at the  
95 latitudes of Drake Passage, the compensating poleward geostrophic transport can only  
96 occur at depth, where submerged topography is able to support a zonal pressure gradient  
97 [Munk and Palmén, 1951]. This leads to a wind-driven overturning “Deacon cell” that  
98 extends much deeper. In concert with surface thermal forcing that maintains a surface  
99 buoyancy gradient, this Deacon cell mechanically pumps down warm, buoyant water to  
100 the north of the ACC, leading to the establishment of a global pycnocline [Gnanadesikan  
101 and Hallberg, 2000; Karsten *et al.*, 2002; Vallis, 2000]. Consistent with this conceptual  
102 picture is the result that Southern Ocean wind forcing is the dominant mechanical energy  
103 source for the global ocean [Wunsch and Ferrari, 2004].

104  
105 The steepening of the isopycnals by the continuous input of momentum from the winds is  
106 ultimately arrested by baroclinic instability, the wind-driven Deacon Cell being opposed  
107 by an eddy-driven bolus overturning cell [Gent *et al.*, 1995]. In early numerical  
108 simulations, this compensation between wind-driven and eddy-driven overturning cells  
109 was nearly exact, resulting in virtually no residual overturning circulation (Danabasoglu  
110 *et al.* [1994]; see also Döös and Webb [1994]). More generally, in thermodynamic  
111 equilibrium, the strength of the residual circulation is related to the surface buoyancy  
112 forcing [Marshall, 1997], with surface wind and buoyancy forcing and interior eddy fluxes  
113 combining to set both the stratification of the ACC, its volume transport through Drake  
114 Passage and the residual overturning circulation [Marshall and Radko, 2003]. These ideas  
115 have been extended and applied to observed air-sea fluxes to infer the residual  
116 overturning [Karsten and Marshall, 2002; Olbers and Visbeck, 2005; Speer *et al.*, 2000].  
117 The schematic of the overturning circulation in the major ocean basins shown in Figure 2  
118 emphasizes the key role of these Southern Ocean processes in the formation and  
119 transformation of globally-important water masses [Lumpkin and Speer, 2007].

120  
121 The preceding discussion has emphasised the role of local forcing over the Southern  
122 Ocean in setting the ACC transport through Drake Passage and the residual overturning  
123 circulation. However, it is important to note also that the ACC is intimately coupled with  
124 the global ocean circulation and stratification, as elegantly articulated in the conceptual  
125 model of *Gnanadesikan* [1999] for the global pycnocline, and its application to the ACC  
126 [*Gnanadesikan and Hallberg*, 2000]. This explains, for example, how Southern Ocean  
127 winds can influence the strength of the North Atlantic meridional overturning circulation  
128 (the “Drake Passage effect” [e.g. *Toggweiler and Samuels*, 1995]) and, conversely, how the  
129 rate of North Atlantic Deep Water (NADW) formation can influence the ACC transport  
130 through Drake Passage [*Fuckar and Vallis*, 2007]. Likewise, *Munday et al.* [2011] have  
131 shown that diapycnal mixing in the northern basins can significantly affect the ACC  
132 transport through Drake Passage. Such models have also been useful in clarifying that  
133 most of the wind forcing of the ACC occurs north of Drake Passage, with the most  
134 appropriate measure of the “Southern Ocean wind stress” being an integral over the  
135 circumpolar streamlines [*Allison et al.*, 2010].

136  
137 Via its strong overturning circulation, the Southern Ocean also has a major influence on  
138 the ocean carbon cycle. Changes in the overturning across the ACC impact the air-sea  
139 carbon flux and biological productivity, and are widely believed to be important for  
140 explaining the large glacial-interglacial changes in atmospheric CO<sub>2</sub> [e.g. *Watson and*  
141 *Naveira Garabato*, 2006]. Outcropping isopycnals in the Southern Ocean also provide an  
142 important pathway for the subduction of anthropogenic CO<sub>2</sub> into the ocean interior  
143 [*Caldeira and Duffy*, 2000; *Sabine et al.*, 2004] via the upper cell. The climate system is  
144 therefore sensitive to changes in the residual overturning circulation with the potential  
145 for feedbacks onto the Southern Ocean sink of anthropogenic CO<sub>2</sub> [*Mignone et al.*, 2006].

146  
147 **1.2) Specific rationale for sustained observations in Drake Passage**  
148  
149 The pivotal role of the ACC in global climate makes it a priority for any global network of  
150 sustained climate observations. Logistically, by far the most practical location to monitor  
151 the ACC is across Drake Passage. Firstly, this is the narrowest constriction across the  
152 Southern Ocean, thus allowing the full meridional extent of the ACC to be covered with  
153 the minimal possible effort. Secondly, with continental landmasses to the north and

154 south, Drake Passage is the only place across which one can unambiguously monitor the  
155 ACC without the complicating influence of subpolar and subtropical flows on its flanks.  
156 Thirdly, Drake Passage lies immediately north of the most inhabited part of Antarctica,  
157 thus it is the region of the Southern Ocean most frequented by supply vessels, presenting  
158 greatest opportunities for the synergistic use of shiptime.

159  
160 As discussed above and illustrated in Figure 2, Drake Passage represents a crossroads for  
161 the global overturning circulation. It is of specific interest because it lies along the “cold  
162 water path” for overturning waters returning to the Atlantic, in contrast to the “warm  
163 water path” via the Indonesian Throughflow and Agulhas leakage [Gordon, 1986]. As one  
164 of the most critical choke points in the global ocean, Drake Passage is a natural point at  
165 which to attempt quantification of the time-varying fluxes of heat, freshwater and other  
166 tracers, in order to provide strong constraints on water mass budgets and circulation  
167 patterns within each of the major basins.

168  
169 Drake Passage is fortuitously situated for monitoring changes in the water masses that  
170 occupy both the upper and lower limbs of the overturning circulation in the Atlantic. For  
171 example, Subantarctic Mode Water (SAMW), formed by deepening of the winter mixed  
172 layer on the equatorward flank of the ACC, has a pronounced source in the southeast  
173 Pacific [Aoki *et al.*, 2007], from where it flows through Drake Passage into the Atlantic.  
174 Lying beneath the SAMW is Antarctic Intermediate Water (AAIW), which forms from  
175 upwelled Circumpolar Deep Water (CDW) that becomes Antarctic Surface Water (AASW)  
176 and subducts at the Polar Front. The AAIW found in Drake Passage originates in the  
177 winter mixed layer of the Bellingshausen Sea [Naveira Garabato *et al.*, 2009]. The eastern  
178 part of Drake Passage is also close to the outflow of the Weddell Sea Deep Water (WSDW)  
179 that forms at the periphery of Antarctica in the southern and western Weddell Sea. Upon  
180 entering the Scotia Sea, WSDW can flow westward toward Drake Passage, or  
181 northeastward toward the Georgia and Argentine basins [Naveira Garabato *et al.*, 2002a].  
182 Since WSDW ultimately constitutes the densest component of the Antarctic Bottom Water  
183 (AABW) in the Atlantic Meridional Overturning Circulation, observations across Drake  
184 Passage can yield information on the lower limb of this overturning, and constitute a  
185 powerful complement to time series generated from within the ice-infested subpolar gyre  
186 [e.g. Gordon *et al.*, 2010; Meredith *et al.*, 2011].

187

188 Each of the water masses in Drake Passage has been seen to be changing significantly in  
189 recent times [Bindoff *et al.*, 2007; Gille, 2008; Jullion *et al.*, 2010; Naveira Garabato *et al.*,  
190 2009]. There is much interest in understanding to what extent these changes are of  
191 anthropogenic origin, as opposed to representing natural variability. A prerequisite for  
192 this is to sample the changes with spatial consistency and with sufficient temporal  
193 resolution to avoid aliasing problems and to permit correct determination of the  
194 timescale of the variability; only in this way can proper attribution even be attempted.  
195 This further underlines the importance of sustained observations, and will be discussed  
196 in more detail below.

197

198 For all of the reasons described above, the Drake Passage is now the most measured  
199 stretch of water in the Southern Ocean, and historically one of the most heavily-  
200 monitored inter-continental straits in the global ocean. Consequently, any changes in  
201 Southern Ocean properties or fluxes are most likely to be recognised and interpreted  
202 correctly here.

203

204 **1.3) Aims and structure of the paper**

205

206 This paper aims to provide a review of sustained observations at Drake Passage since the  
207 very early days of Southern Ocean science, a summary of the most important results that  
208 have been obtained to date, and an assessment of current activities, to guide what might  
209 be done in the future. Section 2 reviews the early attempts to monitor the Southern Ocean  
210 at Drake Passage, including the landmark International Southern Ocean Studies (ISOS)  
211 experiment. Section 3 describes the initiatives that were undertaken during the World  
212 Ocean Circulation Experiment (WOCE), which was the largest-ever physical  
213 oceanographic programme, and which had a specific focus on the Southern Ocean. Many  
214 of these monitoring projects have continued up to the present day, so this section brings  
215 some of the WOCE-era findings up to date. Section 4 outlines some of the newer  
216 initiatives that have been instigated at Drake Passage since the end of WOCE, including  
217 some very recent additions to the monitoring effort that are just beginning to produce  
218 important new results. Section 5 summarises some of the key findings obtained from  
219 these programmes, and considers which aspects of Drake Passage sustained observations  
220 should be maintained into the future, and why, as well as discussing where such  
221 monitoring efforts might be strategically improved.

222

223 **2) Early Drake Passage transport measurements**

224

225 Prior to the ISOS programme, which commenced in the mid-1970s, there was little by  
226 way of sustained observations of the ocean in Drake Passage. Most of the information that  
227 was accumulated during the pre-ISOS period was obtained from temporally-sparse  
228 hydrographic sections, and is reviewed in *Peterson* [1988a]. The main scientific target for  
229 these investigations was to determine the total volume transport through the passage.

230

231 The first such hydrographic-section based estimate of ACC transport was given by *Clowes*  
232 [1933], who used data from the *Discovery* expeditions during 1929-1930 to derive a  
233 transport relative to 3500 m of 110 Sv. The data used for this estimate were collected  
234 using techniques from an early era of oceanography, and much about the spatial structure  
235 of the ACC was unknown, however this value is strikingly similar to modern values for  
236 the transport through Drake Passage. Significantly, *Clowes* [1933] made an early  
237 realisation that the eastward flow of the ACC at Drake Passage extends to great depths.

238

239 In retrospect, this was a very good start, although the transport of the ACC at Drake  
240 Passage subsequently became the topic of considerable uncertainty. Based purely on  
241 hydrographic section data, estimates that followed for this transport ranged from a  
242 maximum of 218 Sv eastward [*Gordon*, 1967] to a minimum of 5 Sv westward [*Foster*,  
243 1972]. This uncertainty was due in part to the very limited number of observations  
244 available for deriving transport (and almost complete lack of knowledge of the degree of  
245 variability in ACC transport, and hence how significant aliasing might be), and also to a  
246 lack of comprehension of how best to reference geostrophic shears to determine total  
247 transport. As noted by *Peterson* [1988a], a single section across Drake Passage  
248 (undertaken by the *Ob* in 1958) yielded ten different estimates for ACC transport, varying  
249 between 218 Sv [*Gordon*, 1967] and just 9 Sv [*Ostapoff*, 1961].

250

251 Despite the large range in transport estimates obtained during this period, *Reid and*  
252 *Nowlin* [1971] noted that such estimates actually became remarkably consistent when  
253 the data were handled and referenced in the same way. This is in accord with current  
254 thinking about the stability of the ACC transport, as will be seen in Section 3. The  
255 uncertainty in how best to reference the geostrophic shears remained however,

prompting deployment of current meters to make direct velocity measurements. A number of deep current meter moorings were deployed in Drake Passage for four days in 1969, giving daily mean current speeds ranging from 0.5 to 14.7 cm.s<sup>-1</sup>. Confusingly, this exercise actually led to an increase in the range of transport estimates, with a maximum transport of 237 Sv derived [Reid and Nowlin, 1971]. It later became clear that this was due to incomplete knowledge of the spatial and temporal variability of the ACC at Drake Passage, and the need to resolve the pertinent scales of both if direct referencing was to prove effective.

264

## 265 **2.1) The International Southern Ocean Studies (ISOS) programme**

### 266 **2.1.1) Transport and variability from the ISOS array**

267

268 Based on the early works described above, it became clear that a dedicated programme of  
269 measurements that resolved the relevant scales of variability in Drake Passage was  
270 needed, if the ACC transport and variability there were to be adequately determined.  
271 Accordingly, the ISOS programme [Nowlin *et al.*, 1977] was designed and conducted, the  
272 centerpiece of which was a large monitoring array (Figure 3b), supplemented with  
273 hydrographic sections. (The reports of the ISOS measurements are spread over a number  
274 of papers, but are conveniently summarised by Cunningham *et al.* [2003], who also  
275 summarise the methods used in the ISOS calculations).

276

277 The specific goals of ISOS were to resolve the structure of the ACC and to obtain a year-  
278 long time series of ACC transport. With regard to the former, analyses of ISOS and pre-  
279 ISOS data around this time led to the now well-established notion of the ACC being a  
280 banded structure, with relatively fast-flowing currents associated with frontal regions,  
281 which are themselves separated by relatively quiescent zones of water. Three narrow  
282 frontal regions were identified, and termed (north to south) the Subantarctic Front (SAF),  
283 the Polar Front (PF), and the Continental Water Boundary [Nowlin *et al.*, 1977; Nowlin  
284 and Clifford, 1982; Whitworth, 1980]. The nomenclature for the first two of these has  
285 survived, whilst the latter has, in general, been superseded [Orsi *et al.*, 1995].

286

287 The first substantial field effort as part of ISOS was termed the First Dynamic Response  
288 and Kinematics Experiment in 1975 (FDRAKE 75), which has a good claim to being the  
289 beginning of the modern era of measurements in Drake Passage. Preliminary estimates of

290 volume transport based on these data were in good agreement, being 110-138 Sv [*Nowlin*  
291 *et al.*, 1977],  $139 \pm 36$  Sv [*Bryden and Pillsbury*, 1977] and  $127 \pm 14$  Sv [*Fandry and Pillsbury*,  
292 1979]. It was recognized that the previous poor agreement of transport estimates was  
293 due to the undersampling of reference velocities, which presented a particular problem  
294 given the greatly meandering nature of the ACC fronts, and their tendency to spawn  
295 isolated eddies [*Legeckis*, 1977; *Sciremammano*, 1979].

296  
297 FDRAKE 75 and the following FDRAKE 76 were precursors to the extensive ISOS  
298 deployments in 1979, and it was this latter campaign that enabled the year-long series of  
299 transport required by ISOS to be derived (Figure 4a). The monitoring experiment  
300 consisted of three separate hydrographic surveys, and the deployment of 17 current  
301 meter moorings deployed between the northern and southern 500 m isobaths, and  
302 bottom pressure gauges located at 500 m. The volume transport of the upper 2500 m was  
303 estimated to be 121 Sv with  $\sim 10\%$  uncertainty, while the total transport through the  
304 whole cross-sectional area of the Passage was calculated to be between 118 and 146 Sv  
305 [Whitworth, 1983]. The baroclinic mode was found to be responsible for 70% of the net  
306 transport, although the transport fluctuations were found to occur predominantly in the  
307 barotropic mode. This was in agreement with the earlier assertion [Reid and Nowlin,  
308 1971] that the internal pressure field at Drake Passage is rather stable.

309  
310 The 121 Sv estimate for ACC transport was later refined to 123 Sv by *Whitworth and*  
311 *Peterson* [1985]. These authors also extended the ISOS transport time series using two  
312 additional years of bottom pressure data obtained at 500m depth at either side of the  
313 passage (Figure 4b). Their calculation was based on the assumption that the transport  
314 variability was predominantly barotropic, and therefore well-represented by the bottom  
315 pressure data alone. (In 1979, there was a maximum difference in transport of 24 Sv  
316 between the net transport and the transport estimated from the across-passage pressure  
317 difference, which was seen to be acceptably small). They concluded that the variability in  
318 the transport through the passage was of the order of 10 Sv, and they noted two examples  
319 (in July 1978 and June-July 1981) of transport fluctuations approaching 50% of the mean  
320 (or approx 50 Sv) over periods as short as 2 weeks (Figure 4b). The veracity of at least  
321 one of these sudden shifts in transport was later questioned (see Section 3).

322

323 With the intention of further extending the ISOS transport time series, *Peterson* [1988b]  
324 compared information obtained from the ISOS bottom pressure measurements with  
325 coastal sea level data obtained from tide gauges at either side of Drake Passage. Sea level  
326 at Puerto Williams in Tierra del Fuego was found to have little correspondence with the  
327 BPR data on the north side of Drake Passage, apparently due to local winds for periods  
328 under 100 days and to annual changes in upper-layer density. Conversely, sea level data  
329 from Faraday (now called Vernadsky) on the Antarctic Peninsula were found to be  
330 coherent with bottom pressure measurements from the south side of Drake Passage on  
331 timescales of 6-600 days. Notwithstanding this, *Peterson* [1988b] stated that 'barotropic  
332 changes in transport cannot be directly estimated using these surface observations', due  
333 to a perceived phase difference between the two datasets at certain frequencies. This  
334 conclusion has since been revisited through WOCE-era studies, discussed in Section 3.

335

336 **2.1.2) Studies of wind-forced transport variability during ISOS**

337

338 A number of studies used the ISOS transport time series to attempt to better elucidate the  
339 dynamics of the ACC wind forcing. The three-year ISOS transport time series was used by  
340 *Wearn and Baker* [1980], alongside wind data obtained from the Australian Bureau of  
341 Meteorology. Whilst no studies of the accuracy of the wind data had at that time been  
342 conducted, this was nonetheless believed to be the most reliable dataset available that  
343 spanned the southern hemisphere. Zonally-averaged eastward wind stress between 43  
344 and 65°S was calculated, and compared with the ISOS bottom pressure data and  
345 transport time series (Figure 4c). Based on the significant relationships found, a  
346 conceptual model was created whereby winds supply momentum to the ocean, which is  
347 removed by a dissipative force representing bottom friction, form drag or lateral friction.  
348 Since momentum input and dissipation are both large, the ocean system is able to  
349 respond rapidly to changes in atmospheric forcing: the expected response time of  
350 transport to a change in winds or dissipation was found to be about seven days.

351

352 Particularly noteworthy is that the significant correlation between the zonal winds and  
353 bottom pressure difference across Drake Passage determined by *Wearn and Baker* [1980]  
354 was due almost entirely to the very strong correlation with pressure at the south side of  
355 the passage. Bottom pressure at the north side bore very little resemblance to the wind  
356 data. No convincing explanation was offered for this, though some possibilities (including

357 seasonal density changes in the north) were suggested. This has relevance to the greater  
358 dynamic understanding of the nature of the bottom pressure variability, as discussed in  
359 Section 3.

360

361 A critique of *Wearn and Baker* [1980] was given by *Chelton* [1982], who made the  
362 observation that strong correlations between the bottom pressure and wind datasets  
363 could be the result of significant seasonality in both datasets, rather than evidence of a  
364 causal relationship. However, a number of more recent studies have addressed this by  
365 investigating the relationship between zonal winds and transport in the frequency  
366 domain rather than the temporal domain, with convincing results (see Section 3).

367

368 A number of investigations were conducted that used ISOS data to investigate other  
369 possibilities for wind-forcing of transport changes. *Peterson* [1988a] derived zonally-  
370 averaged wind stress curl in latitude bands at the northern and southern sides of the ACC,  
371 and conducted cross-spectral analyses with the ISOS bottom pressure data. The  
372 underlying theory was that the time-varying wind stress curl in these bands would  
373 differentially force meridional movements of mass into the ACC flanks, and hence alter  
374 the cross-ACC pressure gradient and thus its transport. Significant coherence was  
375 observed across a range of frequencies, and the seasonality in the bottom pressure data  
376 was seen to match reasonably well that in the corresponding wind stress curl field.  
377 Further to this, *Johnson* [1989] investigated the possibility that changes in the latitude of  
378 zero wind stress curl could be a primary driver of changes in transport through Drake  
379 Passage. Again, a reasonable level of agreement was found between the ISOS bottom  
380 pressure and transport data and the derived time series of the zero wind stress curl  
381 latitude.

382

383 In retrospect, the range of significant relationships identified between winds and ISOS  
384 bottom pressure is perhaps only to be expected – each of the putative meteorological  
385 forcings examined were different measures of the same changing wind field, so (if the  
386 transport changes were to some level wind forced) some degree of correlation or  
387 coherence with a range of derived parameters is not surprising. In practice, the debate  
388 about the nature of wind-forcing of the ACC transport variability was not settled on the  
389 basis of ISOS measurements, though significant further progress was made following  
390 dynamical investigations conducted alongside WOCE-era measurements (Section 3).

391  
392 In summary, ISOS was a landmark experiment that laid much of the foundations for our  
393 current understanding of the ACC at Drake Passage. Significant results included the first  
394 detailed descriptions of the ACC zonation, the first comprehensive characterizations of its  
395 spatio-temporal variability, the first robust insights into ACC transport variability, and  
396 some early insights into the nature of wind-forced variability in the Southern Ocean.  
397 Needless to say, science progresses, and some of the ISOS findings have since been  
398 superseded, including refinements of the level of transport variability, better  
399 understanding of the dynamical nature of the transport variability, and a clearer idea of  
400 which processes the bottom pressure measurements are actually reflecting. Many of  
401 these newer insights were made from measurements instigated during WOCE, discussed  
402 next, but it should be noted that the design of WOCE-era monitoring at Drake Passage  
403 was strongly influenced by ISOS experiences and results, highlighting the ISOS legacy.

404  
405 **3) Sustained monitoring implemented during WOCE**  
406  
407 The World Ocean Circulation Experiment (WOCE) was the largest international physical  
408 oceanographic programme ever conducted. It coordinated the research of nearly 30  
409 countries in making then-unprecedented *in situ* observations of the global ocean between  
410 1990 and 1998. This activity in gathering *in situ* data was coordinated temporally with  
411 some particularly important satellite missions, including the first precise radar altimeters  
412 (ERS-1 and TOPEX/POSEIDON).

413  
414 The field phase of WOCE had two primary goals. The first was to develop models useful  
415 for predicting climate change and to collect the data necessary to test them. The second  
416 was to determine the representativeness of the WOCE data sets for describing the long-  
417 term behaviour of the ocean, and to find methods for determining long-term changes in  
418 the ocean circulation. WOCE planning included a strategy for achieving both goals in  
419 terms of three core projects, one of which focused specifically on the Southern Ocean.  
420 Within this, targeted plans for monitoring the ACC at its Drake Passage, African and  
421 Australian ‘choke points’ were implemented. Southern Ocean research during WOCE has  
422 since been presented in a number of special publications [King, 2001; Siedler *et al.*, 2001];  
423 here we focus specifically on the sustained measurements that were initiated at Drake

424 Passage during WOCE, and, looking back with several years' hindsight, what has been  
425 learned from them.

426

427 **3.1) Bottom pressure and tide gauge measurements during WOCE**

428 **3.1.1) Variability on sub-annual periods**

429

430 The observational effort at Drake Passage during WOCE was predominantly led by the  
431 UK, though with other nations contributing significantly. This included the instigation of  
432 annual repeat hydrographic sections (described in detail below; see also Figure 3c), and,  
433 following ISOS, the resumption of sustained bottom pressure measurements at the flanks  
434 of Drake Passage. These latter measurements were the responsibility of the Proudman  
435 Oceanographic Laboratory (POL, now called the National Oceanography Centre,  
436 Liverpool), whose expertise in such measurements derived from the work of David  
437 Cartwright and colleagues in measuring tides in the deep ocean. (See *Cartwright* [1999]  
438 for an excellent review of the development of bottom pressure recording in several  
439 countries.)

440

441 POL made its first set of deployments of BPR pop-up recorders across Drake Passage in  
442 November 1988, taking advantage of ship access provided by the British Antarctic  
443 Survey. These early deployments were on a line between the Falkland Islands and the  
444 South Orkneys (Figure 3c), after which the deployments were moved close to the  
445 narrowest part of the Passage (the original WOCE "SR1" section). Since then, recorders  
446 have been deployed at each end of a line further to the east, dubbed "SR1b". Most SR1b  
447 deployments were at the WOCE-standard depth of 1000m. Additional sensors, including  
448 the long deployment (~5 years) MYRTLE (Multi Year ReTurn Level Equipment)  
449 instrument [*Spencer and Foden*, 1996], were deployed in certain years at locations  
450 between the two ends of SR1 or SR1b.

451

452 Data from the first few years of POL Drake Passage deployments were used by *Meredith*  
453 *et al.* [1996], who suggested that the standard deviation in transport through the Passage  
454 was between 5 and 9 Sv, compared with the 10 Sv observed in ISOS. A small part of this  
455 difference was attributable to the methods employed for dealing with end-points in the  
456 data, caused when the BPRs were recovered and redeployed, though more significant was  
457 the absence of evidence for large, sudden changes in transport of the sort that were

458 reported to have occurred twice during ISOS [Whitworth and Peterson, 1985]. These ISOS  
459 events were reported to have featured a change in ACC transport of up to half its mean in  
460 the space of just a couple of weeks.

461

462 The absence of any similar shifts in the WOCE BPR data prompted re-examination of  
463 these events in the ISOS data, and it was noted that their temporal correspondence to  
464 changes in wind forcing was not strong, despite the pressure series (and the south-side  
465 data in particular) being strongly related to winds from the data series as a whole  
466 [Meredith *et al.*, 1996]. An incontrovertible explanation for the sudden shifts reported  
467 during ISOS could not be found, and probably never will be. It was noted, however, that  
468 POL BPRs had suffered at least one event of “slippage” up to that time, whereby the gauge  
469 slid down the continental slope a little way, before settling at a deeper level. This is  
470 evident in the data as a rapid, sudden increase in pressure, unrelated to changes in the  
471 winds. (Such slippage can cause apparent transport changes of either sign, depending on  
472 whether it occurs in a north-side or south-side BPR.) When spotted, it is relatively easy to  
473 correct for, but if the slippage were relatively small, it would be easy to misinterpret as a  
474 genuine geophysical signal.

475

476 The SR1b line was chosen to lie along an ascending track of the 35-day repeat orbit of the  
477 ERS-1 mission. Concurrently, the 10-day repeat orbit of the TOPEX/POSEIDON mission  
478 had a sufficiently high inclination to provide coverage of the Passage. Several studies  
479 were undertaken in which *in situ* and altimeter data were used in complementary ways.  
480 However, the results of Woodworth *et al.* [1996] and Hughes *et al.* [2003] indicated that,  
481 while altimetric measurements in Drake Passage can reveal signals of interest, questions  
482 concerning altimetric accuracy, and limitations of data coverage due to winter sea ice,  
483 mean that satellite measurements can not be used as direct replacements for *in situ* data  
484 in estimating transport. The inadequacy of altimetric sampling, and aliasing of sea level  
485 and transport signals, was further explored by Gille and Hughes [2001] and Meredith and  
486 Hughes [2005].

487

488 Because monitoring at the three ACC chokepoints was conducted simultaneously during  
489 WOCE, a natural investigation was to study the correlation between pressure data  
490 between these locations. This was extended to include data from coastal tide gauges  
491 around Antarctica, and a high level of circumpolar coherence was found at timescales

492 shorter than seasonal [Aoki, 2002; Hughes *et al.*, 2003] (Figure 5). This coherent  
493 variability was strongly correlated with the circumpolar westerly winds, as quantified by  
494 the Southern Annular Mode [SAM; Thompson and Wallace, 2000]. The relevance of this  
495 circumpolarly-coherent mode to the flow through Drake Passage was confirmed by  
496 comparison with transport here predicted from the 1/4° OCCAM general circulation  
497 model [Webb, 1998].

498  
499 A small number of the POL BPRs were also equipped with inverted echo sounders (IESs),  
500 with the purpose of monitoring the integrated water column properties (temperature,  
501 predominantly) as well as the bottom pressure [Meredith *et al.*, 1997]. These showed that  
502 pressure changes at the south side of Drake Passage were almost purely barotropic in  
503 nature, in that the overlying density of the water column was almost invariant over the  
504 time scales covered by the length of data. Conversely, bottom pressure at the north side  
505 of Drake Passage was more affected by water column density changes, raising questions  
506 as to how well these data relate to transport. (Meredith *et al.* [1997] argued that the  
507 standard deviation in transport derived from pairs of gauges at either side of the Passage  
508 should best be viewed as upper limits to the true transport variability). Such findings  
509 prompted more detailed investigations into the complexity of the bottom pressure series  
510 at Drake Passage, and what processes the data were really reflecting.

511  
512 **3.1.2) Understanding the dynamics of the bottom pressure signals**

513  
514 Coincident with the WOCE observational campaign in the 1990s, ocean modelling was  
515 rapidly developing, with the first large-scale eddy-permitting ocean models appearing.  
516 This made possible a more realistic examination of the interpretation of observations  
517 made in an energetic, turbulent ocean. The ISOS observations had been interpreted using  
518 a very simple flat-bottomed wind-driven channel model [Peterson, 1988a; Wearn and  
519 Baker, 1980], the essentials of which are still the basis for interpretation of observations  
520 today: zonal wind stress produces an accelerating zonal flow, which ceases to accelerate  
521 over some characteristic decay time scale, typically about 3-10 days. However,  
522 topography must be a strong controlling factor for these transport fluctuations, and  
523 furthermore it was not clear that the large-scale processes normally considered in  
524 analytical and coarse resolution numerical models would be the dominant processes  
525 determining what is measured at a single point in the ocean. New models such as the Fine

526 Resolution Antarctic Model [FRAM, 1991] and the Parallel Ocean Climate Model [POCM;  
527 Tokmakian and Challenor, 1999], with Southern Ocean resolutions of about 25 km, could  
528 begin to reproduce the energetic eddy field of the ocean and its effect on observations.

529  
530 *Hughes et al.* [1999] used these models, together with WOCE BPR and tide gauge data, to  
531 investigate the relationship between Drake Passage pressure measurements and ACC  
532 transport. It became apparent that, in an eddying ocean, a meaningful definition of the  
533 northern boundary of the ACC can not be found except in the choke points, most notably  
534 Drake Passage. Scaling arguments also showed that, at length scales of more than a few  
535 hundred kilometres, fluctuations in Southern Ocean currents must be predominantly  
536 barotropic on time scales shorter than about a year. This means that fluctuations in the  
537 flow will be strongly controlled by the geometry of  $f/H$  contours ( $f$  is the Coriolis  
538 parameter;  $H$  is depth), and will not follow the path of the mean ACC, which is much more  
539 weakly (though still significantly) steered by topography. With this in mind, the channel  
540 model concept had to be reinterpreted: whereas all Drake Passage latitudes can be  
541 considered “open” in a flat-bottomed channel (i.e. these latitudes represent closed  $f$   
542 contours), the only “open” part of a Southern Ocean with topography is the narrow band  
543 of closed  $f/H$  contours that pass right around Antarctica, mostly lying along the Antarctic  
544 continental slope.

545  
546 The suggestion was, therefore, that fluctuations in circumpolar transport should be  
547 predominantly associated with a barotropic flow along, or near to, these closed  $f/H$   
548 contours. Fluctuations should be driven by wind stress acting along those contours, and  
549 should be detectable (if not masked by small scale local disturbances) in terms of bottom  
550 pressure and sea level variations on and near the Antarctic continental slope. This  
551 prediction was borne out within the models, which clearly showed such a mode [*Hughes*  
552 *et al.*, 1999; *Woodworth et al.*, 1996]. Comparison between models and observations of  
553 bottom pressure, sea level and wind stress were also consistent with this interpretation  
554 (Figure 6). A subtlety, which is still a subject worth investigating in more detail, is that  
555 there appears to be rather little transport associated with the “free mode” associated  
556 with the completely closed  $f/H$  contours. Most of the transport is in an “almost-free  
557 mode”, which requires the current to cross  $f/H$  contours in order to pass through Drake  
558 Passage, but is clearly closely associated with the region of closed contours.

559

560 The dominance of this “Southern Mode” of variability in Antarctic transport has been  
561 supported by subsequent observations and model investigations [Kusohara and Ohshima,  
562 2009; Vivier *et al.*, 2005; Weijer and Gille, 2005]. The essentially barotropic nature of this  
563 mode is confirmed by comparison between barotropic and three-dimensional models,  
564 which produce very similar time series at intra-annual periods [Hughes *et al.*, 2003], and  
565 by the success of purely barotropic models in reproducing tide gauge observations  
566 [Hibbert *et al.*, 2010; Hughes and Stepanov, 2004; Kusohara and Ohshima, 2009]. At  
567 interannual time scales, however, barotropic models do not perform well, suggesting the  
568 increasing importance of baroclinic processes at lower frequencies [Meredith *et al.*,  
569 2004].

570  
571 Notwithstanding the limitations of satellite altimeter data mentioned above, the part of  
572 the Southern Mode that extends beyond the sea ice can be seen in such data, and matches  
573 the model predictions well [Hughes *et al.*, 2003; Hughes and Meredith, 2006; Vivier *et al.*,  
574 2005]. More recently, large-scale bottom pressure variations have been measured from  
575 space by the GRACE (Gravity Recovery and Climate Experiment) satellite gravity mission,  
576 and a rather blurred version of the Southern Mode has also been found as the dominant  
577 Southern Ocean mode in these measurements [Ponte and Quinn, 2009].

578  
579 While the Southern Mode is seen to be the dominant structure associated with  
580 circumpolar transport fluctuations, it does not explain all the variability. In fact at Drake  
581 Passage, the relationship between pressure to the south and total transport implies that  
582 the flow (if geostrophic) is occurring at larger values of  $H$  (or smaller values of  $f$ ) than any  
583 that occur within Drake Passage [Hughes *et al.*, 1999]. Pressure on the northern side of  
584 the choke point must also be considered to complete the picture. However, variability on  
585 the northern side is much more complicated, and therefore harder to sample adequately.  
586 For a purely barotropic flow, the transport can be calculated from the near-bottom  
587 velocity multiplied by depth, and integrated across the channel. The baroclinic  
588 component of the flow can then be defined as the integral of the flow relative to the  
589 bottom, using thermal wind balance. Although the Southern Mode is highly barotropic  
590 and coherent both around Antarctica and across the Antarctic continental slope, the  
591 baroclinic contribution to transport fluctuations in FRAM was found to be significant and  
592 highly variable from place to place (e.g. Figure 6 of Hughes *et al.* [1999]). This is a result of  
593 small-scale, baroclinic processes occurring near the northern boundary.

594  
595 A hint as to the origin of these processes was given by *Vivier et al.* [2001] and *Vivier and*  
596 *Provost* [1999], who found signals on the Argentinian continental slope near 41°S that  
597 they suggested may be shelf waves originating in the Pacific and propagating through  
598 Drake Passage. This interpretation was supported by altimeter measurements [*Hughes*  
599 and *Meredith*, 2006], which clearly showed that signals of equatorial Pacific origin  
600 penetrate well into the Atlantic along the South American continental shelf and slope.  
601 These are not the only propagating signals in the northern part of Drake Passage though;  
602 as *Fetter and Matano* [2008] note, there is ample evidence for propagating eddies in this  
603 region also.

604  
605 **3.1.3) Interannual variability in transport from BPRs and tide gauges**  
606  
607 As noted above, the barotropic models that perform well at reproducing the sub-annual  
608 variability associated with the Southern Mode tend to perform poorly at interannual and  
609 longer periods, suggesting the increasing importance of baroclinic processes [*Meredith et*  
610 *al.*, 2004]. This interpretation is supported by the improved agreement with observations  
611 when using a baroclinic model with data assimilation (although not of tide gauge data), as  
612 shown by *Hibbert et al.* [2010]. The switch from barotropic to baroclinic dominance has  
613 been studied in the context of an idealized model (with realistic but somewhat smoothed  
614 topography) by *Olbers and Lettmann* [2007], who found a rather long baroclinic  
615 adjustment time scale of about 16 years, and a cross-over between barotropic and  
616 baroclinic dominance at about 7-9 year periods, although this may be sensitive to the  
617 absence of eddies.

618  
619 Because of the presence of baroclinic variability at interannual periods, there is no *a*  
620 *priori* reason that data from a single depth in the ocean (or from a surface tide gauge)  
621 should be a reliable proxy for transport changes at these periods. Nonetheless, *Meredith*  
622 *et al.* [2004] investigated a long series of annual mean sea level records from the tide  
623 gauge at Faraday station (Figure 5a) on the Antarctic Peninsula in this context. (Faraday  
624 was transferred to Ukrainian control during WOCE, and renamed Vernadsky). Data from  
625 this site represents the longest tide gauge series from Antarctica for which reliable  
626 records exist; a record extending back to the early 1980s was used for this study.

627

628 The time series of sea level from Faraday showed variability that was significantly  
629 correlated with the SAM, even after correction for surface atmospheric pressure changes  
630 (Figure 7) [Meredith *et al.*, 2004]. It was also significantly correlated with interannual  
631 changes in Drake Passage transport predicted by the full version of the 1/4° OCCAM  
632 general circulation model (though not with a purely barotropic version of the same  
633 model). This indicated that, despite the presence of baroclinic signals in the data, the  
634 Faraday tide gauge provided a reliable proxy for interannual changes in transport. This  
635 was fortuitous, and was seen to be indicative of a degree of vertical coherence in the  
636 transport changes, even though they are not purely barotropic.

637

638 Of great interest is the longer-term response of the ACC to the changing SAM, since the  
639 SAM has been exhibiting a marked upward trend (stronger winds) in recent decades  
640 [Thompson *et al.*, 2000]. This has been argued to be forced at least partly by  
641 anthropogenic processes, with greenhouse gases and ozone depletion both suggested as  
642 the cause [Marshall, 2003; Thompson and Solomon, 2002], though with natural variation  
643 also contributing [e.g. Visbeck, 2009]. A key question is: is the ACC strengthening as a  
644 result? Data from the Faraday tide gauge cannot answer this question, since tide gauges  
645 contain trends due to a great number of processes (isostatic rebound, global sea level  
646 rise, etc), and isolating a trend due exclusively to a change in ACC transport is not  
647 possible. However, the BPR data from Drake Passage are useful in this context.

648

649 Whilst BPR data cannot directly inform on transport changes at periods longer than the  
650 lengths of the individual records, they do capture well the seasonal signals in the  
651 transport [Meredith *et al.*, 1996]. A significant factor in the decadal trend in the SAM is  
652 that it is not uniform across the year, but is significantly seasonally modulated [Thompson  
653 and Solomon, 2002]. This allowed examination of the change in seasonality in Drake  
654 Passage transport in the context of the change in seasonality in the SAM over the same  
655 period; the two were seen to be strikingly similar (Figure 8). Whilst this does not  
656 constitute direct proof that the long-term trend in the SAM is accelerating the ACC, it is  
657 nonetheless strongly suggestive that this may be happening. Further, it was argued that,  
658 to the extent that anthropogenic processes are modulating the seasonality of the SAM,  
659 they are also influencing the flow of the ACC [Meredith *et al.*, 2004]. This proposition is  
660 discussed further below (Section 3.2).

661

662 An interesting feature concerning the interannual changes in transport in response to the  
663 SAM is that they seem to be rather small (Figure 7), with peak-to-peak changes in  
664 transport of around 5% of the ACC mean transport, despite much larger relative changes  
665 in the overlying winds. This is consistent with more recent evidence that suggests a  
666 small-amplitude response of ACC transport with respect to winds on decadal timescales  
667 [Böning *et al.*, 2008]. These observations have helped to narrow the range of theoretical  
668 predictions regarding the dependence of ACC transport upon the magnitude of wind  
669 stress. The upper limit of this range (over timescales for which thermodynamic  
670 equilibrium can be assumed to hold) is the linear dependence of Drake Passage transport  
671 upon wind stress [Marshall and Radko, 2003]; at the other end of the spectrum Straub  
672 [1993] developed scaling arguments outlining parameter regimes in which transport is  
673 insensitive to the winds. The latter has become known as the “eddy saturation” limit  
674 [Hallberg and Gnanadesikan, 2006].

675  
676 Eddy saturation can be interpreted on physical grounds as the consequence of the  
677 vertical transport of momentum by eddies: in steady state, a balance exists between  
678 momentum input at the surface and momentum loss at the bottom (due to bottom form  
679 drag). When wind stress is higher, a stronger eddy field more effectively damps zonal  
680 momentum resulting in a weak dependence of transport upon wind stress. Eddy  
681 saturation theory therefore predicts that wind stress has a greater influence on eddy  
682 kinetic energy (EKE) than it does on transport; this prediction has been confirmed using  
683 satellite observations by Meredith and Hogg [2006] (Figure 9). Moreover, a lag of  
684 approximately 2 years between wind stress maxima and EKE is found in both  
685 observations and numerical models in the eddy saturated parameter regime, believed to  
686 be due to a slow feedback between the mean flow, eddies and topography. These findings,  
687 of relatively small variability in ACC transport on interannual and decadal timescales,  
688 have significant implications for the sampling precision and frequency that is needed  
689 when attempting to detect trends in transport (see Section 3.2). These are further  
690 emphasized by theoretical arguments [Allison *et al.*, 2011] that suggest that the baroclinic  
691 ACC adjusts on centennial timescales to changes in wind stress, again consistent with  
692 [Böning *et al.*, 2008].

693  
694 **3.1.4) Relationship of transport changes to low-latitude modes of climate**  
695 **variability**

696

697 As described earlier, a large-scale sea level and circumpolar transport response to  
698 variability in the SAM has been confirmed by a number of studies [Aoki, 2002; Hughes *et*  
699 *al.*, 1999; Hughes *et al.*, 2003; Meredith *et al.*, 2004]. However, in a more recent and  
700 perhaps surprising development, evidence has emerged that this coherent oceanic mode  
701 is also modulated by two major low-latitude atmospheric modes, namely the Madden-  
702 Julian Oscillation [MJO; Madden and Julian, 1971] and the Quasi-Biennial Oscillation  
703 [QBO; Angell and Korshover, 1964].

704

705 The MJO dominates intraseasonal atmospheric variability in the tropics and is  
706 characterised by the generation and eastward propagation of deep convection and  
707 precipitation anomalies on timescales of 30 to 100 days [Xie and Arkin, 1997]. A  
708 wintertime response has been identified in the extratropics in the form of planetary wave  
709 trains that extend southeastward from the tropical Pacific and Indian Oceans. Mindful of  
710 the potential influence of these upon surface wind patterns, Matthews and Meredith  
711 [2004] examined the SAM and Drake Passage BPR data, and found an MJO component in  
712 each. Most striking was the rapidity of the transport adjustment, occurring only 3 days  
713 after the development of the extratropical atmospheric wave train.

714

715 Other research has suggested that the periodic reversal in equatorial stratospheric wind  
716 direction that is described by the QBO could also influence the southern extratropical  
717 atmospheric circulation, and, when the influence of the 11-year solar cycle is taken into  
718 account, the SAM [Roscoe and Haigh, 2007; Wong and Wang, 2003]. Accordingly, Hibbert  
719 *et al.* [2010] examined whether circumpolar transport might similarly be modulated by  
720 the QBO and/or the solar cycle. They found a statistically significant QBO modulation of  
721 the Southern Ocean coherent mode and the circumpolar transport, identifying a key  
722 region of relatively weak westerly winds around 65°S via which the atmospheric signal  
723 might be communicated to the surface ocean.

724

725 As with any large-scale observational programme, a number of serendipitous findings  
726 were made from the Drake Passage BPR data obtained during WOCE, including detection  
727 of internal tides in the ancillary bottom temperature measurements [Heywood *et al.*,  
728 2007], and the first detection of ventilation of intermediate and deep layers at the south  
729 side of Drake Passage by local downslope convection [Meredith *et al.*, 2003]. In addition,

recent studies have demonstrated the usefulness of Drake Passage bottom pressure data for characterizing the 2004 Sumatra tsunami [Rabinovich *et al.*, 2011], and also for generating understanding of the processes that control sea level in coastal and island tide gauges so that correct attribution can be made [e.g. Woodworth *et al.*, 2005]. Whilst interesting, these were peripheral to the core strategic aims of the WOCE monitoring programme, and thus are not discussed in detail here, but the extra scientific value that such findings add to the sustained measurement programme should not be underestimated.

738

### 739 **3.2) Results from hydrographic data**

#### 740 **3.2.1) Transports and fluxes**

741

742 For WOCE, a repeat hydrographic section was initiated by the UK in the 1993/94 season,  
743 on the SR1b line that had already been adopted for BPR measurements (Figure 3c). As  
744 with the BPR deployments, these CTD measurements were made opportunistically from  
745 RRS *James Clark Ross*, on logistics passages to or from the British Antarctic Survey bases  
746 in the Antarctic. As reviewed in Section 2, the definitive estimates of Drake Passage  
747 transport prior to WOCE were from ISOS: a canonical value of  $134 \pm 11.2$  Sv was quoted  
748 by Whitworth and Peterson [1985], with the variation being the standard deviation of a  
749 yearlong dataset, rather than the formal uncertainty of the estimate of the mean.

750

751 The WOCE SR1b hydrographic section consisted of 30 full-depth CTD stations, with  
752 salinity calibrated using up to 12 bottle salinities per station analysed on board. These  
753 sections have been continued post-WOCE, and a full description of the data and analysis  
754 is given in King and Jullion [2011]. For completeness, we report here a summary of their  
755 analyses and results, including data up to the most recent cruise in November 2009.

756

757 Data were collected in every southern summer season since 1993/94, except for 1995/96  
758 and 1998/99, when the CTD work could not be accommodated in the logistics schedule.  
759 Two sections were completed in 2008/09: the first was the usual CTD-only section, the  
760 second was a full CLIVAR/GO-SHIP repeat hydrography cruise with a suite of additional  
761 chemical measurements. Wherever possible, the sections were exact repeats, with the  
762 same nominal station positions every year.

763

764 Many of the cruises acquired shipboard or lowered ADCP data. While it would be possible  
765 to consider these datasets as a means of estimating the absolute water velocities (and  
766 hence a potential means of deriving total volume transport), this was decided against  
767 here primarily because the data are not available for all the early cruises, and to make  
768 partial use would compromise the comparison between years. (The referencing of  
769 transports using lowered ADCP data is discussed further in Section 4). The transports  
770 reported here are thus based on the simplest possible calculation, whereby geostrophic  
771 velocities between adjacent stations are calculated relative to a presumed level of no  
772 motion at the deepest common level. No attempt was made to adjust for the contributions  
773 missed due to ‘bottom triangles’. Volume flux was then calculated by integration of the  
774 product of the velocity and the relevant cross-sectional area. The transport calculated by  
775 this method thus represents the baroclinic structure of the ACC, and any changes in that  
776 structure, rather than being a measure of absolute ACC transport.

777

778 We have departed from this simple calculation just once: for the 2009/10 cruise. In this  
779 year the PF was found to be exceptionally far north, as shown by the dashed line and  
780 overlaid symbol in Figure 10. The PF/SAF system was pushed right up onto the slope  
781 near Burdwood Bank, and a reference level of zero at the deepest common level is  
782 inappropriate. Examination of the lowered ADCP data for stations north of 55.5°S  
783 suggested that near-bottom eastward velocities up to 30 cm/s were present. To allow for  
784 this, the velocity field was set to have a cross-track component of 15 cm/s at the deepest  
785 common level for stations north of 55.5°S for this section alone.

786

787 Temperature and salinity are averaged from adjacent stations onto the derived velocity  
788 field. Temperature flux is obtained by summing the product of each volume flux element  
789 with the element’s ITS-90 temperature in °C; this quantity is dominated by the volume  
790 flux, and it would be meaningless to interpret it as a heat flux. Instead, this temperature  
791 flux is divided by the volume flux to give a transport-weighted mean temperature. This is  
792 referred to as simply the ‘mean temperature’. Changes in this mean temperature enable  
793 us to estimate the change in exceptional heat flux through Drake Passage for some  
794 nominal value of the total volume flux, without requiring a bounded region with a  
795 balanced mass budget. Likewise, salt flux is obtained from the product of volume flux  
796 elements with Practical Salinity, but then reduced to a transport-weighted mean salinity.

797

798 Figure 10 shows the volume flux for each cruise, accumulated from zero at the southern  
799 end of the section. The PF generally occupies the region between 58°S and 56.5°S, shown  
800 by the sharp increase in transport here. Its location is distinctly bimodal, with the five  
801 ‘southern’ years (red lines) being 1993/4, 1996/7, 2000/1, 2003/4 and 2006/7. The  
802 intermediate year (cyan line) is 2005/6. In the southern PF years, there is a distinct  
803 transition zone between the PF and the SAF to the north. In the northern PF years (black  
804 lines), the accumulating transport is less likely to show an obvious inflection between the  
805 fronts. The positions of the PF as defined using the thermohaline criterion (2°C isotherm  
806 crossing 200m) of *Orsi et al.* [1995] for each cruise are also shown (black dots for the  
807 southern PF positions and red dots for the northern PF position). The dashed black line  
808 marks the most northerly position of the PF and corresponds to the exceptional year  
809 2009/2010. Analysis of satellite altimeter and sea surface temperature data for the time  
810 of that cruise (not shown) reveals the presence of a large meander of the PF, which  
811 extended up to the continental slope of South America at that time.

812

813 The mean volume transport from the 16 sections is 136.7 Sv, with a standard deviation of  
814 6.9 Sv. Table 1 lists the range, mean and standard deviation of the volume flux and other  
815 quantities of interest. Figure 11 shows time series of the volume, mean temperature and  
816 mean salinity from the 16 sections, both with (solid lines) and without (dashed) a  
817 seasonal adjustment (described below). The most striking features of the unadjusted time  
818 series are the high mean temperature during the 1999/2000 cruise and the second  
819 2008/09 cruise. This is expected, since these cruises were undertaken later in the season  
820 (February) than the others. The difference in mean temperature, 0.4 °C, is equivalent to  
821 0.2 PW when multiplied by a nominal volume flux of 137 Sv. It is therefore crucial that  
822 any attempt to close a heat budget of the Southern Ocean that involves Drake Passage  
823 sections must consider the month in which data were gathered.

824

825 Figure 12 shows the volume flux, mean temperature and mean salinity for each section,  
826 as a function of year day. Since each set of measurements occupies up to six days of  
827 elapsed time, the central day of each data gathering period is used. Most of the data were  
828 gathered before, or just after, the year-end. The two February cruises provide the high  
829 values to the right of Figure 12b, but even apart from these two late-season cruises there  
830 is a well-resolved trend through the southern spring, shown by the solid line. The full  
831 seasonal cycle is not resolved, but the spring/summer trend can be determined. There is

832 no obvious seasonal variation in the total volume flux (Figure 12a) and a weak freshening  
833 trend in the mean salinity (Figure 12c). The 2002/03 data, centered on day 362, is an  
834 outlier from the underlying seasonal trend in both mean temperature and salinity, for  
835 reasons that have not been identified.

836

837 In order to look for decadal trends in transport and fluxes, a seasonal adjustment has  
838 been made to the total fluxes, using the slopes of the best-fit lines in Figure 12. The slopes  
839 are 0.44°C per 100 days for temperature and -0.015 per 100 days for salinity. Total fluxes  
840 for each cruise have been adjusted to equivalent values at 1 December (day 335). The  
841 seasonally-adjusted time series are the solid lines in Figure 11 (b and c). As noted earlier,  
842 the 2002/03 cruise appears as an outlier in the adjusted time series, and no explanation  
843 has yet been found. Satellite-derived sea surface temperature shows nothing unusual at  
844 the time of this cruise. The 2004/05 cruise is also slightly cooler than other years. Apart  
845 from these, the mean temperature and salinity are remarkably stable. There is no  
846 discernable trend in any of the transports.

847

848 We consider briefly the errors or uncertainty in the calculations presented in Figures 11  
849 and 12. The contribution from measurement error is negligible. Suppose that the CTD  
850 measurements of temperature, salinity and pressure have a random errors of 0.002°C,  
851 0.002 and a random 2 dbar offset on each station. When these errors are combined the  
852 standard deviations of the changes to the mean temperature transport, mean salinity  
853 transport and volume transport are 0.004°C, less than 0.001 and less than 0.1 Sv  
854 respectively, an order of magnitude below the interannual variability. The error bar in  
855 each calculation in Figure 11 is thus too small to plot. In effect we have 16 precise  
856 measurements of a variable quantity, and rather than being one of errors, the issue is one  
857 of representativeness. Our 16 sections have characterized the size of the variability, but  
858 not the time scales on which it occurs.

859

860 Given the apparent lack of trends, it is pertinent to ask the minimum size of change that  
861 could be detected from such annual measurements. First, we suppose that the full  
862 variance of the transport (for example) can be represented by the variance of, say, a  
863 decade of annual measurements. This supposes that while individual realizations of the  
864 section may have aliased the higher frequency variability, a sufficient range of higher-  
865 frequency variability has been sampled by the individual cruises: ten such measurements

866 in our assumption. Then a two-tailed student t-test suggests that the smallest change that  
867 could be detected between two decadal means is roughly equal to the sample standard  
868 deviation in each decadal mean. We therefore conclude that the magnitude of any change  
869 in the transport or mean properties of the ACC at Drake Passage over the period of the UK  
870 repeat CTD cruises is no greater than the standard deviations in the right hand column of  
871 Table 1. This places a useful constraint on how small the response of the ACC transport is  
872 to changing winds, and what impact this might have on associated property fluxes.

873

874 Interestingly, the WOCE SR1b CTD data show no evidence for a southward shift of the PF  
875 (neither using the transport definition or a thermohaline definition of the PF), despite it  
876 having been argued elsewhere that the ACC could be migrating southwards, associated  
877 with the climatic poleward movement of the circumpolar winds [e.g. *Gille*, 2008; *Sprintall*,  
878 2008]. Given the constrained nature of the PF on SR1b (Figure 10), it may be that this  
879 section is unusual in this regard compared with the ACC more generally around its  
880 circumpolar path. This is discussed further in Section 4.

881

882 **3.2.2) The Southern Ocean meridional overturning circulation**

883

884 As seen already (Figure 2), the horizontal circulation of the ACC is associated with a  
885 complex Southern Ocean meridional circulation that is related to the formation,  
886 modification and ventilation of the world ocean water masses. Within this overturning  
887 circulation, CDW upwells close to the surface south of the ACC, whereupon it can be  
888 pushed north under the direct influence of the winds and re-enter the ocean interior as  
889 AAIW and SAMW; alternatively, it can be transformed into dense waters that become  
890 AABW close to the Antarctic continent (Figure 13).

891

892 The two-cell structure of the meridional overturning circulation in the Southern Ocean  
893 was first revealed by the early descriptions of the hydrographic structure [e.g. *Deacon*,  
894 1937]. However, because of the absence of zonal barriers and the importance of the eddy-  
895 induced flow in the overturning circulation, assessing and monitoring its intensity has  
896 been challenging. In contrast to the measurement of ACC transport, determination of the  
897 strength of the overturning circulation can only be achieved by indirect methods such as  
898 inverse models. In this respect, the repeated hydrographic sections of the WOCE era have  
899 proved very useful: in combination with the other Southern Ocean sections, they have

allowed estimates of the strength of the Southern Ocean overturning circulation for the first time.

To enable this, two main methods have been applied to WOCE observations: methods using geostrophic velocity data derived from hydrography with empirically chosen reference levels [e.g. *Talley et al.*, 2003; *Talley*, 2008], and box inverse methods [e.g. *Lumpkin and Speer*, 2007; *Sloyan and Rintoul*, 2001]. Significant uncertainties remain on the estimate of the strength of the overturning circulation, indeed both methods are highly sensitive to empirical choices. For instance, inverse methods depend critically on the choice of the weight matrices, which are, in practice, not possible to derive from observations. In addition, inverse solutions depend on mixing schemes used, treatment of the interactions between the ocean interior circulation and the ocean surface layer, and other critical physical mechanisms that are still not accurately understood. In turn, methods based on geostrophic velocities depend on subjective choices, for instance when adjusting observed geostrophic shear to match the observed property distribution. Notwithstanding this, the comparison of several studies that cover a range of such subjective choices can provide important information on the intensity of the Southern Ocean overturning circulation.

The overturning circulation in the Southern Ocean is estimated to involve a southward transport of CDW over the circumpolar belt of between 20 Sv [*Lumpkin and Speer*, 2007] and 52 Sv [*Sloyan and Rintoul*, 2001] (Figure 13). Although both estimates arise from inverse analysis of WOCE hydrographic sections, *Lumpkin and Speer* [2007] considered twice as many layers in their inverse model as did *Sloyan and Rintoul* [2001], and the two inverse methods also use different air-sea forcing. However, *Lumpkin and Speer* [2007] suggested that the calculation of *Sloyan and Rintoul* [2001] might be biased high by the different treatment of the interaction of Ekman transport and water mass formation, rather than because of the difference in air-sea forcing. The estimates from *Talley et al.* [2003] and *Talley* [2008] from geostrophic velocity data give numbers slightly above the estimate of *Lumpkin and Speer* [2007], with 22-30 Sv of southward transport of CDW over the circumpolar belt. Similar discrepancies exist in the transport of other water-masses. These are due to a number of reasons, including the number of density layers considered, model treatment of mixing and surface layers, velocity reference levels, the

933 error matrix, and the surface forcing. But overall, these observationally-based estimates  
934 provide a generally consistent picture of the Southern Ocean overturning circulation.

935  
936 Additional studies have estimated the intensity of the Southern Ocean overturning,  
937 acknowledging that the transport across the ACC results from a balance between  
938 northward wind-driven flow at surface and eddy-induced flow at depth. The eddy-  
939 induced transport can be parameterized using diffusion coefficients and the  
940 climatological isopycnal structure of the ocean interior [e.g. *Gent and McWilliams*, 1990].  
941 From the climatological isopycnal structure of the Southern Ocean, *Zika et al.* [2009]  
942 produced a quantified relationship between the magnitude of the overturning circulation  
943 and the mixing intensity in the Southern Ocean, suggesting that a mean isopycnal mixing  
944 coefficient of the order of  $300 \text{ m}^2\text{s}^{-1}$  and a mean diapycnal mixing coefficient of the order  
945 of  $10^{-4} \text{ m}^2\text{s}^{-1}$  would be needed to maintain an overturning strength of the magnitude  
946 estimated by inverse methods. The overturning circulation transports are also tightly  
947 linked to water mass transformations, which can be estimated in the near-surface ocean  
948 from air-sea buoyancy fluxes [e.g. *Speer et al.*, 2000]. In the near-surface ocean, both  
949 thermodynamics and the eddy-induced parameterisation method have suggested  
950 upwelling of 10-20 Sv south of the ACC, a northward meridional export, and a re-injection  
951 of 10-20 Sv within or north of the ACC [e.g. *Karsten and Marshall*, 2002; *Marshall et al.*,  
952 2006; *Speer et al.*, 2000]. *Sallée et al.* [2010] pinpointed the regional distribution of this  
953 process, with very large subduction fluxes in SAMW and AAIW layers at Drake Passage.  
954

### 955 **3.2.3) Changes in upper and lower limbs of the Southern Ocean overturning**

956

957 In addition to contributing to information on the mean strength of overturning in the  
958 Southern Ocean, the repeat hydrography programme at Drake Passage instigated during  
959 WOCE has proved especially useful for monitoring the evolution of several globally  
960 significant water masses relevant to this overturning. This is true for both the upper-  
961 ocean SAMW and AAIW that ventilate the pycnocline of the Southern Hemisphere oceans  
962 [*Hanawa and Talley*, 2001; Section 3.2.2], and for the AABW that forms in the nearby  
963 Weddell Sea and that invades large areas of the global ocean abyss [*Orsi et al.*, 1999]. In  
964 the following, we review the character and driving mechanisms of the variability of these  
965 water masses, as revealed by several decades of hydrographic measurements in Drake  
966 Passage, the majority of which were collected from the WOCE SR1b line (Figure 3c).

967  
968 The SAMW that flows through Drake Passage is formed by winter overturning on the  
969 equatorward flank of the ACC, in a region of deep winter mixed layers in the southeast  
970 Pacific and in the passage itself [Naveira Garabato *et al.*, 2009]. SAMW (defined here by  
971 the 26.80-27.23 kg m<sup>-3</sup> neutral density range to the north of the SAF) exhibited  
972 substantial variability between 1969 and 2005 (Figure 14), with potential temperature  
973 ( $\theta$ ), salinity (S) and pressure changes of 0.1 – 0.4°C, 0.01 – 0.04 and 30 – 200 dbar,  
974 respectively. Positive  $\theta$  and S anomalies generally co-vary with layer-mean shoaling,  
975 thinning, and lightening (as expected from a convective formation process), and vice  
976 versa. These changes are mainly driven by variations in wintertime air-sea turbulent heat  
977 fluxes and net evaporation modulated by the El Niño/Southern Oscillation (ENSO)  
978 phenomenon and, to a lesser extent, the SAM [Naveira Garabato *et al.*, 2009]. A prominent  
979 exception to the usual buoyancy-driven overturning of SAMW formation took place in  
980 1998, when strong wind forcing associated with constructive interference between ENSO  
981 and the SAM triggered a transitory shift to a friction-dominated mode of ventilation.

982  
983 The time series of SAMW properties in Figure 14 also reveals significant interdecadal  
984 changes. SAMW is seen to have warmed (by ~0.3°C) and salinified (by ~0.04) during the  
985 1970s, with little change in density, whereas it experienced the reverse trends between  
986 1990 and 2005, resulting in a marked lightening of ~0.06 kg.m<sup>-3</sup>. The coldest, freshest  
987 and lightest SAMW is observed at the end of the time series. Available evidence  
988 (discussed by Naveira Garabato *et al.* [2009]) suggests that the reversing changes in  
989 SAMW characteristics were chiefly forced by a ~30 year oscillation in regional air-sea  
990 turbulent heat fluxes and precipitation associated with the Interdecadal Pacific  
991 Oscillation (IPO). A SAM-driven intensification of the Ekman supply of cold, fresh surface  
992 waters from the south also contributed significantly. The IPO is an interdecadal  
993 fluctuation in SST and atmospheric circulation centred over the Pacific Ocean that may  
994 result from the projection of stochastic ENSO variability onto interdecadal time scales. Its  
995 association with the interdecadal oscillation in SAMW properties is apparent from the  
996 qualitative resemblance between the property time series and the evolution of the IPO  
997 index in Figure 14.

998  
999 The AAIW in Drake Passage is ventilated by the northward subduction at the PF of the  
1000 Winter Water originating in the winter mixed layer of the Bellingshausen Sea. AAIW  
1001 (defined here by the 27.23-27.50 kg m<sup>-3</sup> neutral density range to the north of the PF)

1002 displayed interannual variations comparable in amplitude to those of SAMW during  
1003 1969-2005 (Figure 14), but positive (negative)  $\theta$  and S anomalies now co-vary with layer-  
1004 mean deepening, thinning, and lightening (shoaling, thickening, and densification). These  
1005 changes stem from variations in Winter Water properties resulting from fluctuations in  
1006 wintertime air-sea turbulent heat fluxes and spring sea ice melting, both of which depend  
1007 strongly on the intensity of (partially ENSO- and SAM-forced) meridional winds to the  
1008 west of the Antarctic Peninsula. Coupled with the transitory shift in the mode of SAMW  
1009 ventilation, a 1-2-yr shutdown of AAIW formation was initiated in 1998, driven by the  
1010 extraordinary wind forcing of that winter. This resulted in a rapid warming and  
1011 salinification of AAIW at the time (Figure 14).

1012  
1013 The interdecadal evolution of AAIW is characterized by a significant freshening of  $\sim 0.05$   
1014 between the 1970s and the turn of the century, with little detectable change in  $\theta$ . This  
1015 freshening has been shown to stem from a freshening of the Winter Water in the  
1016 Bellingshausen Sea [Naveira Garabato et al., 2009]. Such change was brought about by  
1017 increased precipitation and a retreat of the winter sea ice edge, forced by an interdecadal  
1018 trend in meridional wind stress (likely associated with a concurrent positive tendency in  
1019 the SAM) and regional positive feedbacks in the air-sea-ice coupled climate system. Thus,  
1020 the AAIW freshening is a deep-ocean manifestation of the extreme climate change that  
1021 has occurred along the West Antarctic Peninsula in recent decades [Meredith and King,  
1022 2005; Vaughan et al., 2003].

1023  
1024 The observed variability in the properties of SAMW and AAIW raises the question of  
1025 whether the rate of subduction of those water masses (and, ultimately, the rate of  
1026 meridional overturning) changes considerably in response to climatic forcing. Whilst we  
1027 have no way of directly measuring the overturning streamfunction from the available  
1028 observations, several aspects of the measured property changes are suggestive of  
1029 significant perturbations in the overturning. Consider, for example, the observed changes  
1030 in the pressure of SAMW and AAIW (Figure 14), which are associated with substantial  
1031 variations in the potential vorticity of those layers [Naveira Garabato et al., 2009]. If we  
1032 portray the Southern Ocean overturning circulation as the residual arising from the  
1033 incomplete cancellation between a wind-driven Eulerian-mean cell and a generally  
1034 opposing eddy-induced cell [e.g., Marshall and Radko, 2003; 2006], we may readily  
1035 conclude that the observed changes in potential vorticity are conducive to variations in

1036 eddy-induced overturning that are not necessarily countered by changes in the Eulerian-  
1037 mean cell (see e.g., discussion in *Naveira Garabato et al.* [2009]). The clearest illustration  
1038 of a perturbation to the overturning circulation associated with wind-forced changes in  
1039 the Eulerian-mean and eddy-induced flows in the Drake Passage region may be found in  
1040 the 2-year period following the winter of 1998 / 99. During that winter, anomalously  
1041 strong upfront winds led to a striking arrest in the formation of AAIW (which ceased to  
1042 be ventilated for 1-2 years, as evidenced by its anomalously warm and salty character  
1043 between 1998 and 2000) and a transitory shift in the formation mechanism of SAMW  
1044 (which was ventilated by a strong Ekman transport of Antarctic surface waters from the  
1045 south, as manifested in its anomalously cold and fresh character in the same period). The  
1046 dynamics underpinning these changes in mode and intermediate water subduction are  
1047 discussed in more detail by *Naveira Garabato et al.* [2009].

1048

1049 The AABW found in Drake Passage is a recently-ventilated variety of the water mass that  
1050 leaves the Weddell Sea through clefts in the South Scotia Ridge and flows westward in a  
1051 deep boundary current at the southern edge of the Scotia Sea [*Gordon et al.*, 2001;  
1052 *Naveira Garabato et al.*, 2002b]. Significant variation in AABW properties and transports  
1053 within the Weddell Sea has been observed, on timescales from seasonal to interannual  
1054 and beyond [*Fahrbach et al.*, 2004; *Gordon et al.*, 2010; *Robertson et al.*, 2002], though the  
1055 absence of a clearly-defined decadal trend in AABW temperatures in the Weddell Sea  
1056 seemingly conflicts with observations of significant AABW warming along the length of  
1057 the Atlantic [*Johnson and Doney*, 2006; *Johnson et al.*, 2008; *Meredith et al.*, 2008].  
1058 Consequently, much attention has focused on understanding the processes that control  
1059 the properties and flux of AABW as it exits the Weddell Sea, and Drake Passage  
1060 hydrographic data have proved valuable in this context.

1061

1062 A time series of Drake Passage AABW properties between 1993 and 2008 (Figure 15)  
1063 shows significant variability, although the characteristic time scale of the measured  
1064 changes is believed to be shorter than 1 year, and thus some level of aliasing must occur  
1065 [*Jullion et al.*, 2010]. Notwithstanding this, the time series in Figure 15 is useful in  
1066 elucidating the controls of the properties of the AABW exported from the Weddell Sea.  
1067 This is demonstrated by Figure 16, which displays the correlation between the  $\theta$  of AABW  
1068 and the zonal wind stress over the Southern Ocean. High positive correlations occur over  
1069 the northern limb of the Weddell gyre with a lag of  $\sim$ 5 months, suggesting that instances

1070 of stronger (weaker) wind forcing of the gyre lead to warmer (colder) AABW in Drake  
1071 Passage a few months later. Examination of mooring records in the region further shows  
1072 that fluctuations in wind forcing and AABW temperature occur in synchrony with  
1073 variations in AABW outflow speed, with an association of anomalously strong winds and  
1074 positive anomalies in AABW flow [Meredith *et al.*, 2011]. These findings are consistent  
1075 with (and expand upon) the ‘Weddell gyre intensity’ hypothesis [Meredith *et al.*, 2008], in  
1076 which baroclinic adjustment of the gyre to changes in wind stress curl results in  
1077 variations in the density horizon (and therefore  $\theta$  and  $S$ ) of the AABW overflowing the  
1078 South Scotia Ridge, though they emphasize more the significance of local winds and  
1079 processes within the vicinity of the South Scotia Ridge. Wind stress fluctuations along this  
1080 ridge and over the broader Weddell gyre have been shown to respond substantially to  
1081 changes in the SAM [Jullion *et al.*, 2010] suggesting that this coupled mode of climate  
1082 variability may exert a significant influence on the properties and flux of the AABW  
1083 escaping the Weddell Sea.

1084  
1085 Overall, the time series of hydrographic measurements in Drake Passage lends an  
1086 important new perspective to the problem of modern global ocean climate change. On  
1087 one hand, it suggests that the interdecadal freshening of SAMW and AAIW observed  
1088 widely across the subtropical oceans since the 1960s [Bindoff *et al.*, 2007] may have  
1089 distinctly different origins, and that the concurrent AABW warming measured across  
1090 much of the Atlantic Ocean [Johnson and Doney, 2006; Meredith *et al.*, 2008] may have  
1091 been caused by wind-driven changes in AABW export rather than modified source water  
1092 properties. On the other hand, it reveals that the major modes of atmospheric variability  
1093 play a key role in driving ocean climate evolution, and that this forcing occurs on  
1094 surprisingly short time scales (of several months, even at abyssal depths). It was only via  
1095 the sustained, systematic observation of the full depth ocean that these findings were  
1096 obtainable.

1097  
1098 **4) Observational programs implemented since WOCE**  
1099

1100 A legacy of WOCE is the global oceanographic dataset that was collected under its  
1101 auspices. WOCE raised awareness of the importance of implementing a sustained global  
1102 ocean observing system (GOOS) in order to describe and understand the physical  
1103 processes responsible for climate variability and to extend the range and accuracy of

prediction on time scales from seasonal to decadal. A number of its programmes such as repeat hydrography have continued under its immediate successor, CLIVAR (Climate Variability and Prediction). Under the umbrella of GOOS, a scientific rationale and strategy for a Southern Ocean Observing System (SOOS; <http://www.scar.org/soos/>) has been proposed with recommendation for continued choke point monitoring [*Rintoul et al., 2010*]. The 2007-2009 International Polar Year (IPY) provided a timely stimulus to the SOOS planning. Although IPY was the fourth polar year of its kind (following those in 1882-3, 1932-3 and 1957-8) it was the first during which the Southern Ocean was measured in a truly comprehensive way, and it carried out some of the central observational elements proposed for the SOOS.

In this section, we focus on new sustained observational programmes begun in Drake Passage since the end of WOCE. These include the U.S. Drake Passage repeat XBT/ADCP line, the U.S. IPY cDrake array of Current and Pressure Recording Inverted Echo Sounders (CPIES), the French DRAKE program and mooring line, and the U.K./U.S. DIMES programme.

#### 4.1) Drake Passage XBT/ADCP repeat line

Year-round monitoring of upper-ocean temperature variability in Drake Passage was begun in 1996 through repeat expendable bathythermograph (XBT) surveys from the United States' Antarctic supply vessel. The XBTs are dropped at intervals of 5 to 15 km spacing (closest spacing across the Subantarctic and Polar Fronts) between the 200-m isobaths at either side of Drake Passage on approximately 6 crossings per year [*Sprintall, 2003*]. The three most frequently repeated tracks are shown in Figure 3d. The XBT probes consistently return water temperatures down to 850 m, with 1-m depth bins. Sampling has expanded in recent years to include expendable CTD (XCTD) probes; twelve XCTDs are deployed at intervals of 25 to 50 km and measure temperature and salinity to around 1000 m. XBT temperature profiles are combined with historical hydrography and XCTDs to calculate salinity profiles.

Continuous upper ocean current profiling from a hull-mounted 150 kHz shipboard acoustic Doppler current profiler (ADCP) was added in September 1999; a second 38 kHz ADCP was added in late 2004. The 150 kHz ADCP provides velocity measurements at 8-m

1138 vertical resolution over a 300-m depth range. The 38kHz ADCP provides velocity  
1139 measurements at 24-m vertical resolution over a 1000-m depth range. Measurements of  
1140 the atmospheric partial pressure of CO<sub>2</sub> (pCO<sub>2</sub>) and dissolved CO<sub>2</sub> in the surface waters  
1141 were added in 2003. The underway ADCP and pCO<sub>2</sub> observations are made on all  
1142 crossings (about 20 per year); the dissolved CO<sub>2</sub> surface sampling is limited to the 6 XBT  
1143 transects.

1144

#### 1145 **4.1.1) Defining ACC streamlines in Drake Passage**

1146

1147 While the ISOS picture of a banded frontal structure has proved to be a robust description  
1148 of the mean ACC, higher resolution measurements from ships and satellites [e.g. *Hughes*  
1149 and *Ash*, 2001; *Sokolov and Rintoul*, 2007] have shown that the frontal structure is more  
1150 complex than earlier sampling suggested. At high temporal and spatial resolution, the  
1151 principal ACC fronts comprise multiple filaments that subsequently merge and diverge  
1152 along the circumpolar path of the current. The multiple filaments exhibit substantial  
1153 persistence in space and time, with as many as eight or nine identified in the wide  
1154 chokepoint south of Tasmania [*Sokolov and Rintoul*, 2007]. Multiple filaments of the SAF,  
1155 PF and Southern ACC Front (SACCF) upstream of Drake Passage converge into three main  
1156 frontal jets as they enter its narrowest horizontal constriction. High resolution sampling  
1157 identifies the mean positions of the SAF and PF about 50 km north of their climatological  
1158 positions [*Lenn et al.*, 2007; *Orsi et al.*, 1995]. The apparent northward displacement of  
1159 the means is likely due to uncertainty in determining front locations from the coarser  
1160 sampling (~50 km spacing) characteristic of the earlier period. While the Drake Passage  
1161 mean ACC is dominated by three frontal jets, consistent with *Nowlin et al.* [1977], the  
1162 variability is dominated by mesoscale eddies and meanders of the fronts, with smaller  
1163 contributions from inertial currents and the baroclinic tide. Horizontal wavenumber  
1164 spectra of ocean currents are consistent with aspects of geostrophic turbulence [*Lenn et*  
1165 *al.*, 2007]. Along the repeat XBT/ADCP line, EKE is concentrated in northern Drake  
1166 Passage between the SAF and PF. This contrasts with the distribution observed along  
1167 SR1b, downstream of the Shackleton Fracture Zone, where mesoscale variance increases  
1168 to the south. The DRAKE moorings sample both these local maxima in mesoscale  
1169 variability (Figure 3d).

1170

1171 A geostrophic streamfunction estimated from objective analysis of the mean ADCP  
1172 currents and altimetry [Lenn *et al.*, 2008] improves on the resolution of the ACC fronts  
1173 observed in recent climatologies [Maximenko and Niiler, 2005; Olbers *et al.*, 1992].  
1174 Although the means are from different time periods (Figure 17), interannual variability  
1175 estimated from differences in mean sea-level anomalies for the respective periods do not  
1176 account for the differences [Lenn *et al.*, 2008]. A total height change of about 140 cm  
1177 across the ACC is comparable between the ADCP-based mean streamfunction and the  
1178 highest resolution climatology examined [Maximenko and Niiler, 2005]. However, the  
1179 ADCP streamfunction better resolves the banded structure of the ACC, with narrower jets  
1180 associated with the ACC fronts separated by quiescent zones of much weaker flow  
1181 (Figure 17). Using the ADCP streamfunction together with sea level anomalies, distinct  
1182 streamlines associated with particular ACC fronts can be identified and are tracked in  
1183 time-dependent maps of dynamic height [Lenn *et al.*, 2008]. Varying degrees of  
1184 topographic control can be observed in the preferred paths of the mean fronts through  
1185 Drake Passage. These streamlines define a natural coordinate system for the ACC in  
1186 Drake Passage.

1187

#### 1188 **4.1.2) Seasonal to interannual variability of temperature**

1189

1190 One-time hydrographic CTD transects, such as undertaken during WOCE, provide  
1191 snapshots of the top-to-bottom mass and property transports. In the eddy-populated  
1192 Southern Ocean, however, there are questions regarding the representativeness of single  
1193 hydrographic sections with station spacing of  $\sim$ 50 km for estimation of the mean state of  
1194 the ocean; additionally, they cannot easily be used to address questions of seasonal to  
1195 interannual variability. In contrast, the broad-scale sampling of the profiling float array  
1196 has provided information on the long-term changing heat content of the Southern Ocean  
1197 [Gille, 2002; 2008], but these data do not adequately sample the strong jets, fronts and  
1198 eddies that require finer resolution. The high-resolution XBT/XCTD sampling is a hybrid  
1199 of these sampling strategies, with an eddy-resolving station spacing of 0(5-15 km) and a  
1200 short crossing time (2.5 days) making the survey closer to a true snapshot. Beyond single  
1201 transects, the Drake Passage XBT/XCTD program samples in the time domain. The long-  
1202 term, spatially coherent nature of the XBT/XCTD sampling programme enables detailed  
1203 studies of statistics, structures and features in the seasonal to interannual variability of

1204 the upper ocean water masses in Drake Passage that are not possible using other  
1205 sampling modes.

1206

1207 The relatively dense sampling of the XBT transect was designed to capture the mesoscale  
1208 features and frontal systems in Drake Passage. The position of the PF defined as the  
1209 northern extent of the 2°C isotherm at 200 m depth [Botnikov, 1963] is also associated  
1210 with a strong velocity jet and a large increase in surface (0-250 m) transport [Lenn *et al.*,  
1211 2007]. The sharp temperature gradient across the PF is frequently resolved within just 2-  
1212 3 XBT profiles. The PF has the strongest temporal variability within Drake Passage with a  
1213 standard deviation of ~2°C in the upper 75 m of Drake Passage and is generally located  
1214 between 58° and 59°S (Figure 18). The closely spaced XBT profiles show the isotherms  
1215 are near vertical in the PF from the surface to ~300-m depth during austral winter, but  
1216 weaken in summer due to surface heating. South of the PF, cold (<0°C) AASW is found in  
1217 the upper 150 m during winter, and is capped by surface heating in spring and summer  
1218 that traps a well-defined temperature-minimum layer. Below the AASW lies the Upper  
1219 CDW that is characterized by temperatures of ~2°C and is strongly homogenous,  
1220 although there is a weak temperature maximum found at ~400-600 m depth. The Upper  
1221 CDW has the lowest temperature variability of all water masses found in the Drake  
1222 Passage XBT sections (Figure 18). The largest temperature variability occurs north of the  
1223 PF, and is associated with mesoscale variations from meanders and eddies. In this region  
1224 of Drake Passage, eddies are predominantly found north of the PF [Sprintall, 2003], and  
1225 estimates of EKE from the direct ADCP velocity measurements and altimetry are elevated  
1226 there [Lenn *et al.*, 2007].

1227

1228 Distinct differences are also found north and south of the PF in long-term trends and  
1229 interannual variability of the upper ocean temperature from 1969 to 2004 in Drake  
1230 Passage [Sprintall, 2008]. North of the PF, statistically significant warming trends of ~  
1231 0.02°C yr<sup>-1</sup> are observed that are largely depth independent between 100-700 m. A  
1232 statistically significant cooling trend of -0.07°C yr<sup>-1</sup> is observed at the surface south of the  
1233 PF, which is smaller (-0.04°C yr<sup>-1</sup>) but still significant when possible seasonal sampling  
1234 biases are accounted for. The observed annual temperature anomalies are highly  
1235 correlated with variability in sea-ice, and also with the SAM and ENSO climate indices.  
1236 The temperature trends are largely consistent with a poleward shift of the PF due to a  
1237 strengthening and southward shift of the westerly winds in the Southern Ocean, which is

1238 shown by models to be associated with the increasing positive polarity of the Southern  
1239 Annular Mode [*Hall and Visbeck*, 2002; *Oke and England*, 2004; *Thompson and Solomon*,  
1240 2002]. In *Sprintall* [2008], a complete 36-year time series of the PF position in Drake  
1241 Passage was not sufficiently well-resolved, primarily because the available individual  
1242 data from the historical archives were not necessarily part of a complete transect across  
1243 the passage. In addition, the coarser ~50 km station spacing of the historical transects  
1244 made the determination of the PF problematic. However, the time series of the PF  
1245 location determined from 13 years of the high-resolution Drake Passage XBT  
1246 temperature measurements suggests a poleward trend of ~40 km/decade, consistent  
1247 with that suggested by the models. No significant trend is evident in the SAF, which in  
1248 Drake Passage is located in the very north of the passage. We note here the apparent  
1249 conflict with the results from the WOCE SR1b CTD stations, which indicate a bipolar  
1250 position of the PF at that line and no significant trend in its position (see Section 3 above;  
1251 also *King and Jullion* [2011]). The SR1b results are independent of which definition of PF  
1252 location is used (transport maximum or thermohaline criterion), thus the apparent  
1253 difference cannot be due to different concepts of what determines the PF. Consequently,  
1254 it appears most likely that the different locations of the sections are responsible, with the  
1255 SR1b CTD stations being conducted further east in Drake Passage compared with the XBT  
1256 transects. It is possible that topographic effects play a role in constraining the location of  
1257 the PF on SR1b, lying as it does just east of the Shackleton Fracture Zone.

1258

1259 **4.1.3) Eddy momentum and heat fluxes**

1260

1261 Mesoscale eddies are ubiquitous within the Southern Ocean and have long been thought  
1262 to be the mechanism for fluxing heat poleward while transmitting wind momentum  
1263 downward through the water column [*Bryden*, 1979; *Johnson and Bryden*, 1989; *Olbers*,  
1264 1998]. However, the proposed link between the Southern Ocean momentum balance and  
1265 overturning circulation, via an interfacial form stress dependent on the eddy heat flux  
1266 [*Johnson and Bryden*, 1989], has been challenging to assess. Confirmation requires  
1267 observations of sufficient duration and temporal and spatial resolution so that the  
1268 divergence of the eddy fluxes can be estimated with statistical significance. While Drake  
1269 Passage is one of a few Southern Ocean regions in which moored observations have  
1270 yielded consistently poleward eddy heat flux estimates, these vary widely with depth and  
1271 are sensitive to the record length used [*Bryden*, 1979; *Johnson and Bryden*, 1989;

1272 *Sciremammano*, 1979]. An ISOS-inferred interfacial form stress suggested a downward  
1273 transfer of momentum that exceeded the surface wind stress in Drake Passage [Johnson  
1274 and Bryden, 1989]. South of Tasmania, where other moored observations have provided  
1275 the necessary vertical resolution, the interfacial form stress was found to be of roughly  
1276 equal magnitude to the surface wind stress [Phillips and Rintoul, 2000]. Estimates of eddy  
1277 momentum fluxes have likewise proved spatially inhomogeneous, resulting in small  
1278 lateral gradients of varying sign [Gille, 2003; Hughes and Ash, 2001; Morrow et al., 1994].  
1279

1280 The long-term nature and high spatial resolution of the XBT/ADCP sampling enables an  
1281 evaluation of the contribution of the eddy momentum and heat fluxes to the ACC  
1282 momentum balance in the upper 250-m of Drake Passage. Using seven years of  
1283 observations, Lenn et al. [2011] averaged gridded eddy flux estimates along mean ACC  
1284 streamlines to form time-mean vertical cross-stream sections of eddy momentum and  
1285 heat fluxes. Statistically significant stream-averaged cross-stream eddy momentum fluxes  
1286 confirm that the eddies exchange momentum with the mean SAF and PF, acting to  
1287 strengthen and sharpen the fronts over the observed depth range while decelerating the  
1288 flow in the interfrontal zones. The XBT/ADCP observations resolve large poleward eddy  
1289 heat fluxes of up to -290 kW/m<sup>2</sup> in the near-surface layer of the PF and SACCF, exceeding  
1290 deep moored estimates by an order of magnitude. Interfacial form stress could only be  
1291 calculated in the SAF. It varied little with depth between 100 m (the Ekman depth) and  
1292 250 m and was in approximate balance with the surface wind stress. Its vertical  
1293 divergence, estimated over the depth range 100-250 m was about an order of magnitude  
1294 greater than the eddy momentum forcing.  
1295

#### 1296 **4.1.4) Characteristics of the Southern Ocean Ekman layer**

1297 Wind-driven Ekman currents have been difficult to observe directly because, even when  
1298 forced by strong winds as in the Southern Ocean, their magnitudes are small compared to  
1299 the background geostrophic circulation. Therefore, despite their importance, Ekman  
1300 currents are usually inferred from the wind using classical Ekman theory. Without direct  
1301 measurement of the vertical profile of Ekman currents, accurate predictions of the Ekman  
1302 layer depth, mean temperature, eddy viscosity and associated Ekman layer heat fluxes  
1303 cannot be made. In Drake Passage, repeated upper-ocean current profiling has resolved  
1304 the characteristics of the mean Ekman layer [Lenn and Chereskin, 2009]. Mean Ekman  
1305

1306 currents decay in amplitude and rotate anticyclonically with depth, penetrating to 100 m,  
1307 above the base of the annual mean mixed layer at 120 m. Transport estimated from the  
1308 observed currents is mostly equatorward and in good agreement with the Ekman  
1309 transport computed from wind. Since the Ekman layer is shallower than the mixed layer,  
1310 the mixed layer temperature together with Ekman transport inferred from the wind can  
1311 be used to estimate the Ekman heat flux contribution to the shallow upper cell of the  
1312 meridional overturning circulation [Deacon, 1937; Speer *et al.*, 2000]. Turbulent eddy  
1313 viscosities estimated from the time-averaged stress are  $O(100\text{-}1000 \text{ m}^2\text{s}^{-1})$  and decrease  
1314 in magnitude with depth.

1315

#### 1316 **4.1.5) Patterns of small-scale mixing inferred from XCTDs**

1317

1318 Mixing rates in the Southern Ocean remain poorly constrained primarily because few  
1319 direct observations exist in the region, and this has led to different views concerning how  
1320 mixing should be incorporated into models of the Southern Ocean meridional circulation.  
1321 Southern Ocean observational mixing studies have often focused on abyssal mixing  
1322 processes, and although they clearly show that mixing is intense and widespread, it is  
1323 characterized by spatial intermittency [e.g. Heywood *et al.*, 2002; Naveira Garabato *et al.*,  
1324 2004]. None of these studies have addressed the temporal variability of the mixing  
1325 events. Thompson *et al.* [2007] used the time series of XCTD temperature and salinity  
1326 data collected in Drake Passage to diagnose the mean and seasonal upper-ocean  
1327 diapycnal eddy diffusivities with a view towards understanding what processes dominate  
1328 upper-ocean mixing in the Southern Ocean. Patterns of turbulent diffusivity were inferred  
1329 from density/temperature inversions using Thorpe scale techniques [Dillon, 1982], and  
1330 independently from vertical strain spectra. As for other properties in Drake Passage, the  
1331 PF separates two dynamically different regions. In the upper 400 m, turbulent  
1332 diffusivities are higher north of the PF (of order  $10^{-3} \text{ m}^2 \text{s}^{-1}$ ) compared with south of the  
1333 PF (of order  $10^{-4} \text{ m}^2 \text{s}^{-1}$  or smaller), and this meridional pattern corresponds to local  
1334 maxima and minima in both wind stress and wind stress variance [Thompson *et al.*,  
1335 2007]. The near-surface diffusivities are also larger during winter months north of the PF.  
1336 Below 400 m, diffusivities typically exceed  $10^{-4} \text{ m}^2 \text{s}^{-1}$ . Diffusivities decay weakly with  
1337 depth north of the PF, whereas south of the PF diffusivities increase with depth and peak  
1338 near the local temperature maximum. Thompson *et al.* [2007] suggest wind-driven near-  
1339 inertial waves, strong mesoscale activity and double-diffusive convection as possible

1340 mechanisms that could give rise to these elevated mixing rates and the observed spatial  
1341 patterns.

1342

1343 **4.1.6) Seasonal to interannual variability of ADCP backscatter**

1344

1345 Evidence suggests that the west Antarctic Peninsula region has warmed every decade for  
1346 the last half century, affecting populations from penguins to krill [Loeb *et al.*, 1997;  
1347 Meredith and King, 2005; Schofield *et al.*, 2010]. Monitoring Antarctic krill distribution is  
1348 of particular interest since krill are a major source of food for higher predators, and their  
1349 dominance represents a potential source of instability in the ecosystem. Intensive  
1350 sampling of zooplankton assemblages in Drake Passage has thus focused on krill  
1351 spawning habitat, located primarily in the coastal waters adjacent to the Antarctic  
1352 Peninsula and South Shetland Islands, with sampling limited to the ice-free spring and  
1353 summer months [e.g. Hewitt *et al.*, 2003]. North of the SACC, the Discovery Expeditions  
1354 [Mackintosh, 1934] remain the best comprehensive reference for zooplankton taxa  
1355 throughout much of Drake Passage.

1356

1357 Quantifying krill populations is challenging due to patchiness in their spatial distribution.  
1358 The ADCP backscatter, while not calibrated absolutely, has been shown to be strongly  
1359 correlated with the biomass of planktivores [e.g. Zhou *et al.*, 1994]. While the ADCP  
1360 backscatter amplitude is not calibrated against net tows, it is calibrated from bottom  
1361 echoes along a repeated transect of the Patagonian shelf. The long-term and highly  
1362 spatially-resolved nature of the ADCP sampling provides a valuable estimate of the space-  
1363 time variability of backscatter and inferred biomass [Chereskin and Tarling, 2007]. Depth-  
1364 averaged backscatter strength shows a well-defined seasonal cycle, with a peak in  
1365 summer and a trough in winter, consistent with seasonal changes in planktivore  
1366 populations. The time series resolves interannual variations in spring transition that can  
1367 be aliased by seasonal sampling. There is a trend in backscatter strength across the PF,  
1368 with higher values in northern Drake Passage, in agreement with patterns observed in  
1369 net tows of the Discovery Expedition [Mackintosh, 1934]. South of the SACC, both  
1370 planktivores and backscatter have declined over a six year period (1999-2006),  
1371 coincident with a decline in the populations of planktivorous higher-predators (e.g.  
1372 Adelie penguins) in nearby islands [Forcada *et al.*, 2006]. The backscatter time series

1373 provides a useful guideline for future, dedicated studies examining the response of the  
1374 zooplankton community to recent warming trends in the surface waters of this region as  
1375 well as the changing ice dynamics [Vaughan *et al.*, 2003].

1376

## 1377 **4.2) The DRAKE project**

### 1378 **4.2.1) Experimental aims and design**

1379

1380 The DRAKE project is a recently concluded experiment consisting of *in situ*  
1381 measurements made over a period of about 3 years (February 2006 to April 2009), which  
1382 are tightly coupled to satellite altimetry (TOPEX/POSEIDON and Jason-1). The  
1383 measurement array consisted of 10 subsurface current meter moorings deployed below  
1384 Jason track 104, with individual moorings located at altimeter crossover points (Figure  
1385 3d). A total of 5 full-depth hydrographic sections were occupied on the R/V Polarstern  
1386 cruises that serviced the moorings [Provost *et al.*, 2011]. Early results from analyses of  
1387 satellite data and the hydrographic data are summarized below, while the time series  
1388 from the moorings are still preliminary.

1389

### 1390 **4.2.2) Early DRAKE results**

1391

1392 Altimetric time-series were used to document the long-term trends in sea surface height,  
1393 the recurrence of major frontal meanders and statistical links between them [Barré *et al.*,  
1394 2011]. Trends are not homogeneous in Drake Passage; for example, a strong positive  
1395 trend between the Phoenix Antarctic Ridge (PAR) and the Shackleton Fracture Zone (SFZ)  
1396 is consistent with a southward shift of the PF there, in agreement with the observations  
1397 along the XBT/ADCP repeat tracks (Figure 19). The trend changes sign in the adjacent  
1398 Yaghan Basin, however, suggesting a regional effect caused by the complicated  
1399 bathymetry and geometry. Topography favors the recurrence of some meanders and  
1400 eddies in specific spots in Drake Passage. For example a dipole occurring with a close to  
1401 annual periodicity is observed at the entrance to Drake Passage over the PAR and  
1402 corresponds to adjacent meanders of the SAF and PF [Barré *et al.*, 2011 and Figure 20].  
1403 An anticyclonic meander of the PF was found to recur over the Ona sea floor depression  
1404 to the northwest of the Ona Basin ( $54^{\circ}\text{W}$ ,  $58^{\circ}\text{S}$ ) and constitutes an important element of  
1405 the cyclonic recirculation in the Ona Basin [Barré *et al.*, 2008].

1406

1407 Barré *et al.* [2011] used isolines of absolute dynamic topography from satellite altimetry  
1408 data to map out locations of fronts and eddies, providing a temporal and spatial context  
1409 for the 2006 DRAKE mooring deployment cruise (ANT-XXIII/3, January–February 2006).  
1410 Eight fronts were identified from local maxima in SSH gradients and associated with SSH  
1411 values. Consistent with Lenn *et al.* [2008], the multiple branches of the ACC fronts were  
1412 observed to merge into single jets in the narrowest part of the passage, with two  
1413 branches of the SAF merging at about 61°W and three branches of the PF merging over  
1414 the SFZ. The SACC branches could also be traced using altimetry, and a remarkable  
1415 agreement was found between the location of the frontal branches and eddies detected  
1416 by altimetry and the patterns observed in sea surface temperature and ocean color. The  
1417 crest of the SFZ was found to constitute a barrier in the south of Drake Passage, causing  
1418 the two SACC branches to separate by about 400 km, and creating sheltered conditions  
1419 in partial isolation from the ACC, while promoting an active recirculation region in the  
1420 Ona Basin. This recirculation, marked by cyclonic eddies carrying cold, fresh and  
1421 oxygenated water from south of the Southern Boundary of the ACC, causes effective  
1422 ventilation of the whole CDW density range [Provost *et al.*, 2011].

1423  
1424 In 2006 a highly-resolved (20-km station spacing) hydrographic/LADCP section under  
1425 Jason track 104 was occupied twice within 3 weeks, providing a unique opportunity to  
1426 document full depth in situ variability at about a 10-day interval. Between the two  
1427 occupations, the contributions of frontal meanders and eddies to the total volume  
1428 transport changed notably, although the net transport changed by only 10% and agreed  
1429 within confidence limits with prior WOCE and ISOS estimates [Renault *et al.*, 2011].  
1430 Encouragingly, estimates of total transport by two different methods agreed within  
1431 errors: a mean estimate of transport for the repeated section computed from LADCP  
1432 observations was  $142 \pm 9.7$  Sv, in good agreement with  $133 \pm 7$  Sv estimated from  
1433 geostrophic velocities referenced to full-depth LADCP profiles via least squares.

1434  
1435 Considerable differences in properties between the 10-day-apart sections are observed  
1436 throughout the whole water column with values as high as  $0.2^\circ\text{C}$  in temperature,  $0.01$  in  
1437 salinity,  $0.03 \text{ kg m}^{-3}$  in neutral density and  $10 \mu\text{mol kg}^{-1}$  in dissolved-oxygen  
1438 concentration found below a depth of 3000 m [Provost *et al.*, 2011; Sudre *et al.*, 2011].  
1439 Only part of the difference is attributable to frontal or eddy displacements along the  
1440 section. The other part results from the spatial heterogeneity of water properties

1441 upstream of the section and the funnelling of the flow due to the topographic constraints  
1442 of the SFZ. The considerable short-term differences in water properties in rather large-  
1443 scale structures that cannot be accounted for by frontal motions along the section points  
1444 to the need for highly-resolved measurements in both time and space in order to avoid  
1445 aliasing.

1446

#### 1447 **4.3) The cDrake experiment**

##### 1448 **4.3.1) Experimental aims and design**

1449

1450 cDrake is a field experiment to resolve the seasonal to interannual variability of the ACC  
1451 transport and dynamics over a four year period using bottom-moored Current and  
1452 Pressure-recording Inverted Echo Sounders (CPIES). The cDrake array (Figure 3d)  
1453 comprises a transport line of 21 CPIES spanning 800 km across the passage, and a local  
1454 dynamics array (LDA) of 21 CPIES spanning 120 km cross-stream and 240 km  
1455 downstream. The LDA is situated where surface variability observed by altimetry and  
1456 shipboard ADCP is a local maximum [Lenn *et al.*, 2007]. The goal for the transport line is  
1457 to determine the time-varying total ACC transport, its vertical structure partitioned  
1458 between barotropic and baroclinic components and its lateral structure partitioned  
1459 among the multiple ACC jets. The goal for the LDA is to make 4-D streamfunction maps  
1460 with mesoscale resolution in order to quantify the vertical transport of momentum in the  
1461 ACC from the surface to the sea floor, to describe the mesoscale eddy field and to quantify  
1462 eddy-mean flow interactions. The cDrake array was deployed during the 2007-2008  
1463 International Polar Year. Data is collected annually by acoustic telemetry to a ship, and  
1464 instrument recovery is planned for late 2011.

1465

1466 The pressure-recording inverted echo sounder (PIES) moored on the seafloor measures  
1467 bottom pressure and emits sound pulses to measure the round-trip travel times of these  
1468 pulses to the sea surface and back ( $\tau$ ). The CPIES includes a Doppler current sensor  
1469 tethered 50 m above it to measure the near-bottom current outside the benthic boundary  
1470 layer. The instrument internally processes data using typical post-processing techniques  
1471 and saves a daily mean value to a file that resides in the instrument. Internal processing  
1472 of pressure and current data ensures that tides are not aliased. Results described here are  
1473 based primarily on telemetered data and, when available, from the recovered records of  
1474 instruments that required replacement.

1475  
1476 Measurements of  $\tau$  from the IES are used to estimate full-water-column profiles of  
1477 temperature, salinity and density. These profiles are based upon historical hydrography  
1478 for the region, from which an empirical look-up table (the so-called gravest empirical  
1479 mode or GEM) is established to use as an index for vertical profiles of temperature,  
1480 salinity, and density. Through geostrophy, laterally separated pairs of these density  
1481 profiles yield vertical profiles of baroclinic velocity. The deep pressure and current  
1482 measurements provide the reference velocity to render the velocity profiles absolute.  
1483 Deep pressures are leveled by adjusting records to the same geopotential surface under  
1484 the assumption that long time-averages of near bottom currents and bottom pressures  
1485 are in geostrophic balance. These methods have been successful in many regions,  
1486 including the ACC [Meinen *et al.*, 2003; Watts *et al.*, 2001].

1487  
1488 **4.3.2) Early cDrake results**  
1489  
1490 The first year of daily-averaged currents measured at 50-m above bottom revealed  
1491 extremely large mean velocities in northern Drake Passage, exceeding  $10 \text{ cm s}^{-1}$  at 15  
1492 sites north of the PF, with mean directions that were not aligned with the surface fronts  
1493 (Figure 21 and Chereskin *et al.* [2009]). The large bottom currents suggest that bottom  
1494 friction may play a more significant role in the ACC momentum balance than previously  
1495 thought, at least locally. Topographic steering was most evident at the continental  
1496 margins. Deep EKE was maximum at about  $200 \text{ cm}^2 \text{ s}^{-2}$  between the SAF and PF,  
1497 coinciding with the location, but about one quarter of the value, of a maximum in surface  
1498 EKE [Chereskin *et al.*, 2009]. The LDA observations showed multiple high-speed current  
1499 events, with peak speeds of  $60\text{-}70 \text{ cm s}^{-1}$  and lasting 30 to 70 days, that were coherent  
1500 across sites separated by 45 km. These events corresponded to the spinup of deep eddies  
1501 coinciding with meanders in the surface fronts, consistent with deep cyclogenesis (Figure  
1502 21). A longer 2-year record is consistent with the first year results.

1503  
1504 Two-year bottom-pressure variance within the LDA was two times higher than variance  
1505 to the north and three times higher than variance to the south [Donohue *et al.*, 2011].  
1506 Bottom pressure in the LDA was strongly influenced by the meandering of the two  
1507 northern ACC fronts. Transport was sensitive to the choice of endpoints, particularly the  
1508 northern endpoint. A suite of reasonable calculations yielded barotropic transport

variability with standard deviations near 10 Sv. In all cases, large transport fluctuations, as high as 30 Sv, occurred over time scales of weeks to days. Ultimately a multiple-site average reduced local small-scale eddy variability at both the southern and northern end points and best described barotropic transport in Drake Passage. Neither time series by itself captured all the transport variability across the Passage. Within the frequency band 1/200 to 1/3 d<sup>-1</sup>, the northern (southern) time series explained about 44 (32) percent of the variance in transport. This is largely consistent with *Hughes et al.* [2003], who derived a correlation around 0.7 between south-side pressure and modeled total transport, indicating that around half the total transport variability could be captured by a single gauge. Coherence between northern and southern time series existed, and the phase relationship changed with frequency. To focus on large-scale bottom-pressure variability, empirical orthogonal functions were calculated for frequencies greater than 1/200 d<sup>-1</sup> within four bands. Two transport modes were identified that both correlated with the Antarctic Oscillation Index. In the 12-to-8-day band, a transport mode with spatial decay of 1/800 km<sup>-1</sup> existed with northern sites in phase with southern sites. In the 40-to-12-day band, a passage-wide transport mode has northern sites out of phase with southern sites. The broad scale of both modes suggests that in Drake Passage the southern Antarctic transport mode exists along f/H contours that are both blocked and unblocked.

The cDrake pressure and IES measurements show the relative contributions of the mass-loading and steric constituents of sea surface height anomaly (SSHA). Round-trip travel time measurements were converted to geopotential using historical hydrography [*Cutting, 2010*]. Geopotential was then divided by gravity to determine the steric component of SSHA. The mass-loading component of SSHA was computed by dividing the bottom pressure anomaly by the product of density and local gravity. In Drake Passage, the mass-loading and steric SSHA components are uncorrelated, except in the LDA at times when strong cyclogenesis occurs. Relative contributions of steric and mass-loading components varied along the transport line. North of 57°S, steric SSHA variance exceeded 60% of the total SSHA variance. South of 59°S, the mass-loading SSHA variance exceeded 40% of the total SSHA variance and in places reached 65% of the total variance. CPIES SSHA complements altimetric SSHA in several ways. First, the time series can quantify the aliasing of the SSHA signal from satellite altimeters. Based on the first year of cDrake estimates, the near-10-day repeat sampling (e.g., T/P, Jason-1, and Jason-2) likely leads to

1543 aliased variance that exceeds 20% of the total signal variance within the LDA and on the  
1544 southern end of the transport line south of 58°S. Second, bottom-pressure data  
1545 contributes to the validation of numerical models used to reduce the aliased variance in  
1546 the altimeter SSHA data set.

1547

#### 1548 **4.3.3) Ongoing cDrake investigations**

1549

1550 CPIES are an integrating measurement technique and offer a complementary view to  
1551 point current meter observations such as those made during ISOS and DRAKE. Whilst  
1552 point current meters have poor vertical resolution, CPIES are limited to geostrophic and  
1553 barotropic velocities, so future work to combine contemporaneous cDrake and DRAKE  
1554 observations during their overlap measurement period should yield a more complete  
1555 description of the vertical and horizontal structure of the ACC through exploitation of the  
1556 different sampling strengths.

1557

1558 cDrake observations will be used to assess aliasing in ongoing time series (e.g., altimetry,  
1559 XBTs) and to guide future monitoring systems. The cDrake observations will also provide  
1560 metrics for model validation. cDrake observations will be assimilated in the Southern  
1561 Ocean State Estimate (SOSE; [Mazloff *et al.*, 2010]). The initial fit of the observations with  
1562 the SOSE solution will provide information as to the uncertainty of dynamical estimates  
1563 drawn from the state estimate. In return, the SOSE will provide a framework for dynamic  
1564 interpolation useful in interpreting the observations.

1565

#### 1566 **4.4) The DIMES experiment**

1567

1568 The Diapycnal and Isopycnal Mixing Experiment in the Southern Ocean (DIMES) is an  
1569 international (U.K./U.S.), multi-cruise experiment seeking to obtain the first systematic  
1570 measurements of mixing processes in two contrasting regimes (the Southeast Pacific and  
1571 Southwest Atlantic) of the ACC centered around Drake Passage. The project is motivated  
1572 by the perceived acute sensitivity of the oceanic overturning circulation and a range of  
1573 important features of the wider climate system to the representation of mixing processes  
1574 in the Southern Ocean, and by the existence of seemingly conflicting observational clues  
1575 on the character and controlling dynamics of diapycnal and isopycnal mixing in the  
1576 region. For example, whereas much of the theoretical work on understanding the

1577 Southern Ocean overturning assumes weak diabaticity below the surface mixed layer  
1578 [e.g., *Marshall and Radko*, 2003; 2006], intense turbulent mixing has been suggested to  
1579 occur due to the breaking of internal waves generated by ACC flow over small-scale  
1580 topography [*Naveira Garabato et al.*, 2004; *Naveira Garabato et al.*, 2007; *Nikurashin and*  
1581 *Ferrari*, 2010]. Similarly, the structure of eddy-induced isopycnal stirring in the Southern  
1582 Ocean remains a matter of contention, with analyses of various observations suggesting  
1583 that it is either enhanced [e.g. *Sallée et al.*, 2008; *Waugh and Abraham*, 2008] or reduced  
1584 [e.g., *Ferrari and Nikurashin*, 2010; *Naveira-Garabato et al.*, 2011] at the core of the eddy-  
1585 rich ACC jets. Against this backdrop, DIMES seeks to test and, if necessary, redefine the  
1586 present paradigm of Southern Ocean mixing and how it shapes meridional overturning.  
1587

1588 In order to achieve this overarching goal, DIMES investigators are presently in the course  
1589 of obtaining multiple, concurrent measures of the rates of isopycnal and diapycnal mixing  
1590 and upwelling, and their underpinning physical processes, throughout the study region.  
1591 The focal element of the experiment is the spreading of a chemical tracer (trifluoromethyl  
1592 sulphur pentafluoride,  $\text{CF}_3\text{SF}_5$ ) that was released in the Upper CDW layer of the SE Pacific  
1593 zone of the ACC in January – February 2009, with which the spatially and temporally  
1594 averaged rates of mid-depth mixing and upwelling throughout the experimental domain  
1595 are being assessed. In order to measure diapycnal mixing at other depths and investigate  
1596 the physical processes driving it, full-depth profiles of oceanic microstructure are being  
1597 collected with three different free-falling profilers during five further austral summer  
1598 cruises, and finestructure profiles obtained year-round with EM-APEX floats within and  
1599 above the tracer cloud. Isopycnal stirring by mesoscale eddies is also being measured at  
1600 two different vertical levels by monitoring the dispersion of isopycnal RAFOS floats  
1601 deployed in clusters at various stages of the experiment and tracked acoustically using  
1602 moored sound sources. The dynamics regulating the coupling between mesoscale eddies  
1603 and internal waves are being studied with a sub-mesoscale cluster of 6 moorings  
1604 deployed in eastern Drake Passage between December 2009 and January 2012. This  
1605 portfolio of observations is being complemented by a range of inverse and numerical  
1606 modeling efforts that seek to optimize the methodology of the observational analyses,  
1607 investigate the controlling dynamics of the mixing processes under scrutiny, and assess  
1608 the sensitivity of large-scale overturning to those processes. The initial results of the  
1609 DIMES fieldwork reveal that the Southeast Pacific sector hosts remarkably weak

1610 turbulent diapycnal mixing at mid-depth [Ledwell *et al.*, 2011]. The fieldwork phase of the  
1611 experiment is due to conclude in the austral summer of 2013 / 14.

1612

1613 **5) Discussion and Conclusions**

1614

1615 Because of its long history of sustained measurements, Drake Passage is the best-  
1616 observed region of the Southern Ocean, and arguably the best understood. Indeed, it  
1617 stands as one of the most comprehensively monitored continent-to-continent sections in  
1618 the world. Scientific progress here since the early hydrographic sections and the days of  
1619 ISOS has been profound. In particular, the sustained nature of the measurement  
1620 programmes at Drake Passage has enabled some particular insights to be made that  
1621 would not have been possible without such targeted, long-term measurements. These  
1622 include (but are certainly not limited to):-

1623

1624 • Quantification of the transport fluctuations at sub-annual periods, leading to an  
1625 understanding of the wind-forcing of such fluctuations and their dynamical  
1626 interaction with topography.

1627

1628 • A realization that the ACC transport is remarkably steady on interannual and longer  
1629 timescales relative to much larger proportional changes in the overlying winds, and a  
1630 growing understanding of the mesoscale processes and feedbacks responsible for  
1631 this.

1632

1633 • Recognition of the role of coupled climate modes in dictating the horizontal  
1634 transport, and the role of anthropogenic processes in this.

1635

1636 • Identification of changes in properties of water masses relevant to both the upper  
1637 and lower limbs of the overturning circulation in the Southern Ocean, and an  
1638 understanding of the dynamics and climatic processes responsible for these, as well  
1639 as their impacts.

1640

1641 • Realisation of the pivotal role of Southern Ocean eddies in setting the ACC transport  
1642 through Drake Passage, the residual overturning circulation across the ACC, and the  
1643 global stratification.

1644  
1645 The sustained monitoring programmes that generated these advances in understanding  
1646 of the Southern Ocean almost all chose Drake Passage primarily for logistical reasons, it  
1647 being the narrowest section that captures all of the ACC, and also a trade route for many  
1648 vessels travelling to and from the most populated part of Antarctica. However, it is  
1649 noteworthy that most of the major findings to have come from Drake Passage monitoring  
1650 have applicability and implications that extend well beyond providing a baseline  
1651 understanding of the oceanography of the Passage itself. For example, elucidation of the  
1652 dynamics behind the transport fluctuations is relevant to the ACC in all sectors of the  
1653 Southern Ocean, whilst the changes in the Southern Ocean overturning observed at Drake  
1654 Passage have implications for regional and even global climate via processes such as the  
1655 drawdown of anthropogenic carbon from the atmosphere. There is an implicit criterion  
1656 here – of producing results which have a significance that transcends the location of the  
1657 measurements – which is, in many ways, a critical test of the value of a sustained  
1658 monitoring programme. In this context, and against the background of what has been  
1659 learned at Drake Passage over the past several decades, it is worth asking whether the  
1660 monitoring efforts here should be continued, and if so why and how.

1661  
1662 With regard to determining the horizontal flow through Drake Passage and its variability,  
1663 a Devil's advocate might claim that this task has almost been completed. In particular,  
1664 given that the long-term transport appears to have been remarkably stable, with changes  
1665 in flow of around 5% of the mean on interannual timescales despite much larger relative  
1666 changes in wind stress, the argument could be advanced that future changes in transport  
1667 are also likely to be small (howsoever one defines "small"), and thus the need to monitor  
1668 them is less compelling. This argument is perhaps not without some merit, however the  
1669 counterpoint is that the dynamics that control the transport variability on interannual  
1670 and longer periods (and that are responsible for it being small) are still imperfectly  
1671 known. For example, the feedbacks between the mean flow, eddies and topography that  
1672 generate the observed lag between transport changes and changes in eddy intensity is a  
1673 topic deserving of further investigation. Coarse-resolution coupled climate models  
1674 represent such processes only very crudely, and if their depictions of the Southern Ocean  
1675 are to be improved, there is a need to improve dynamical understanding, and to test this  
1676 understanding with observations.

1677

1678 A related point that should be made is that the previously-recognised low level of  
1679 transport variability on interannual and decadal timescales does not, in fact, necessarily  
1680 imply that future changes will be equally small. In an inherently non-linear system, there  
1681 is the possibility of moving to a different dynamical regime, where horizontal flow  
1682 responds differently to forcing. For example, if it is accepted that the ACC is currently  
1683 close to an eddy-saturated state (where transport varies little with respect to winds, but  
1684 eddy intensity changes more), there is a question concerning what will happen if the  
1685 wind strength reduces significantly in future decades. Such a decrease in wind is  
1686 conceivable as recovery from the ozone hole progresses, and is predicted by a number of  
1687 climate models that include stratospheric ozone processes.

1688

1689 A further driver for sustaining the monitoring of the flow at Drake Passage is that the  
1690 measurements are increasingly seen as being key in the design of a system for monitoring  
1691 the overturning circulation in the South Atlantic (see  
1692 <http://www.aoml.noaa.gov/phod/SAMOC/> for details on the South Atlantic Meridional  
1693 Overturning Circulation initiative). In this context, the Drake Passage data provide the  
1694 boundary conditions for fluxes entering the Atlantic via the cold water path route. SAMOC  
1695 aims to monitor both this and the corresponding warm water path fluxes as functions of  
1696 time, as well as their impacts on the meridional overturning and gyre circulations in the  
1697 South Atlantic. This is also strongly connected with the emerging SOOS, which includes a  
1698 focus on ocean circulation and its role in climate, and also on the need for sustained  
1699 interdisciplinary measurements in the Southern Ocean in response to a variety of  
1700 strategic drivers.

1701

1702 Whilst Drake Passage monitoring was largely initiated to elucidate the characteristics of  
1703 the horizontal flow, numerous other important findings have emerged from the datasets  
1704 collected to date. Perhaps the most significant amongst these is the recognition of  
1705 changes in properties in both the upper and lower limbs of the Southern Ocean  
1706 overturning, i.e. changes in the AAIW and SAMW temperatures and salinities at the  
1707 location where these water masses enter the Atlantic, and changes in the AABW  
1708 properties as this water mass exits the Weddell Sea to become the abyssal layer of the  
1709 Atlantic circulation. Such changes are increasingly seen to be of global significance:  
1710 Southern Ocean overturning is a key process in modulating the concentrations of  
1711 atmospheric CO<sub>2</sub>, including the anthropogenic component, and the sequestration of this

1712 CO<sub>2</sub> in the region of the ACC is one of the reasons why this area is particularly susceptible  
1713 to ocean acidification.

1714  
1715 Our judgement is thus that continuing the sustained measurements in Drake Passage is  
1716 important, though increasingly it is the measurements that relate to the three-  
1717 dimensional circulation of the Southern Ocean (and the dynamical controls thereon),  
1718 rather than just the horizontal flow, that are seen to be the most compelling strategic  
1719 drivers. If such monitoring is to be continued, the scientific community must challenge  
1720 itself to deliver the key measurements in the most strategic, cost-effective and  
1721 scientifically beneficial way. There is also the need to target the monitoring to be as  
1722 societally beneficial as possible, to justify its continuation against the pressures of  
1723 different nations' funding systems.

1724  
1725 In terms of a monitoring system capable of meeting these criteria, there are some  
1726 requirements that are already clearly established. Specifically there is a need for  
1727 sampling with a frequency that is sufficiently high to avoid aliasing of the short-period  
1728 variability when trying to determine long-period changes in transport, and there is also a  
1729 need for internal measurements of the water column from which to infer and attribute  
1730 changes in overturning. Satellite-based measurements of sea surface height (e.g. the  
1731 Jason series of altimeters) and of temporal and spatial variations in space gravity (GRACE  
1732 and GOCE) can add useful information, but cannot meet the requirements by themselves.  
1733 In practice, this means that a combination of ship-based hydrographic work and *in situ*  
1734 observations from coastal tide gauges, moorings and/or bottom lander systems will be  
1735 needed for the foreseeable future.

1736  
1737 There are aspects of existing and previous Drake Passage monitoring programmes that  
1738 are far from optimal. For example, chemical and biogeochemical tracers have only been  
1739 measured sporadically on Drake Passage sections, despite routine drawing of water  
1740 samples for salinity analysis. The Drake Passage monitoring effort should be developed to  
1741 incorporate some of the more compelling of such measurements, including regular full-  
1742 depth profiles of carbonate system parameters, dissolved oxygen, and so on.

1743  
1744 Further, it is very much the case that the current effort at Drake Passage has evolved  
1745 rather than being planned. Various nations are contributing very significantly, but their

efforts are not especially well-coordinated spatially, nor is there a particularly optimal use of resource (either human or technological). To some extent this is inevitable, and a direct consequence of the opportunistic nature of many of the measurements being made. Nonetheless, improved international strategic oversight and planning would be beneficial in maximizing the usefulness and cost-effectiveness of Drake Passage observations. This should be a key challenge to the newly-described SOOS.

It is worth recognizing that the effort currently expended at Drake Passage is close to the maximum that is likely to be sustainable for the future, in terms of both human and technical resources, especially with regard to ship-based hydrography, moorings and bottom landers. If substantially more data are required in the future, for example to provide the year-round and multi-year coverage needed to resolve the seasonal cycles and interannual variability of key properties such as heat flux, then new strategies and technologies will need to be brought to bear. Profiling floats have revolutionized our ability to obtain near real-time data from the Southern Ocean; however, the strong flow means that such floats tend to pass very rapidly through Drake Passage, and because they move generally parallel to streamlines they are of limited value for flux calculations. To make substantial progress would require the development and deployment of other new technologies, such as long-duration autonomous underwater vehicles (AUVs) and gliders capable of profiling to the seabed in Drake Passage, and capable of navigating autonomously in regions of rapid flow. Existing technologies such as bottom pressure measurement also need development, such that they provide well-calibrated long-term datasets with minimized drift and minimum requirements for maintenance and refurbishment.

Overall, Drake Passage stands as the region of the harsh, remote Southern Ocean from which the most data and understanding have been obtained. Many of the science drivers for sustained observations here remain strong and relevant, though these are evolving, and the measurements undertaken and the technologies used to obtain them need to evolve in parallel. The challenges are significant, but need to be addressed if the scientific and societal worth of the measurements are to remain demonstrable, and for the monitoring to be sustained into the future.

1778  
1779

1780 **Acknowledgements**

1781 The success of Southern Ocean monitoring at Drake Passage over many decades has been  
1782 due to the efforts of many hundreds of scientists, technicians, ships' officers, crew and  
1783 support staff. They are all thanked profusely. We also thank the attendees of a Drake  
1784 Passage workshop held in 2009 at the Proudman Oceanographic Laboratory (now  
1785 National Oceanography Centre, Liverpool), U.K., for many stimulating discussions and  
1786 useful thoughts. Robert Smith is thanked for helping with preparation of diagrams, and  
1787 the Editor, Martin Visbeck, John Marshall and an anonymous reviewer are thanked for  
1788 useful comments that helped improve the original manuscripts.

1789 **Tables**1790  
1791

|                            | No seasonal adjustment |        |        |       | With seasonal adjustment |        |        |       |
|----------------------------|------------------------|--------|--------|-------|--------------------------|--------|--------|-------|
|                            | min                    | mean   | max    | sd    | min                      | mean   | max    | std   |
| Volume (Sv)                | 126.3                  | 136.7  | 147.1  | 6.9   | 126.3                    | 136.7  | 147.1  | 6.9   |
| Potential Temperature (°C) | 2.05                   | 2.21   | 2.55   | 0.15  | 1.94                     | 2.15   | 2.24   | 0.07  |
| Practical Salinity         | 34.430                 | 34.444 | 34.464 | 0.009 | 34.434                   | 34.446 | 34.468 | 0.008 |

1792  
1793  
1794 **Table 1.** Minimum, mean, maximum and standard deviation of transports at Drake  
1795 Passage for the UK repeat hydrography cruises. Data are shown with and without  
1796 seasonal adjustment to 1 December of each season. There is no seasonal adjustment for  
1797 the volume transport so the numbers are unchanged. The potential temperature and  
1798 practical salinity are transport-weighted mean properties.

1799  
1800  
1801 **Figures**  
1802  
1803 **Figure 1.** Bathymetry and topography of the Southern Ocean and Antarctica. Marked  
1804 schematically is the Antarctic Circumpolar Current (ACC), here denoted by the  
1805 approximate positions of its main frontal features [Orsi *et al.*, 1995]. Drake Passage,  
1806 between South America and the Antarctic Peninsula, is the most significant choke  
1807 point for the ACC as it circumnavigates Antarctica.  
1808  
1809 **Figure 2:** Schematic diagram of the global overturning circulation, reproduced from  
1810 *Lumpkin and Speer* [2007]. The arrows indicate the net overturning circulation,  
1811 integrated across each ocean basin, with the numbers indicating the volume  
1812 transports of each water mass (Sv). The figure illustrates the critical role of the  
1813 Southern Ocean in connecting the overturning cells in each of the basins to the north.  
1814  
1815 **Figure 3.** Top left panel shows bathymetry of Drake Passage, and a schematic  
1816 depiction of the main frontal features, namely the Subantarctic Front (SAF), the Polar  
1817 Front (PF), the Southern ACC Front (SACCF) and the Southern Boundary (SB). Various  
1818 topographic features are also marked: Yaghan Basin (YB), Ona Basin (OB), Phoenix  
1819 Antarctic Ridge (PAR), Shackleton Fraction Zone (SFZ), West Scotia Ridge (WSR), Ona  
1820 Seafloor Depression (OSD). Top right panel shows the Drake Passage monitoring  
1821 system during the ISOS era: red circles denote current meter moorings; white circles  
1822 denote bottom pressure recorders (BPRs); occluded symbols are current meter  
1823 moorings with incomplete data return. Bottom left panel shows the Drake Passage  
1824 monitoring system during WOCE: blue circles denote BPRs; red lines denote WOCE  
1825 repeat hydrography lines SR1 (western line) and SR1b (eastern line). Bottom right  
1826 panel shows the contemporary monitoring system in Drake Passage: green lines  
1827 denote repeat XBT/ADCP lines; blue triangles denote the CPIES array; red squares  
1828 denote the DRAKE current meter array; black line denotes the SR1b repeat  
1829 hydrography line; black circles denote BPRs.  
1830

1831   **Figure 4a.** 1-year transport time series through Drake Passage from ISOS (redrawn  
1832   from *Whitworth*, 1983), showing the net transport (upper) and the baroclinic  
1833   transport of the top 2500 m (lower).

1834

1835   **Figure 4b.** Extended transport time series through Drake Passage from ISOS, redrawn  
1836   from *Whitworth and Peterson* [1985].

1837

1838   **Figure 4c.** Low-pass filtered zonally-averaged eastward wind stress and ISOS bottom  
1839   pressure and cross-passage pressure difference, after *Wearn and Baker* [1980].

1840

1841   **Figure 5(a)** Map showing the positions of tide gauges (white) and bottom pressure  
1842   recorders (black) for which long records are available. VF is Vernadsky/Faraday, DS is  
1843   Drake South (1000 m), Myr is Myrtle (2354 m), Si is Signy, Sa is Sanae, Sy is Syowa, Ma  
1844   is Mawson, Da is Davis, Ca is Casey, CR is Cape Roberts and SB is Scott Base.  
1845   Measurements for which a depth is not given are coastal. The 3000 m depth contour is  
1846   also shown. **(b)** Time series (from *Hibbert et al.* [2010]) of monthly mean bottom  
1847   pressures or inverse barometer corrected sea levels from the sites shown in (a). Each  
1848   time series has been detrended, and an annual sinusoid has been removed by least-  
1849   squares fitting. The Cape Roberts time series is a composite of data from Cape Roberts  
1850   and Scott Base.

1851

1852   **Figure 6.** Geometry of the Southern Mode, as shown by the correlation of monthly  
1853   mean values of bottom pressure in a barotropic model [*Hughes and Stepanov*, 2004]  
1854   with tide gauge data. The tide gauge time series is the average of those data available  
1855   (from Figure 9) at each time over the period 1992 to 1999. Annual cycles have been  
1856   removed from each time series before correlating. Contours show the  $f/H$  contours  
1857   which correspond to depths of 3000 m (black) and 4000 m (blue) at  $60^{\circ}\text{S}$ .

1858

1859   **Figure 7.** Annual-mean time series of (top) the SAM index, (middle) atmospheric-  
1860   pressure corrected sea level from the Faraday tide gauge, and (bottom) transport  
1861   through Drake Passage from the quarter-degree OCCAM model. Note significant anti-  
1862   correlation between the upper two traces, and the direct correlation between the  
1863   upper and lower tracers. These indicate that interannual changes in ACC transport

1864 through Drake Passage are forced by changes in the SAM, and are well-monitored by  
1865 sea level from the Faraday tide gauge. From *Meredith et al.* [2004].

1866

1867 **Figure 8.** (a) Trends in bottom pressure from the south Drake BPR during the 1990s,  
1868 displayed by month. (b) Monthly trends in the SAM over the same period, here  
1869 displayed inverted for comparison. Significant trends are displayed in red. The  
1870 similarity between the trends indicates modulation of the seasonal cycle in transport  
1871 through Drake Passage due to the changing seasonality of the SAM. From *Meredith et*  
1872 *al.* [2004].

1873

1874 **Figure 9.** Annual mean changes in Eddy Kinetic Energy (EKE) in different sectors of  
1875 the Southern Ocean, plotted alongside changes in the SAM index (light blue). Note the  
1876 circumpolar increase in EKE during 2000-2002, 2-3 years after an anomalous peak in  
1877 SAM. Redrawn from *Meredith and Hogg* [2006].

1878

1879 **Figure 10.** Cumulative transport across Drake Passage, accumulated south to north,  
1880 for the 15 UK repeat hydrography cruises. The PF is bimodal in location, with the five  
1881 'southern' years (1993/4, 1996/7, 2000/1, 2003/4 and 2006/7) marked as red lines,  
1882 an intermediate year (2005/6) marked in cyan, and 'northern' years marked in black.  
1883 From *King and Jullion* [2011].

1884

1885 **Figure 11.** Time series of transports at Drake Passage for the UK repeat hydrography  
1886 cruises. Upper panel (a): volume transport. Middle (b): transport-weighted mean  
1887 temperature. Lower (c): transport-weighted mean salinity. In (b) and (c), dashed lines  
1888 denote values calculated relative to the time of the cruises, and solid lines denote  
1889 values following seasonal adjustment to be made relative to 1 December. From *King*  
1890 *and Jullion* [2011].

1891

1892 **Figure 12.** Seasonal variation of transports at Drake Passage for UK repeat  
1893 hydrography cruises. Upper panel (a): volume transport. Middle (b): transport-  
1894 weighted mean temperature. Lower (c): transport-weighted mean salinity. Panel (a)  
1895 has no significant slope. Panels (b) and (c) show the least-squares best fit, used for  
1896 subsequent adjustment of the data. From *King and Jullion* [2011].

1897

1898   **Figure 13.** Schematic two-cell meridional overturning circulation in the Southern  
1899   Ocean (adapted from *Speer et al. [2000]*). Five observationally-based estimates of the  
1900   volume transports in different water mass classes at 30-40°S are superimposed.  
1901  
1902   **Figure 14.** Upper three panels show time series of potential temperature, salinity and  
1903   pressure in the Subantarctic Mode Water (SAMW) and Antarctic Intermediate Water  
1904   (AAIW) layers in Drake Passage. All variables show layer-mean values except pressure  
1905   for SAMW (left), which is the average value at the lower boundary of this water mass.  
1906   In 1998/99 for SAMW potential temperature and salinity, the red symbols indicate the  
1907   exceptional presence of a second SAMW mode (see *Naveira Garabato et al. [2009]* for  
1908   details). Error bars amalgamate systematic, standard and sampling errors as  
1909   estimated by *Naveira Garabato et al. [2009]*. Bottom panels show times series of  
1910   indices of three major modes of Southern Hemisphere climate variability: ENSO, SAM  
1911   and IPO.  
1912  
1913   **Figure 15.** Time series of potential temperature, salinity and neutral density of  
1914   Antarctic Bottom Water (AABW) on the WOCE SR1b section (Figure 3). Also shown  
1915   are 1-year low-pass filtered ENSO and SAM indices over the same period. From *Jullion*  
1916   *et al. [2010]*.  
1917  
1918   **Figure 16.** Spatial correlation at 5 months lag between zonal wind anomalies and the  
1919   potential temperature of AABW in Drake Passage (Figure 15). The black lines are the  
1920   90 and 95% significance limits. The marked zonality in the correlation field is strongly  
1921   indicative of the SAM. From *Jullion et al. [2010]*.  
1922  
1923   **Figure 17:** Streamlines (white) correspond to surface height; contour interval is 5 cm.  
1924   Streamlines from (Left:) the Southern Ocean Atlas dynamic topography relative to  
1925   2500 m [*Olbers et al., 1992*], (Center:) the mean dynamic ocean topography of  
1926   *Maximenko and Niiler [2005]* and (Right:) streamfunction derived from the  
1927   objectively-mapped ADCP mean currents by *Lenn et al. [2008]*. Bathymetry is shown  
1928   in grayscale with contours (black) drawn at 500-m intervals starting at 0 m. Adapted  
1929   from *Lenn et al. [2008]*.  
1930

1931   **Figure 18:** Upper: Mean (color) and standard deviation (white contours) of  
1932   temperature from 90 Drake Passage XBT transects. Typical XBT drop locations are  
1933   shown on the upper axis. Lower: As in upper panel but for January-March; April-June;  
1934   July-September; and October-December.

1935

1936   **Figure 19:** Linear trends in dynamic topography (mm per year) from January 1993 to  
1937   December 2009. The significance of the trend was computed using a two-sided  
1938   Student t-test with a confidence limit of 99%. Areas where the trend is not significant  
1939   are colored in green. White areas correspond to the regions where the time series are  
1940   incomplete, and the data from over the continental slope (depth less than 500 m) are  
1941   disregarded. Black contours represent the bathymetry between 4000 m and 1000 m  
1942   with contour intervals of 500 m. The black diagonal line indicates Jason track 104.  
1943   Black dashed lines represent repeat XBT/ADCP tracks from the US Antarctic supply  
1944   vessel (west of track 104) and the repeat hydrographic section SR1b (east of track  
1945   104). (Updated from Barré *et al.* [2011]).

1946

1947   **Figure 20:** **a** Time series of sea level anomaly (SLA) over a  $1^\circ \times 1^\circ$  box centered at  
1948    $68^\circ\text{W}$  and  $58.5^\circ\text{S}$  (location P1). The linear trend has been removed. The gray shading  
1949   represents one standard deviation. **b** Regression of SLA, in Drake Passage, on the  
1950   normalized time-series in Fig.3a. *Solid black contours* represent the correlation at the  
1951   90% confidence level; *dashed black contours* represent the 95% confidence level. The  
1952   regression map suggests that the strong anomaly (P1) on the western side of the PAR  
1953   can be associated with an anomaly of the opposite sign (N1) on the eastern side of the  
1954   PAR. Thin black lines are bathymetry isobaths (2000, 3000 and 4000 m). (Updated  
1955   from Barré *et al.* [2011])

1956

1957   **Figure 21:** cDrake bottom currents and pressures. Left panel: Record-length (1-year)  
1958   means and standard deviation ellipses for currents observed 50-m above bottom. Fifteen  
1959   sites have means in excess of 10 cm/s, all in northern Drake Passage. Mean directions do  
1960   not, in general, coincide with the mean fronts, shown here as gray lines from the Lenn *et al.*  
1961   [2008] streamline analysis. Right lower panel: Time series for 3 sites during the most  
1962   energetic cyclogenesis event (there were about 5 in a year) show a peak pressure anomaly  
1963   of 0.5 dbar; currents peak at 60 cm/s. Right upper panel: Pressure anomaly (dbar, color)

1964 where blues are low pressure and daily-mean currents on 24 Feb 2008, when a deep  
1965 cyclone center was near site E01. Adapted from *Chereskin et al.* [2009].  
1966

1967    **References**

1968

- 1969    Allison, L. C., et al. (2010), Where do winds drive the Antarctic Circumpolar Current?,  
1970         *Geophysical Research Letters*, 37(L12605).
- 1971    Allison, L. C., et al. (2011), Spin-up and Adjustment of the Antarctic Circumpolar  
1972         Current and Global Pycnocline, *Journal of Marine Research*, submitted.
- 1973    Angell, J. K., and J. Korshover (1964), Quasi-biennial variations in temperature, total  
1974         ozone and tropopause height, *Journal of Atmospheric Science*, 21, 479-492.
- 1975    Aoki, S. (2002), Coherent sea level response to the Antarctic Oscillation, *Geophysical  
1976         Research Letters*, 29(20), 10.1029/2002GL015733.
- 1977    Aoki, S., et al. (2007), Formation regions of Subantarctic Mode Water detected by  
1978         OFES and Argo profiling floats., *Geophysical Research Letters*, 34(L10606).
- 1979    Barker, P. F. (2001), Scotia Sea regional tectonic evolution: implications for mantle  
1980         flow and palaeocirculation, *Earth-Science Reviews*, 55, 1-39.
- 1981    Barker, P. F., et al. (2007), Onset of Cenozoic Antarctic Glaciation, *Deep Sea Research II*,  
1982         54, 2293-2307.
- 1983    Barré, N., et al. (2008), Circulation in the Ona Basin, southern Drake Passage, *Journal  
1984         of Geophysical Research*, 113.
- 1985    Barré, N., et al. (2011), Mesoscale activity in Drake Passage during the cruise survey  
1986         ANT-XXIII/3: a satellite perspective, *Deep-Sea Research II, In press*.
- 1987    Bindoff, N. L., et al. (2007), Observations: Oceanic climate change and sea level.  
1988         Contribution of Working Group I to the Fourth Assessment Report of the  
1989         Intergovernmental Panel on Climate Change,, in *Climate Change 2007: The  
1990         Physical Science Basis.*, edited by D. Q. S. Solomon, M. Manning, Z. Chen, M.  
1991         Marquis, K.B. Averyt, M. Tignor and H.L. Miller, Cambridge University Press,,  
1992         Cambridge, U.K., and New York, U.S.A.
- 1993    Böning, C. W., et al. (2008), The response of the Antarctic Circumpolar Current to  
1994         recent climate change, *Nature Geoscience*, 1, 864-869.
- 1995    Botnikov, V. N. (1963), Geographical position of the Antarctic Convergence Zone in the  
1996         Southern Ocean, *Information of the Soviet Antarctic Expedition*, 4, 324-327.
- 1997    Bryden, H. (1979), Poleward heat flux and conversion of available potential energy in  
1998         Drake Passage, *Journal of Marine Research*, 37(1), 1-22.

- 1999 Bryden, H. L., and R. D. Pillsbury (1977), Variability of the deep flow in Drake Passage  
2000 from yearlong current measurements, *Journal of Physical Oceanography*, 7(803-  
2001 810).
- 2002 Caldeira, K., and P. B. Duffy (2000), The role of the Southern Ocean in uptake and  
2003 storage of anthropogenic carbon dioxide, *Science*, 287, 620-622.
- 2004 Cartwright, D. E. (1999), *Tides: a scientific history*, Cambridge University Press,  
2005 Cambridge.
- 2006 Chelton, D. B. (1982), Statistical reliability and the seasonal cycle: comments on  
2007 "Bottom pressure measurements across the Antarctic Circumpolar Current and  
2008 their relation to the wind", *Deep-Sea Research*, 29(11A), 1381-1388.
- 2009 Chereskin, T. K., and G. A. Tarling (2007), Interannual to diurnal variability in the  
2010 near-surface scattering layer in Drake Passage., *ICES Journal of Marine Science*.
- 2011 Chereskin, T. K., et al. (2009), Strong bottom currents and cyclogenesis in Drake  
2012 Passage, *Geophysical Research Letters*, 36(L23602).
- 2013 Clowes, A. J. (1933), Influence of the Pacific on the circulation in the southwest  
2014 Atlantic Ocean, *Nature*, 131, 189-191.
- 2015 Cunningham, S. A., et al. (2003), Transport and variability of the Antarctic Circumpolar  
2016 Current in Drake Passage, *Journal of Geophysical Research*, 108,  
2017 10.1029/2001JC001147.
- 2018 Cutting, A. L. (2010), Constituents of Sea Surface Height Variability, 68 pp, University  
2019 of Rhode Island.
- 2020 Danabasoglu, G., et al. (1994), The role of mesoscale tracer transports in the global  
2021 ocean circulation, *Science*, 264, 1123-1126.
- 2022 Deacon, G. E. R. (1937), *The Hydrology of the Southern Ocean*, 1-124 pp.
- 2023 Dillon, T. M. (1982), Vertical overturns: A comparison of Thorpe and Ozmidov scales,  
2024 *Journal of Physical Oceanography*, 87, 9601-9613.
- 2025 Donohue, K. A., et al. (2011), Barotropic transport variability in Drake Passage from  
2026 the cDrake experiment, *Submitted*.
- 2027 Döös, K., and D. J. Webb (1994), The Deacon Cell and the other meridional cells of the  
2028 Southern Ocean, *Journal of Physical Oceanography*, 24, 429-442.
- 2029 Fahrbach, E., et al. (2004), Decadal-scale variations of water mass properties in the  
2030 deep Weddell Sea, *Ocean Dynamics*, 54(77-91).

- 2031 Fandry, C., and R. D. Pillsbury (1979), On the estimation of absolute geostrophic  
2032 volume transport applied to the Antarctic Circumpolar Current, *Journal of*  
2033 *Physical Oceanography*, 9, 449-455.
- 2034 Ferrari, R., and M. Nikurashin (2010), Suppression of eddy mixing across jets in the  
2035 Southern Ocean, *Journal of Physical Oceanography*, 40, 1501-1519.
- 2036 Fetter, A. F. H., and R. P. Matano (2008), On the origins of the Malvinas Current in a  
2037 global, eddy-permitting numerical simulation, *Journal of Geophysical Research*,  
2038 113(C11018).
- 2039 Forcada, J., et al. (2006), Contrasting population changes in sympatric penguin species  
2040 in association with climate warming., *Global Change Biology*, 12, 411-423.
- 2041 Foster, L. A. (1972), Current measurements in the Drake Passage, 61 pp, Dalhousie  
2042 University, Halifax, N.S.
- 2043 FRAM (1991), An eddy-resolving model of the Southern Ocean, in *EOS, Transactions of*  
2044 *the American Geophysical Union*, edited, pp. 169-175.
- 2045 Fuckar, N. S., and G. K. Vallis (2007), Interhemispheric influence of surface boundary  
2046 conditions on a circumpolar current, *Geophysical Research Letters*, 34(L14605).
- 2047 Gent, P. R., and J. C. McWilliams (1990), Isopycnal mixing in ocean circulation models,  
2048 *Journal of Physical Oceanography*, 20, 150-155.
- 2049 Gent, P. R., et al. (1995), Parameterizing eddy-induced tracer transports in ocean  
2050 circulation models., *Journal of Physical Oceanography*, 25, 463-474.
- 2051 Gille, S. T., and C. W. Hughes (2001), Aliasing of high-frequency variability by  
2052 altimetry: Evaluation from bottom pressure recorders, *Geophysical Research  
Letters*, 28(9), 1755-1758.
- 2053 Gille, S. T. (2002), Warming of the Southern Ocean Since the 1950s, *Science*, 295, 1275-  
2055 1277.
- 2056 Gille, S. T. (2003), Float observations of the Southern Ocean. Part II: Eddy Fluxes,  
2057 *Journal of Physical Oceanography*, 33, 1182-1196.
- 2058 Gille, S. T. (2008), Decadal-scale temperature trends in the Southern Hemisphere  
2059 ocean, *Journal of Climate*, 21(18), 4749-4764.
- 2060 Gnanadesikan, A. (1999), A simple predictive model for the structure of the oceanic  
2061 pycnocline., *Science*, 283, 2077-2079.
- 2062 Gnanadesikan, A., and R. W. Hallberg (2000), On the relationship of the Circumpolar  
2063 Current to Southern Hemisphere winds in coarse-resolution ocean models.,  
2064 *Journal of Physical Oceanography*, 30, 2013-2034.

- 2065 Gordon, A. L. (1967), Geostrophic transport through the Drake Passage, *Science*, 156,  
2066 1732-1734.
- 2067 Gordon, A. L. (1986), Intercean exchange of thermocline water, *Journal of Geophysical  
2068 Research*, 91, 5037-5046.
- 2069 Gordon, A. L., et al. (2001), Export of Weddell Sea Deep and Bottom Water, *Journal of  
2070 Geophysical Research*, 106(C5), 9005-9017.
- 2071 Gordon, A. L., et al. (2010), A seasonal cycle in the export of bottom water from the  
2072 Weddell Sea, *Nature Geoscience*, 3.
- 2073 Hall, A., and M. Visbeck (2002), Synchronous Variability in the Southern Hemisphere  
2074 Atmosphere, Sea Ice, and Ocean Resulting from the Annular Mode, *Journal of  
2075 Climate*, 15, 3043-3057.
- 2076 Hallberg, R., and A. Gnanadesikan (2006), The role of eddies in determining the  
2077 structure and response of the wind-driven Southern Hemisphere overturning:  
2078 Results from the Modeling Eddies in the Southern Ocean (MESO) project, *Journal  
2079 of Physical Oceanography*, 36, 2232-2252.
- 2080 Hanawa, K., and L. D. Talley (2001), Mode Waters, in *Ocean Circulation and Climate*,  
2081 edited by G. Siedler and J. Church, pp. 373-386, Academic Press.
- 2082 Hewitt, R. P., et al. (2003), An 8-year cycle in krill biomass density inferred from  
2083 acoustic surveys conducted in the vicinity of the South Shetland Islands during  
2084 the austral summers of 1991-1992 through 2001-2002., *Aquatic Living  
2085 Resources*, 16, 205-213.
- 2086 Heywood, K. J., et al. (2002), High mixing rates in the abyssal Southern Ocean, *Nature*,  
2087 415, 1011-1014.
- 2088 Heywood, K. J., et al. (2007), On the Detectability of Internal Tides in Drake Passage,  
2089 *Deep Sea Research I*, 54(11), 1972-1984.
- 2090 Hibbert, A., et al. (2010), Quasi-biennial modulation of the Southern Ocean coherent  
2091 mode, *Quarterly Journal of the Royal Meteorological Society*, 136, 755-768.
- 2092 Hughes, C. W., et al. (1999), Wind-forced transport fluctuations at Drake Passage: a  
2093 southern mode, *Journal of Physical Oceanography*, 29(8), 1971-1992.
- 2094 Hughes, C. W., and E. R. Ash (2001), Eddy forcing of the mean flow in the Southern  
2095 Ocean, *Journal of Geophysical Research*, 106(C2), 2713-2722.
- 2096 Hughes, C. W., et al. (2003), Coherence of Antarctic sea levels, Southern Hemisphere  
2097 Annular Mode, and flow through Drake Passage, *Geophysical Research Letters*,  
2098 30(9), 10.1029/2003GL017240.

- 2099 Hughes, C. W., and V. Stepanov (2004), Ocean dynamics associated with rapid J2  
2100 fluctuations: Importance of circumpolar modes and identification of a coherent  
2101 Arctic mode, *Journal of Geophysical Research*, 109(C6), 10.1029/2003JC002176.
- 2102 Hughes, C. W., and M. P. Meredith (2006), Coherent sea-level fluctuations along the  
2103 global continental slope, *Philosophical Transactions of the Royal Society A*, 364,  
2104 885-901.
- 2105 Johnson, G. C., and H. Bryden (1989), On the strength of the Circumpolar Current,  
2106 *Deep-Sea Research*, 36, 39-53.
- 2107 Johnson, G. C., and S. C. Doney (2006), Recent western South Atlantic bottom water  
2108 warming, *Geophysical Research Letters*, 33(L14614), 10.1029/2006GL026769.
- 2109 Johnson, G. C., et al. (2008), Reduced Antarctic meridional overturning circulation reaches  
2110 the North Atlantic Ocean, *Geophysical Research Letters*, 35(L22601),  
2111 doi:10.1029/2008GL035619.
- 2112 Johnson, M. A. (1989), Forcing the Volume Transport Through Drake Passage, *Journal*  
2113 *of Geophysical Research*, 94(C11), 16115-16124.
- 2114 Jullion, L., et al. (2010), Wind-controlled export of Antarctic Bottom Water from the  
2115 Weddell Sea, *Geophysical Research Letters*, 37(L09609).
- 2116 Karsten, R., et al. (2002), The role of eddy transfer in setting the stratification and  
2117 transport of a circumpolar current., *Journal of Physical Oceanography*, 32, 39-54.
- 2118 Karsten, R. H., and J. Marshall (2002), Constructing the residual circulation of the ACC  
2119 from observations, *Journal of Physical Oceanography*, 32, 3315-3327.
- 2120 King, B. A. (2001), Introduction to special section: World Ocean Circulation  
2121 Experiment: Southern Ocean results, *Journal of Geophysical Research*, 106(C2),  
2122 2691.
- 2123 King, B. A., and L. Jullion (2011), Transport of mass, heat and salt through Drake  
2124 Passage, 1993-2009, *In preparation*.
- 2125 Kusohara, K., and K. I. Ohshima (2009), Dynamics of the wind-driven sea level  
2126 variations around Antarctica, *Journal of Physical Oceanography*, 39, 658-674.
- 2127 Ledwell, J. R., et al. (2011), Diapycnal mixing in the Antarctic Circumpolar Current,  
2128 *Journal of Physical Oceanography*, 41(1), 241-246.
- 2129 Legeckis, R. (1977), Oceanic polar front in the Drake Passage - satellite observations  
2130 during 1976, *Deep Sea Research*, 24, 701-704.

- 2131 Lenn, Y.-D., et al. (2007), Mean jets, mesoscale variability and eddy momentum fluxes  
2132 in the surface-layer of the Antarctic Circumpolar Current in Drake Passage,  
2133 *Journal of Marine Research*, 65, 27-58.
- 2134 Lenn, Y.-D., et al. (2008), Improving estimates of the Antarctic Circumpolar Current  
2135 streamlines in Drake Passage, *Journal of Physical Oceanography*, 38, 1000-1010.
- 2136 Lenn, Y.-D., and T. K. Chereskin (2009), Observations of Ekman Currents in the  
2137 Southern Ocean, *Journal of Physical Oceanography*, 39, 768-779.
- 2138 Lenn, Y.-D., et al. (2011), Near-surface eddy heat and momentum fluxes in the  
2139 Antarctic Circumpolar Current in Drake Passage, *Journal of Physical*  
2140 *Oceanography, in press.*
- 2141 Livermore, R., et al. (2005), Paleogene opening of Drake Passage, *Earth and Planetary*  
2142 *Science Letters*, 236, 459-470.
- 2143 Loeb, V., et al. (1997), Effects of sea-ice extent and krill or salp dominance on the  
2144 Antarctic food web, *Nature*, 387, 897-900.
- 2145 Lumpkin, R., and K. Speer (2007), Global ocean meridional overturning, *Journal of*  
2146 *Physical Oceanography*, 37, 2550-2562.
- 2147 Mackintosh, N. A. (1934), Distribution of the macroplankton in the Atlantic sector of  
2148 the Antarctic, edited, pp. 65-160.
- 2149 Madden, R. A., and P. R. Julian (1971), Detection of a 40-50 Day Oscillation in the Zonal  
2150 Wind in the Tropical Pacific, *Journal of Atmospheric Science*, 28, 702-708.
- 2151 Marshall, D. P. (1997), Subduction of water masses in an eddying ocean, *Journal of*  
2152 *Marine Research*, 55, 201-222.
- 2153 Marshall, G. J. (2003), Trends in the Southern Annular Mode from Observations and  
2154 Reanalyses, *Journal of Climate*, 16, 4134-4143.
- 2155 Marshall, J., and T. Radko (2003), Residual-mean solutions for the Antarctic  
2156 Circumpolar Current and its associated overturning circulation, *Journal of*  
2157 *Physical Oceanography*, 33, 2341-2354.
- 2158 Marshall, J., and T. Radko (2006), A model of the upper branch of the meridional  
2159 overturning circulation of the Southern Ocean, *Progress in Oceanography*, 70,  
2160 331-345.
- 2161 Marshall, J., et al. (2006), Estimates and Implications of Surface Eddy Diffusivity in the  
2162 Southern Ocean Derived from Tracer Transport, *Journal of Physical*  
2163 *Oceanography*, 36, 1806-1821.

- 2164 Matthews, A. J., and M. P. Meredith (2004), Variability of the Antarctic circumpolar  
2165 transport and the Southern Annular Mode associated with the Madden-Julian  
2166 Oscillation, *Geophysical Research Letters*, 31(24), L24312.
- 2167 Maximenko, N., and P. P. Niiler (2005), Hybrid decade-mean global sea level with  
2168 mesoscale resolution, in *Recent Advances in Marine Science and Technology*,  
2169 edited by N. Saxena, pp. 55-59, Honolulu.
- 2170 Mazloff, M. R., et al. (2010), An Eddy Permitting Southern Ocean State Estimate,  
2171 *Journal of Physical Oceanography*, 40, 880-899.
- 2172 Meinen, C. S., et al. (2003), Mean stream coordinates structure of the Subantarctic  
2173 Front: temperature, salinity and absolute velocity, *Journal of Geophysical*  
2174 *Research*, 108(C8).
- 2175 Meredith, M. P., et al. (1996), On the temporal variability of the transport through  
2176 Drake Passage, *Journal of Geophysical Research*, 101(C10), 22,485-422,494.
- 2177 Meredith, M. P., et al. (1997), The Processing and Application of Inverted Echo  
2178 Sounder Data from Drake Passage, *Journal of Atmospheric and Oceanic*  
2179 *Technology*, 14(4), 871-882.
- 2180 Meredith, M. P., et al. (2003), Downslope convection north of Elephant Island,  
2181 Antarctic Peninsula: Influence on deep waters and dependence on ENSO,  
2182 *Geophysical Research Letters*, 30(9), 10.1029/2003GL017074.
- 2183 Meredith, M. P., et al. (2004), Changes in the ocean transport through Drake Passage  
2184 during the 1980s and 1990s, forced by changes in the Southern Annular Mode,  
2185 *Geophysical Research Letters*, 31(21), 10.1029/2004GL021169.
- 2186 Meredith, M. P., and C. W. Hughes (2005), On the sampling timescale required to  
2187 reliably monitor interannual variability in the Antarctic circumpolar transport,  
2188 *Geophysical Research Letters*, 32(3), 10.1029/2004GL022086.
- 2189 Meredith, M. P., and J. C. King (2005), Rapid climate change in the ocean to the west of  
2190 the Antarctic Peninsula during the second half of the twentieth century,  
2191 *Geophysical Research Letters*, 32(L19604), 10.1029/2005GL024042.
- 2192 Meredith, M. P., and A. M. Hogg (2006), Circumpolar response of Southern Ocean eddy  
2193 activity to changes in the Southern Annular Mode, *Geophysical Research Letters*,  
2194 33(16)(L16608), 10.1029/2006GL026499.
- 2195 Meredith, M. P., et al. (2008), Evolution of the Deep and Bottom Waters of the Scotia  
2196 Sea, Southern Ocean, 1995-2005, *Journal of Climate*, 21(13), 3327-3343.

- 2197 Meredith, M. P., et al. (2011), Synchronous intensification and warming of Antarctic  
2198 Bottom Water outflow from the Weddell Gyre, *Geophysical Research Letters*,  
2199 38(L03603), 4.
- 2200 Mignone, B. K., et al. (2006), Central role of southern hemisphere winds and eddies in  
2201 modulating the oceanic uptake of anthropogenic carbon, *Geophysical Research  
2202 Letters*, 33(L01604).
- 2203 Morrow, R. A., et al. (1994), Surface eddy momentum flux and velocity variances in the  
2204 Southern Ocean from Geosat altimetry, *Journal of Physical Oceanography*, 24,  
2205 2050-2071.
- 2206 Munday, D. R., et al. (2011), Remote forcing of the Antarctic Circumpolar Current by  
2207 diapycnal mixing, *Geophysical Research Letters*, 38(L08609).
- 2208 Munk, W. H., and E. Palmén (1951), Note on the dynamics of the Antarctic Circumpolar  
2209 Current, *Tellus*, 3, 53-55.
- 2210 Naveira Garabato, A. C., et al. (2002a), Modification and pathways of Southern Ocean  
2211 Deep Waters in the Scotia Sea, *Deep-Sea Research I*, 49, 681-705.
- 2212 Naveira Garabato, A. C., et al. (2002b), On the export of Antarctic Bottom Water from  
2213 the Weddell Sea, *Deep-Sea Research II*, 49, 4715-4742.
- 2214 Naveira Garabato, A. C., et al. (2004), Widespread intense turbulent mixing in the  
2215 Southern Ocean, *Science*, 303, 210-213.
- 2216 Naveira Garabato, A. C., et al. (2007), Short-circuiting of the overturning circulation of  
2217 the Antarctic Circumpolar Current, *Nature*, 447, 194-197.
- 2218 Naveira Garabato, A. C., et al. (2009), Variability of Subantarctic Mode Water and  
2219 Antarctic Intermediate Water in Drake Passage during the Late 20th and Early  
2220 21st Centuries, *Journal of Climate*, 22(7), 3661-3688.
- 2221 Naveira Garabato, A. C., et al. (2011), Eddy mixing in the Southern Ocean, *Journal of  
2222 Geophysical Research, submitted*.
- 2223 Nikurashin, M., and R. Ferrari (2010), Radiation and dissipation of internal waves  
2224 generated by geostrophic motions impinging on small-scale topography:  
2225 Application to the Southern Ocean, *Journal of Physical Oceanography*, 40, 2025-  
2226 2042.
- 2227 Nowlin, W. D., et al. (1977), Structure and transport of the Antarctic Circumpolar  
2228 Current at Drake Passage from short-term measurements, *Journal of Physical  
2229 Oceanography*, 7, 788-802.

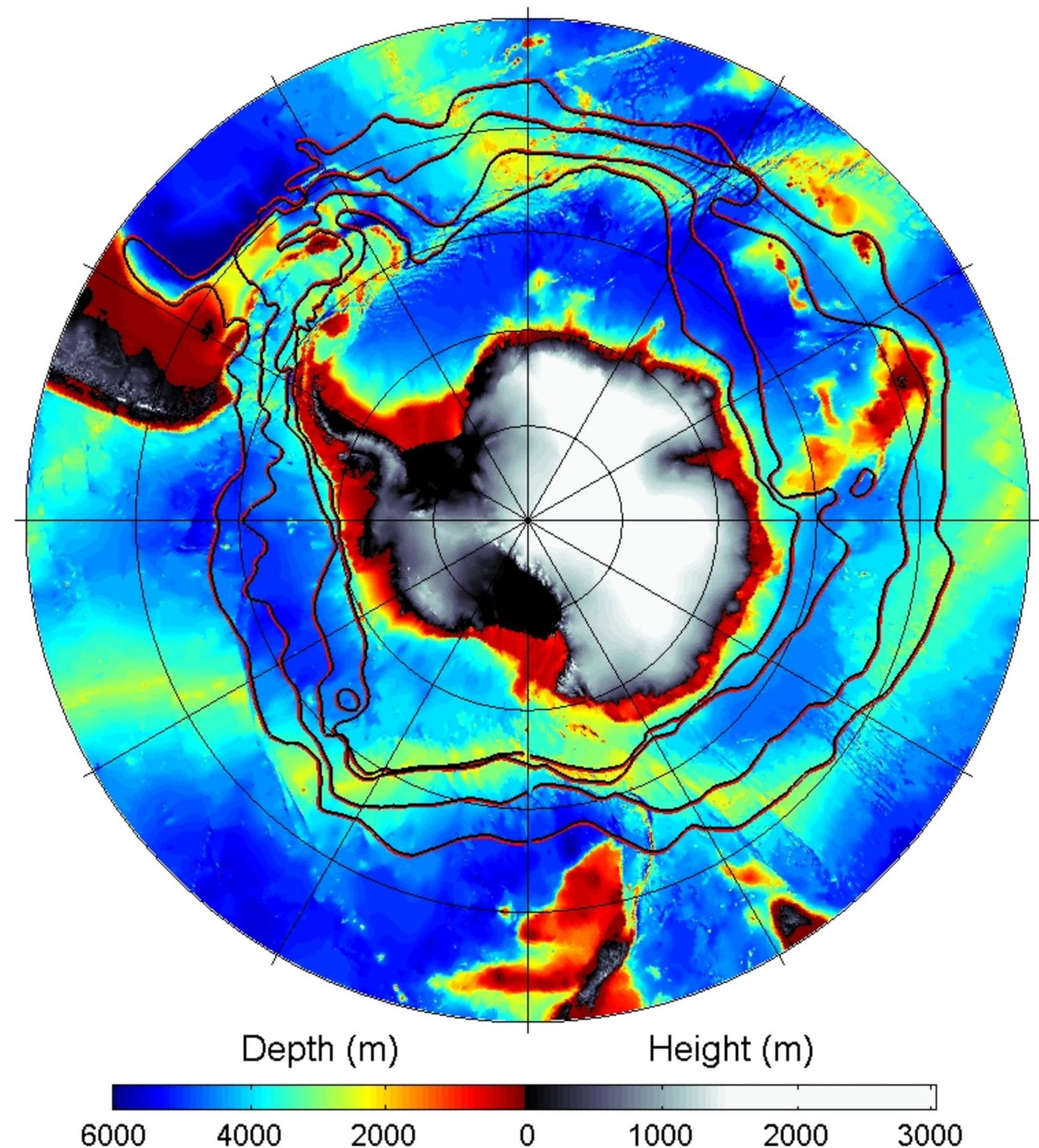
- 2230 Nowlin, W. D., and M. Clifford (1982), The kinematic and thermohaline zonation of the  
2231 Antarctic Circumpolar Current at Drake Passage, *Journal of Marine Research*, 40,  
2232 481-507.
- 2233 Oke, P. R., and M. H. England (2004), Oceanic response to changes in the latitude of the  
2234 Southern Hemisphere subpolar westerly winds, *Journal of Climate*, 17, 1040-  
2235 1054.
- 2236 Olbers, D., et al. (1992), *Hydrographic Atlas of the Southern Ocean*, Alfred-Wegener  
2237 Institute, Bremerhave, Germany.
- 2238 Olbers, D. (1998), Comments on "On the obscurantist physics of 'form drag' in  
2239 theorizing about the Antarctic Circumpolar Current", *Journal of Physical  
2240 Oceanography*, 28, 1647-1654.
- 2241 Olbers, D., and M. Visbeck (2005), A model of the zonally averaged stratification and  
2242 overturning in the Southern Ocean, *Journal of Physical Oceanography*, 35, 1190-  
2243 1205.
- 2244 Olbers, D., and K. Lettmann (2007), Barotropic and baroclinic processes in the  
2245 transport variability of the Antarctic Circumpolar Current, *Ocean Dynamics*, 57,  
2246 559-578.
- 2247 Orsi, A. H., et al. (1995), On the Meridional Extent and Fronts of the Antarctic  
2248 Circumpolar Current, *Deep-Sea Research I*, 42(5), 641-673.
- 2249 Orsi, A. H., et al. (1999), Circulation, mixing, and production of Antarctic Bottom  
2250 Water, *Progress in Oceanography*, 43(1), 55-109.
- 2251 Ostapoff, F. (1961), A contribution to the problem of the Drake Passage transport,  
2252 *Deep Sea Research* 8, 111-120.
- 2253 Peterson, R. G. (1988a), On the Transport of the Antarctic Circumpolar Current  
2254 Through Drake Passage and Its Relation to Wind, *Journal of Geophysical  
2255 Research*, 93(C11), 13993-14004.
- 2256 Peterson, R. G. (1988b), Comparisons of sea level and bottom pressure measurements  
2257 at Drake Passage, *Journal of Geophysical Research*, 93, 12439-12448.
- 2258 Phillips, H. E., and S. R. Rintoul (2000), Eddy variability and energetics from direct  
2259 current measurements in the Antarctic Circumpolar Current south of Australia,  
2260 *Journal of Physical Oceanography*, 30(12), 3050-3076.
- 2261 Ponte, R. M., and K. J. Quinn (2009), Bottom pressure changes around Antarctica and  
2262 wind-driven meridional flows, *Geophysical Research Letters*, 36(L13604).

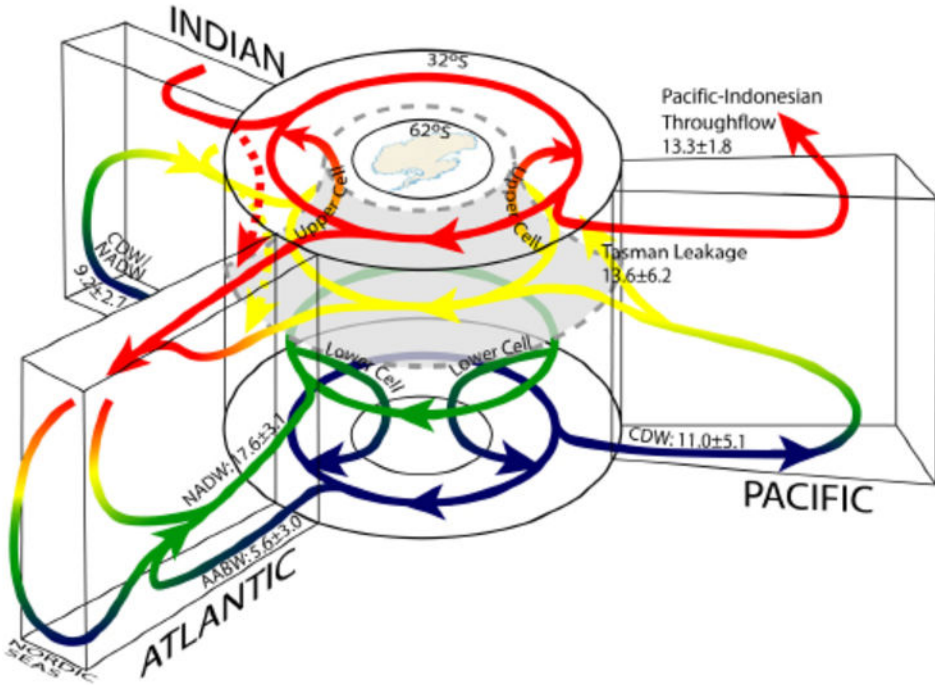
- 2263 Provost, C., et al. (2011), Two repeat crossings of Drake Passage in austral summer  
2264 2006: short term variations and evidence for considerable ventilation of  
2265 intermediate and deep waters., *Deep-Sea Research II, In press.*
- 2266 Rabinovich, A. B., et al. (2011), Deep-sea observations and modelling of the 2004  
2267 Sumatra tsunami in Drake Passage, *Geophysical Research Letters, Submitted.*
- 2268 Reid, J. L., and W. D. Nowlin (1971), Transport of water through the Drake Passage,  
2269 *Deep Sea Research, 18*, 51-64.
- 2270 Renault, A., et al. (2011), Two LADCP surveys in the Drake Passage in 2006: transport  
2271 estimates, *Deep-Sea Research II, In press.*
- 2272 Rintoul, S. R., et al. (2001), The Antarctic Circumpolar System, in *Ocean Circulation and*  
2273 *Climate*, edited by G.Sielder, et al., pp. 271-302, Academic Press.
- 2274 Rintoul, S. R., et al. (2010), Southern Ocean Observing System (SOOS): Rationale and  
2275 strategy for sustained observations of the Southern Ocean, in *OceanObs '09:*  
2276 *Ocean information for society: Sustaining the benefits, realizing the potential.*,  
2277 edited by J. Hall, et al., p. 9, ESA.
- 2278 Robertson, R., et al. (2002), Long-term temperature trends in the deep waters of the  
2279 Weddell Sea, *Deep-Sea Research II, 49*, 4791-4806.
- 2280 Roscoe, H. K., and J. D. Haigh (2007), Influences of ozone depletion, the solar cycle and  
2281 the QBO on the Southern Annular Mode, *Quarterly Journal of the Royal*  
2282 *Meteorological Society, 133*, 1855-1864.
- 2283 Sabine, C. L., et al. (2004), The oceanic sink for anthropogenic CO<sub>2</sub>, *Science, 305*, 367-  
2284 371.
- 2285 Sallée, J. B., et al. (2008), An estimates of Lagrangian eddy statistics and diffusion in  
2286 the mixed layer of the Southern Ocean, *Journal of Marine Research, 66*(4), 441-  
2287 463.
- 2288 Sallée, J. B., et al. (2010), Southern Ocean thermocline ventilation, *Journal of Physical*  
2289 *Oceanography, 40*(3), 509-529.
- 2290 Scher, H. D., and E. E. Martin (2006), Timing and Climatic Consequences of the  
2291 Opening of Drake Passage, *Science, 312*, 428-430.
- 2292 Schofield, O., et al. (2010), How Do Polar Marine Ecosystems Respond to Rapid  
2293 Climate Change?, *Science, 328*(1520).
- 2294 Sciremammano, F. (1979), Observations of Antarctic Polar Front motions in a deep  
2295 water expression, *Journal of Physical Oceanography, 9*(1), 221-226.

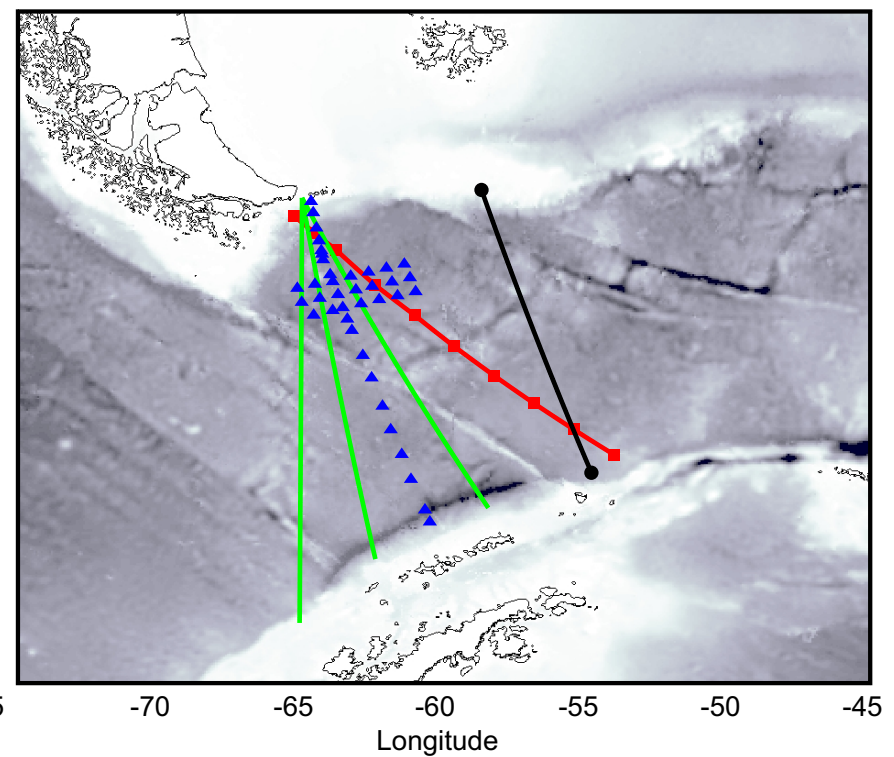
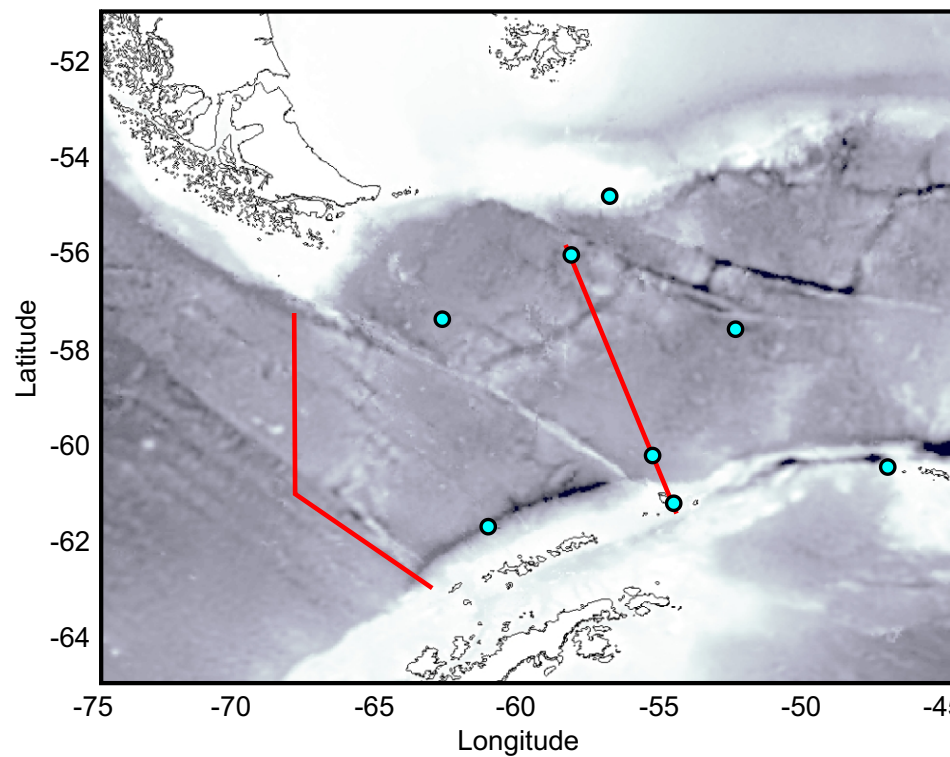
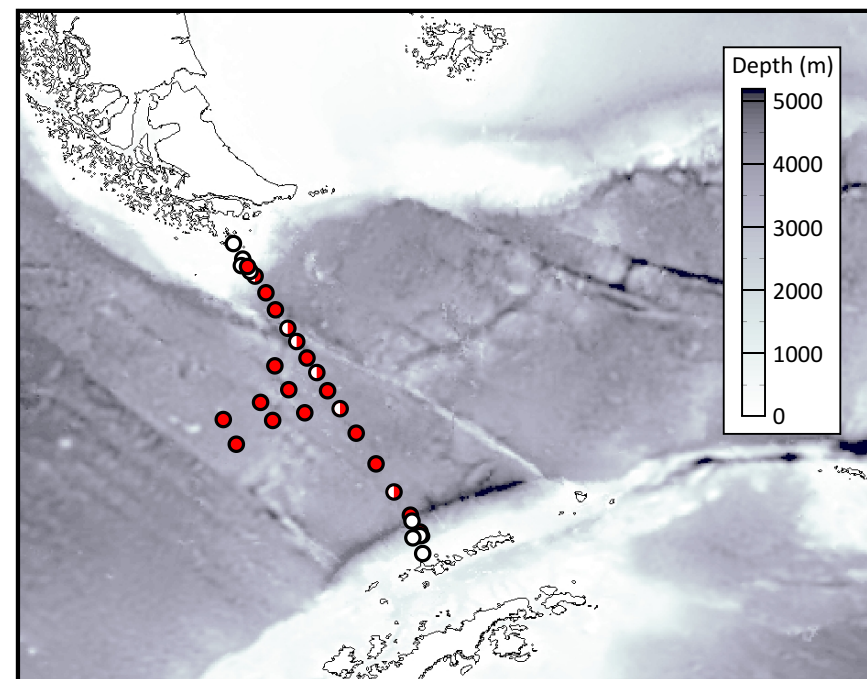
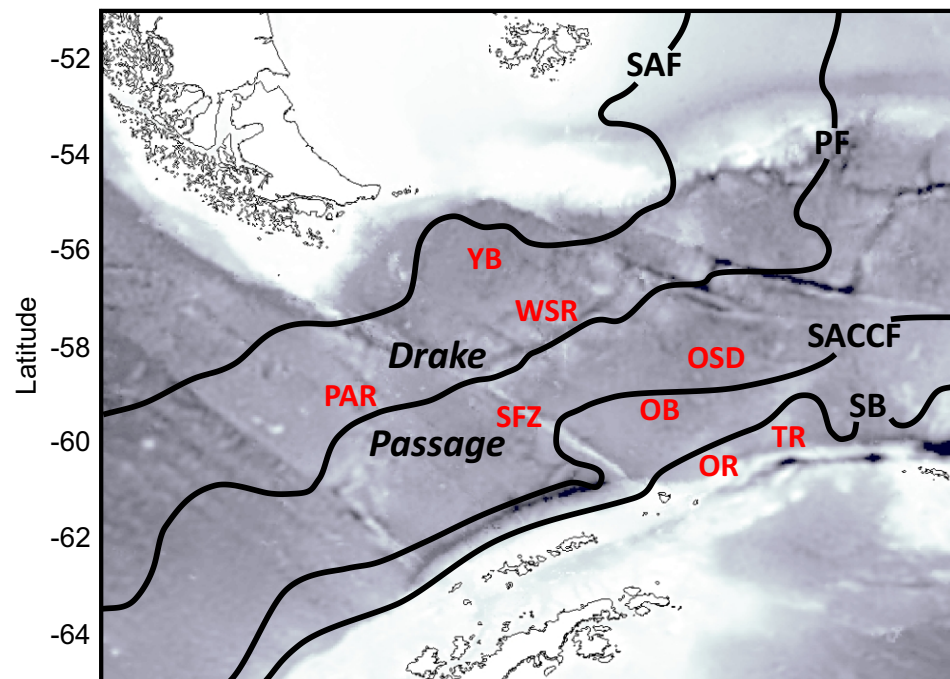
- 2296 Siedler, G., et al. (2001), *Ocean Circulation and climate: Observing and modelling the*  
2297 *global ocean*, Academic Press.
- 2298 Sloyan, B. M., and S. R. Rintoul (2001), The Southern Ocean limb of the global deep  
2299 overturning circulation, *Journal of Physical Oceanography*, 31(1), 143-173.
- 2300 Sokolov, S., and S. R. Rintoul (2007), Multiple jets of the Antarctic Circumpolar Current  
2301 south of Australia, *Journal of Physical Oceanography*, 37, 1394-1412.
- 2302 Speer, K., et al. (2000), The diabatic Deacon cell, *Journal of Physical Oceanography*,  
2303 30(12), 3212-3222.
- 2304 Spencer, R., and P. R. Foden (1996), Data from the deep ocean via releasable data  
2305 capsules, *Sea Technology*, 37(2), 10-12.
- 2306 Sprintall, J. (2003), Seasonal to interannual upper-ocean variability in the Drake  
2307 Passage, *Journal of Marine Research*, 61, 27-57.
- 2308 Sprintall, J. (2008), Long-term trends and interannual variability of temperature in  
2309 Drake Passage, *Progress in Oceanography*, 77, 316-330.
- 2310 Straub, D. N. (1993), On the transport and angular momentum balance of channel  
2311 models of the Antarctic Circumpolar Current, *Journal of Physical Oceanography*,  
2312 23, 776-782.
- 2313 Sudre, J., et al. (2011), Short-term variations of deep water masses in Drake Passage  
2314 revealed by a multiparametric analysis of the ANT-XXIII/3 bottle data, *Deep-Sea*  
2315 *Research II, In press*.
- 2316 Talley, L. D., et al. (2003), Data-based meridional overturning streamfunctions for the  
2317 global ocean, *Journal of Climate*, 16, 3213-3226.
- 2318 Talley, L. D. (2008), Freshwater transport estimates and the global overturning  
2319 circulation: shallow, deep and throughflow components, *Progress in*  
2320 *Oceanography*, 78, 257-303.
- 2321 Thompson, A. F., et al. (2007), Spatial and temporal scales of small-scale mixing in  
2322 Drake Passage, *Journal of Physical Oceanography*, 37, 572-592.
- 2323 Thompson, D. W. J., and J. M. Wallace (2000), Annular modes in the extratropical  
2324 circulation. Part I: Month-to-month variability., *Journal of Climate*, 13, 1000-  
2325 1016.
- 2326 Thompson, D. W. J., et al. (2000), Annular modes in the extratropical circulation. Part  
2327 II: Trends, *Journal of Climate*, 13, 1018-1036.
- 2328 Thompson, D. W. J., and S. Solomon (2002), Interpretation of recent Southern  
2329 Hemisphere climate change, *Science*, 296, 895-899.

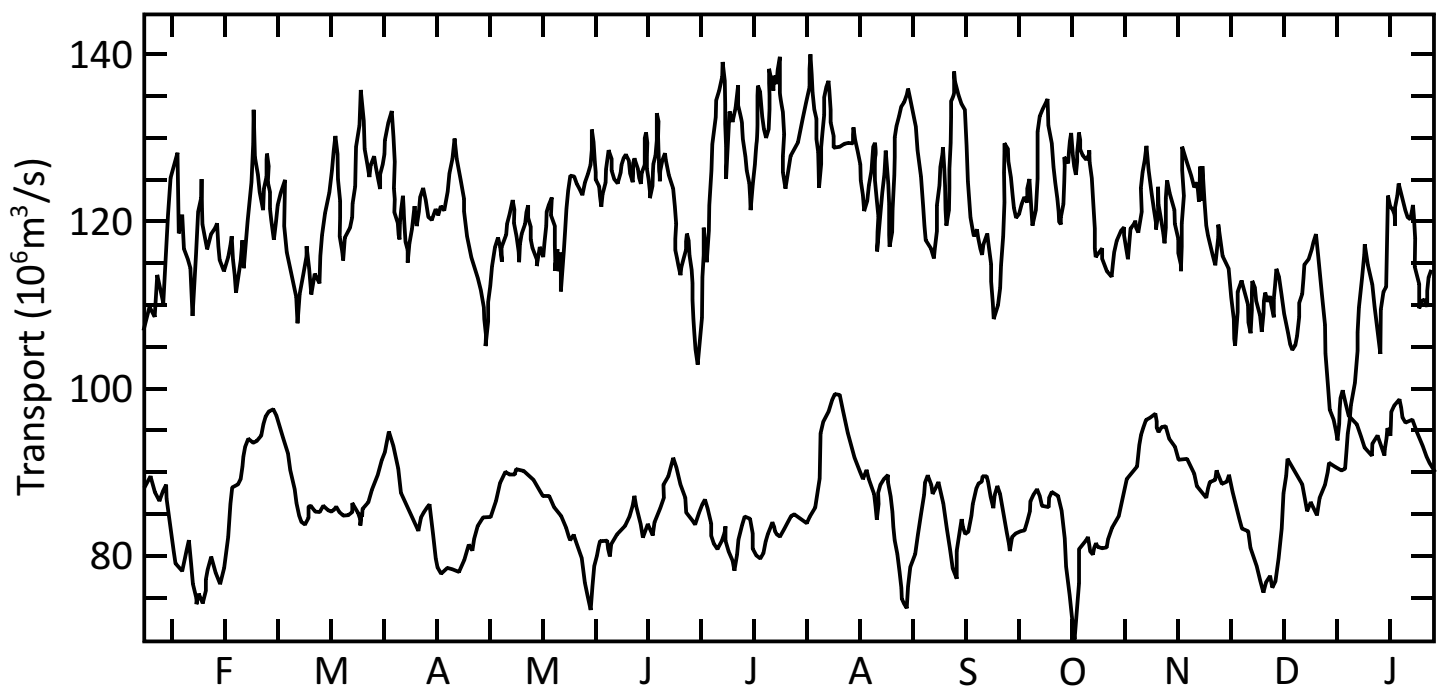
- 2330 Toggweiler, J. R., and B. Samuels (1995), Effect of Drake Passage on the global  
2331 thermohaline circulation, *Deep Sea Research I*, 42, 477-500.
- 2332 Tokmakian, R., and P. G. Challenor (1999), On the joint estimation of model and  
2333 satellite sea surface height anomaly errors, *Ocean Modelling*, 1, 39-52.
- 2334 Vallis, G. K. (2000), Large scale circulation and production of stratification: effects of  
2335 wind, geometry and diffusion, *Journal of Physical Oceanography*, 30, 933-954.
- 2336 Vaughan, D. G., et al. (2003), Recent rapid regional climate warming on the Antarctic  
2337 Peninsula, *Climatic Change*, 60(3), 243-274.
- 2338 Visbeck, M. (2009), A station-based Southern Annular Mode index from 1884 to 2005,  
2339 *Journal of Climate*, 22, 940-950.
- 2340 Vivier, F., and C. Provost (1999), Volume transport of the Malvinas Current: Can the  
2341 flow be monitored by TOPEX/Poseidon?, *Journal of Geophysical Research*, 104,  
2342 21105-21122.
- 2343 Vivier, F., et al. (2001), Remote and local forcing in the Brazil-Malvinas Region, *Journal*  
2344 *of Physical Oceanography*, 31(4), 892-913.
- 2345 Vivier, F., et al. (2005), Causes of large-scale sea level variations in the Southern  
2346 Ocean: Analyses of sea level and a barotropic model, *Journal of Geophysical*  
2347 *Research*, 110(C9), C09014.
- 2348 Watson, A. J., and A. C. Naveira Garabato (2006), The role of Southern Ocean mixing  
2349 and upwelling in glacial-interglacial atmospheric CO<sub>2</sub> change, *Tellus*, 58B, 73-87.
- 2350 Watts, D. R., et al. (2001), A two-dimensional gravest empirical mode determined from  
2351 hydrographic observations in the Subantarctic Front, *Journal of Physical*  
2352 *Oceanography*, 31, 2186-2209.
- 2353 Waugh, D. W., and E. R. Abraham (2008), Stirring in the global surface ocean,  
2354 *Geophysical Research Letters*, 35(L20605).
- 2355 Wearn, R. B., and D. J. Baker (1980), Bottom pressure measurements across the  
2356 Antarctic Circumpolar Current and their relation to the wind, *Deep Sea Research*,  
2357 *Part A*(27), 875-888.
- 2358 Webb, D. J. (1998), The first main run of the OCCAM Global Ocean Model, *Southampton*  
2359 *Oceanography Centre, internal document*, 34.
- 2360 Weijer, W., and S. T. Gille (2005), Adjustment of the Southern Ocean to wind forcing on  
2361 synoptic timescales, *Journal of Physical Oceanography*, 35, 2076-2089.
- 2362 Whitworth, T. (1980), Zonation and geostrophic flow of the Antarctic Circumpolar  
2363 Current at Drake Passage, *Deep Sea Research, Part A*, 27, 497-507.

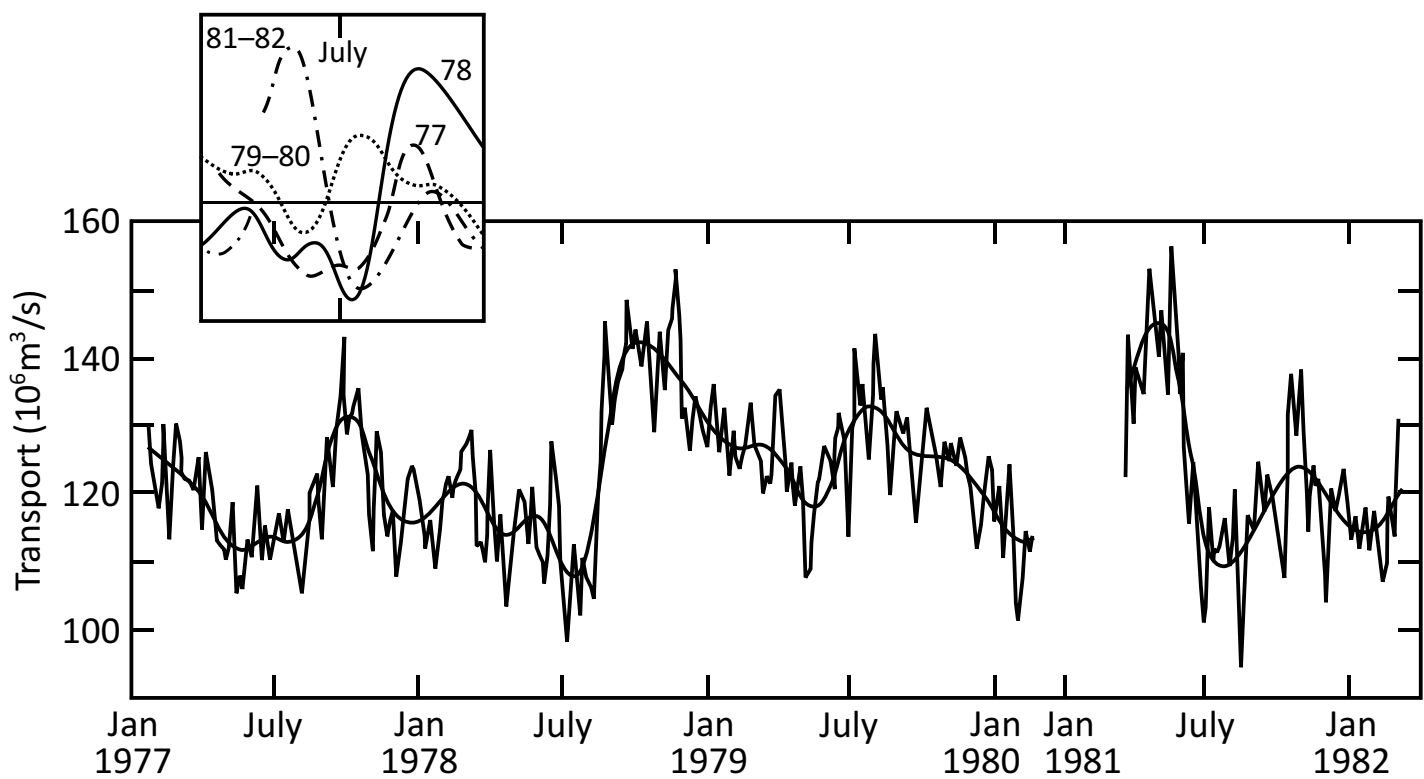
- 2364 Whitworth, T. (1983), Monitoring the transport of the Antarctic Circumpolar Current  
2365 at Drake Passage, *Journal of Physical Oceanography*, 13(11), 2045-2057.
- 2366 Whitworth, T., and R. G. Peterson (1985), Volume Transport of the Antarctic  
2367 Circumpolar Current from Bottom Pressure Measurements, *Journal of Physical*  
2368 *Oceanography*, 15(6), 810-816.
- 2369 Wong, S., and W. Wang (2003), Tropical-extratropical connection in interannual  
2370 variation of the tropopause: Comparison between NCEP/NCAR reanalysis and an  
2371 atmospheric general circulation model simulation, *Journal of Geophysical*  
2372 *Research*, 108(D2), 4043.
- 2373 Woodworth, P. L., et al. (1996), A test of the ability of TOPEX/POSEIDON to monitor  
2374 flows through the Drake Passage, *Journal of Geophysical Research*, 101(C5),  
2375 11,935-911,947.
- 2376 Woodworth, P. L., et al. (2005), Sea level changes at Port Stanley, Falkland Islands,  
2377 *Journal of Geophysical Research*, 110(C06013).
- 2378 Wunsch, C., and R. Ferrari (2004), Vertical mixing, energy, and the general circulation  
2379 of the oceans, *Annual Reviews of Fluid Mechanics*, 36, 281-314.
- 2380 Xie, P., and P. A. Arkin (1997), Global Precipitation: A 17-year monthly analysis based  
2381 on gauge observations, satellite estimates and numerical model outputs, *Bulletin*  
2382 *of the American Meteorological Society*, 78, 2539-2558.
- 2383 Zachos, J., et al. (2001), Trends, rhythms and aberrations in global climate 65 Ma to  
2384 present, *Science*, 292, 686-693.
- 2385 Zhou, M., et al. (1994), ADCP measurements of the distribution and abundance of  
2386 euphausiids near the Antarctic Peninsula in winter, *Deep-Sea Research I*, 41,  
2387 1425-1445.
- 2388 Zika, J. D., et al. (2009), Diagnosing the Southern Ocean overturning from tracer fields,  
2389 *Journal of Physical Oceanography*, 39, 2926-2940.
- 2390  
2391

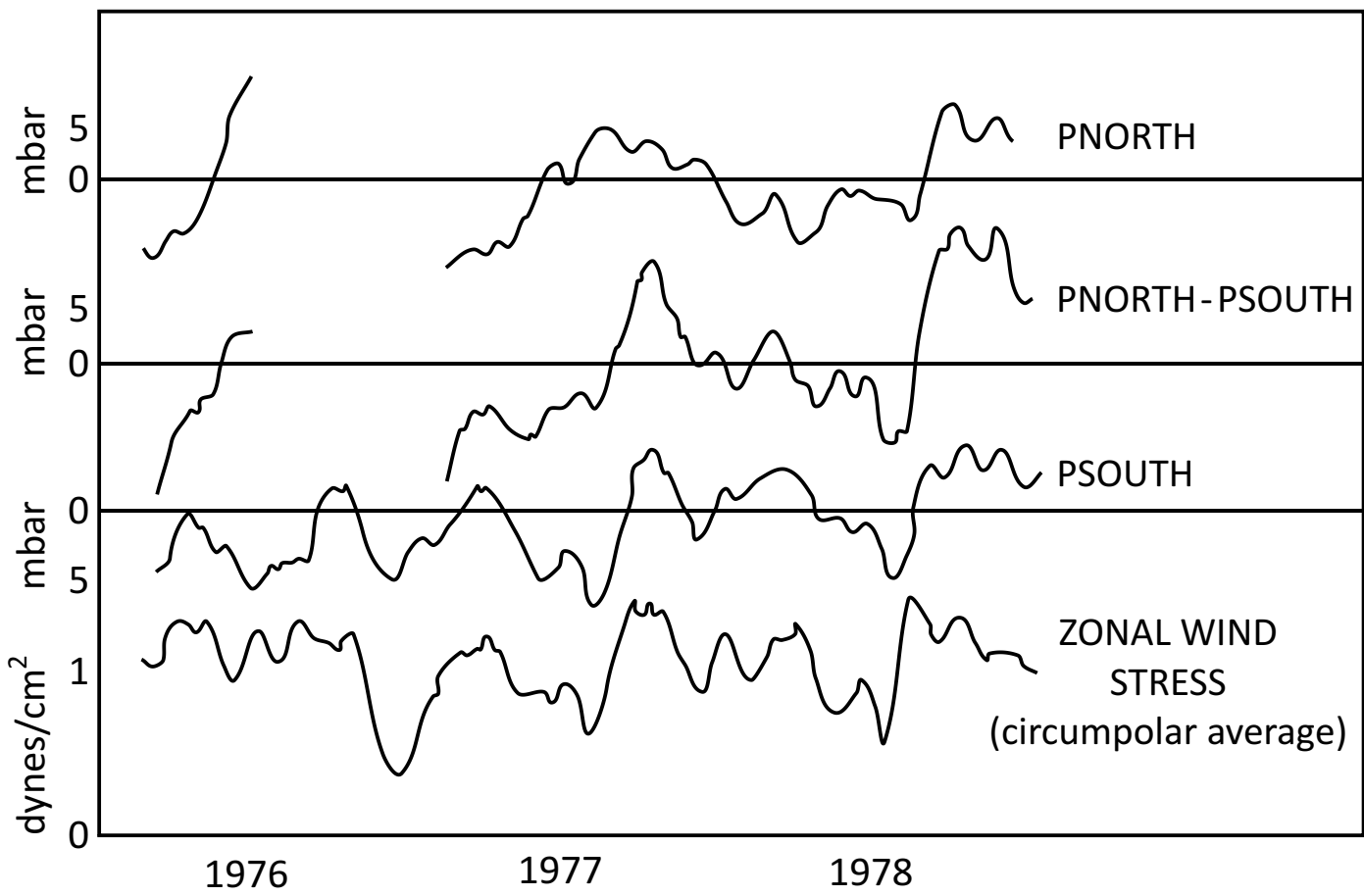


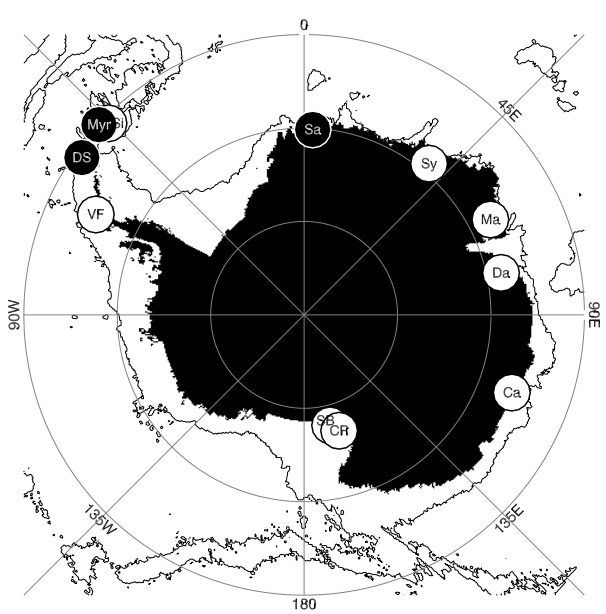




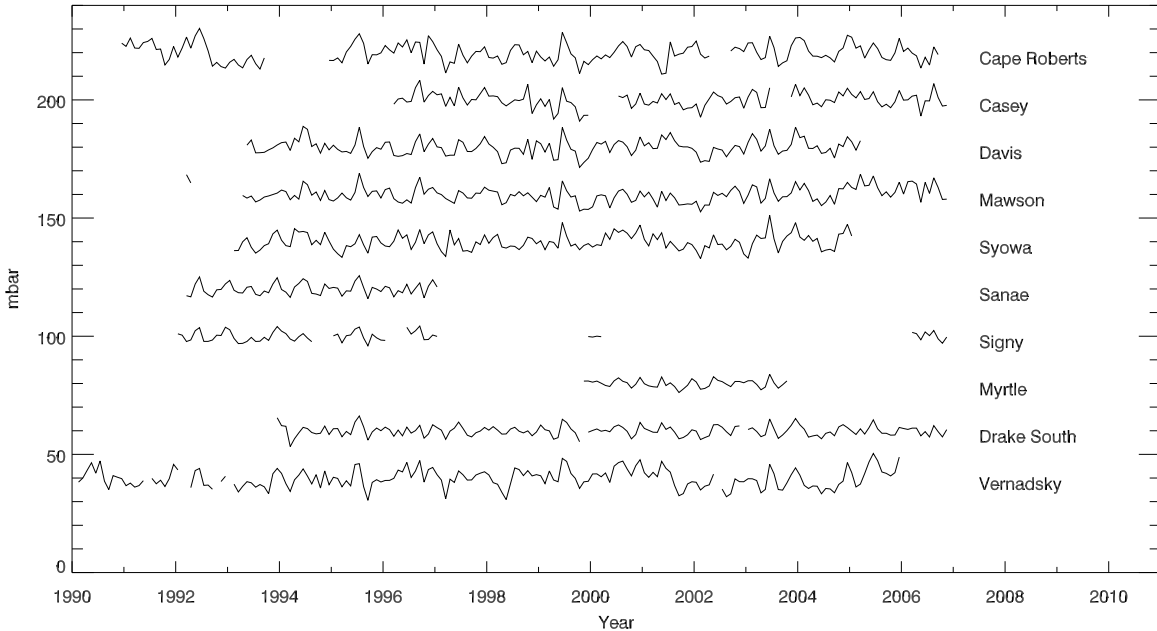




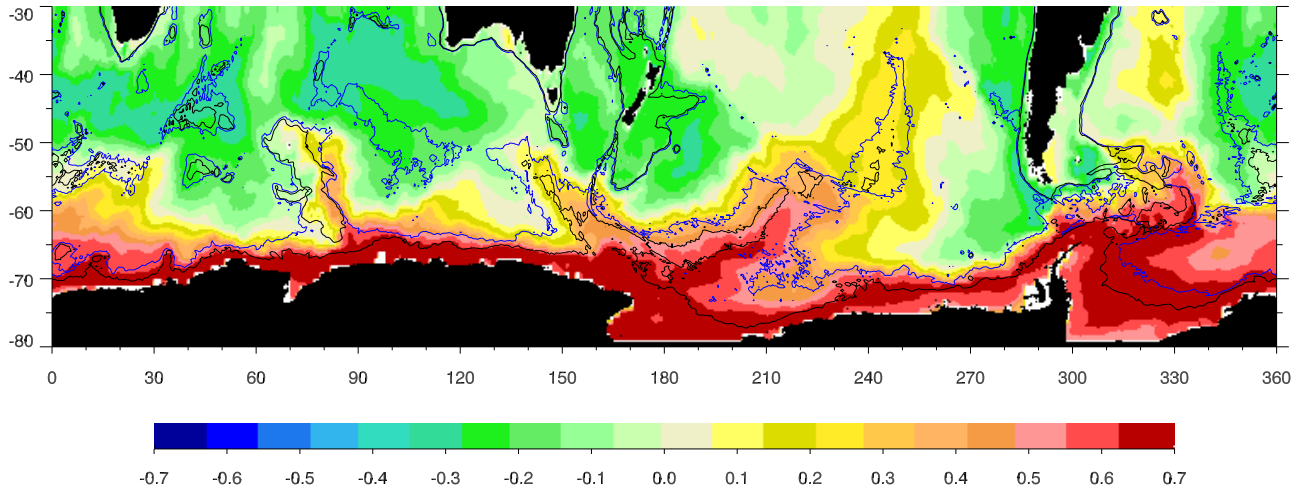


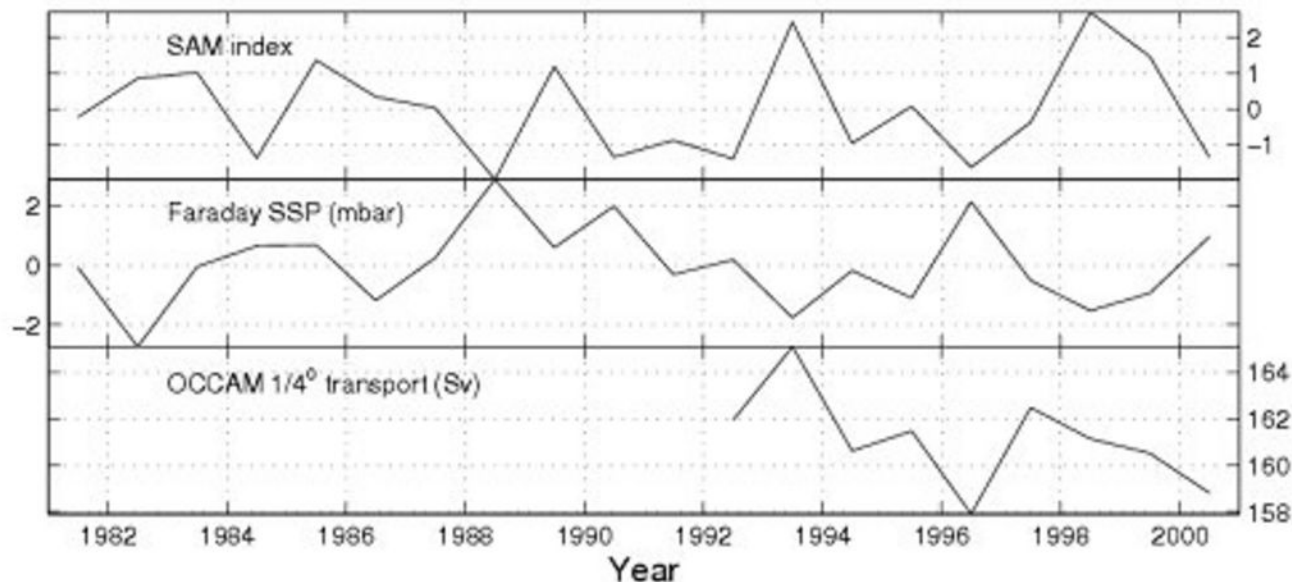


Monthly mean subsurface or bottom pressure, annual cycle removed

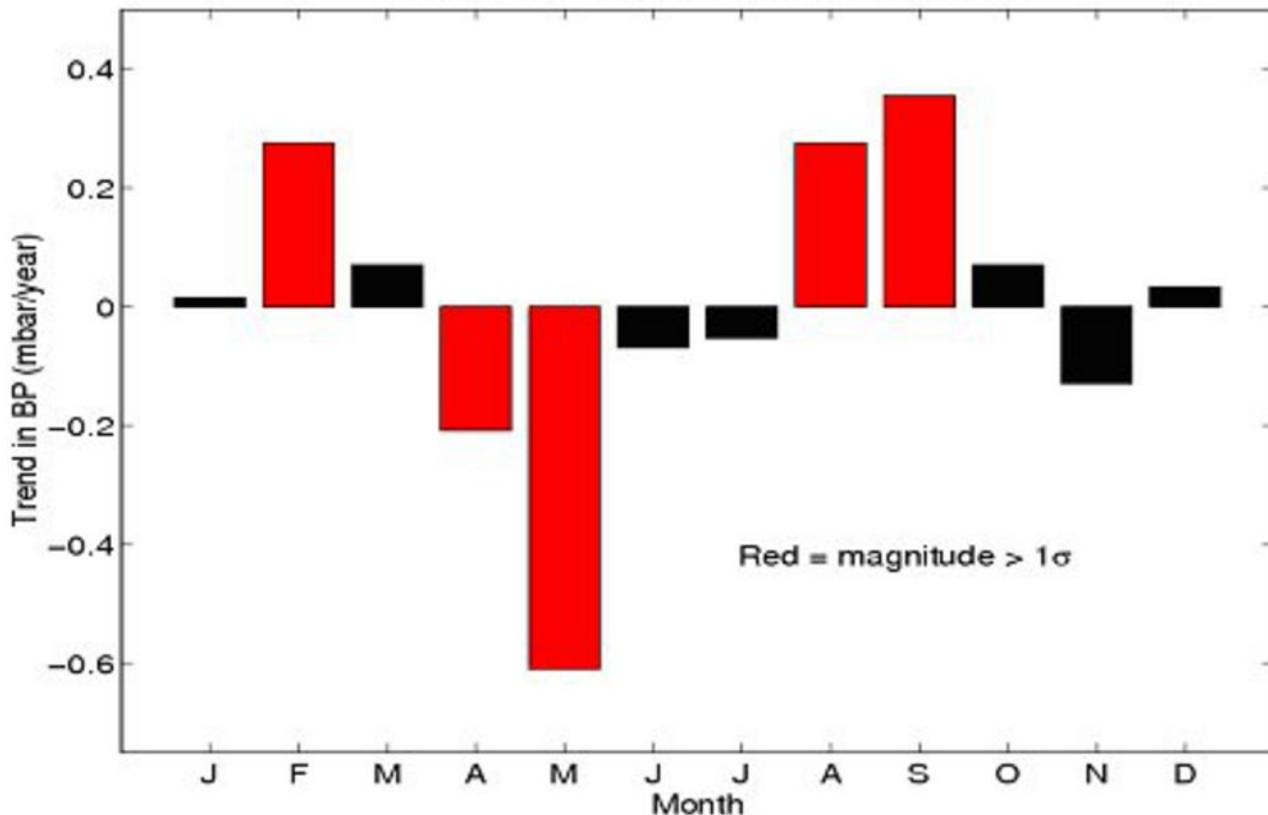


Correlation of model pressure with tide gauge data, annual cycle removed

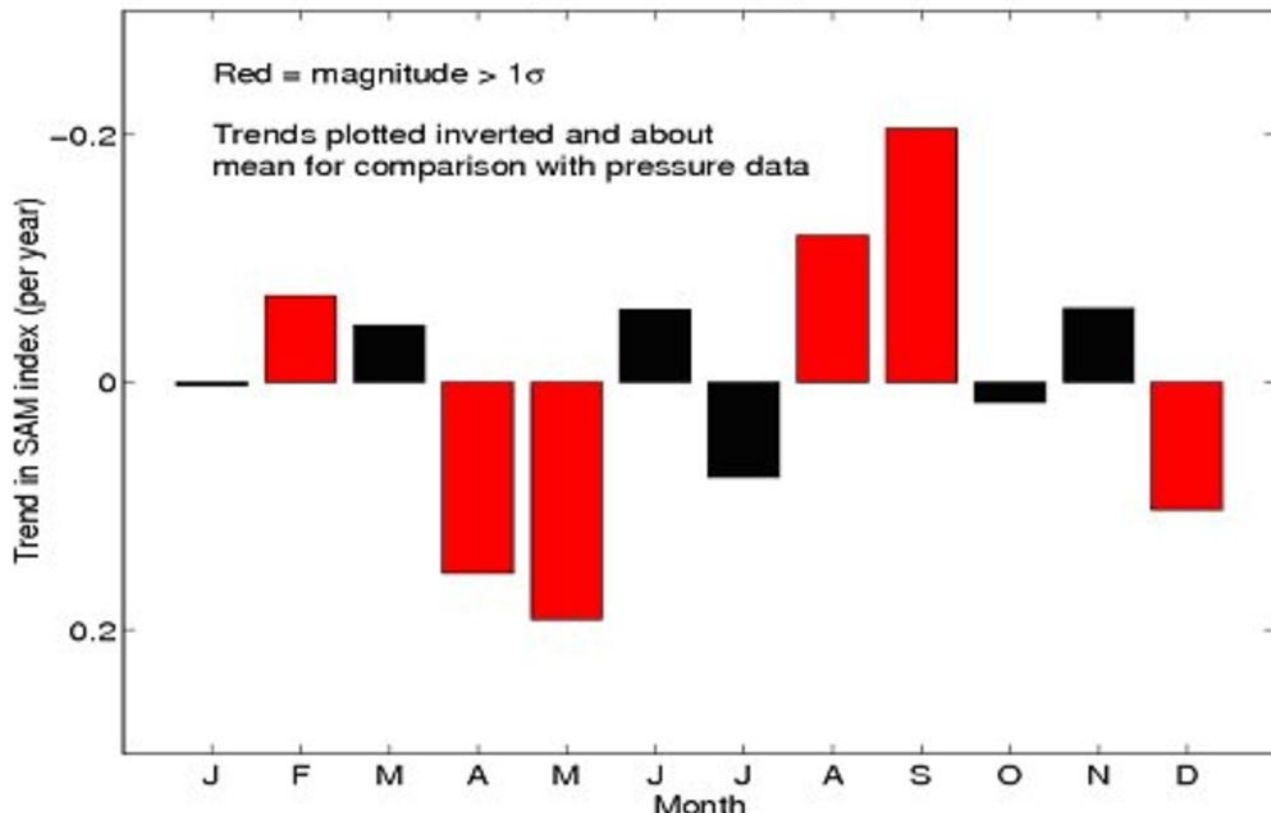


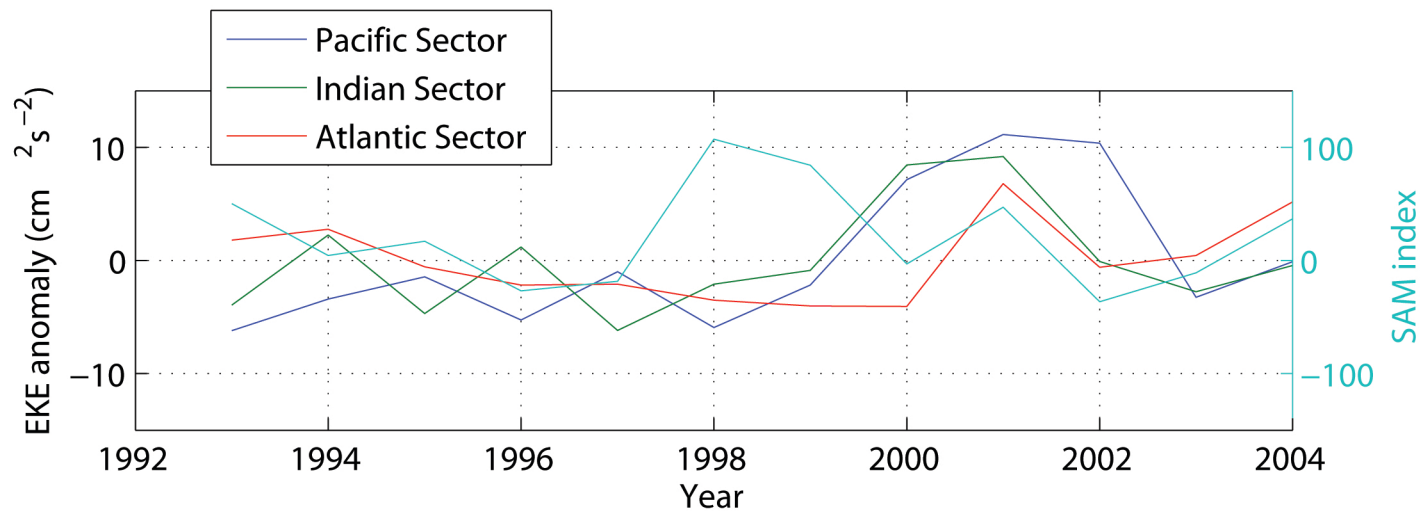


Monthly trends in BP (SD2), 1990–1999

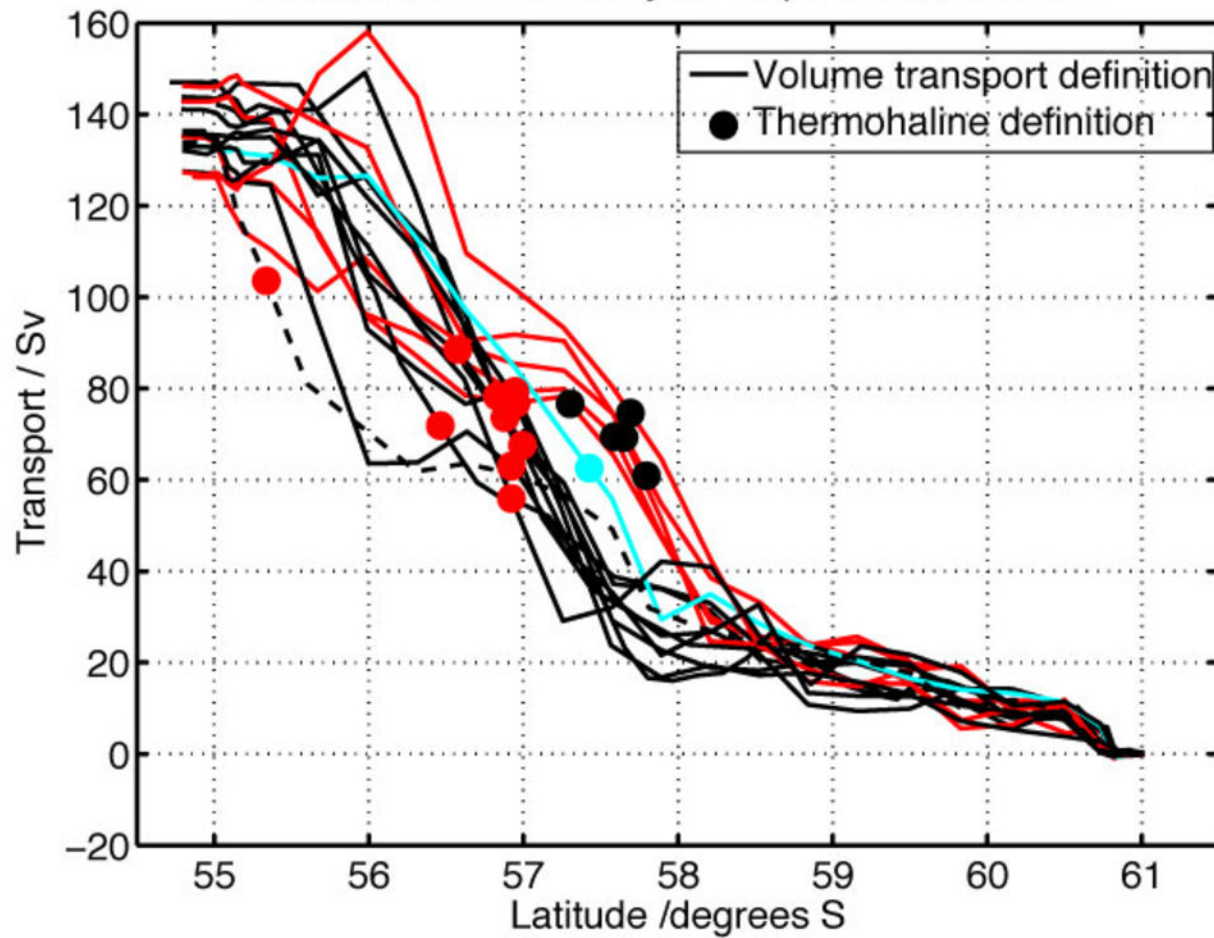


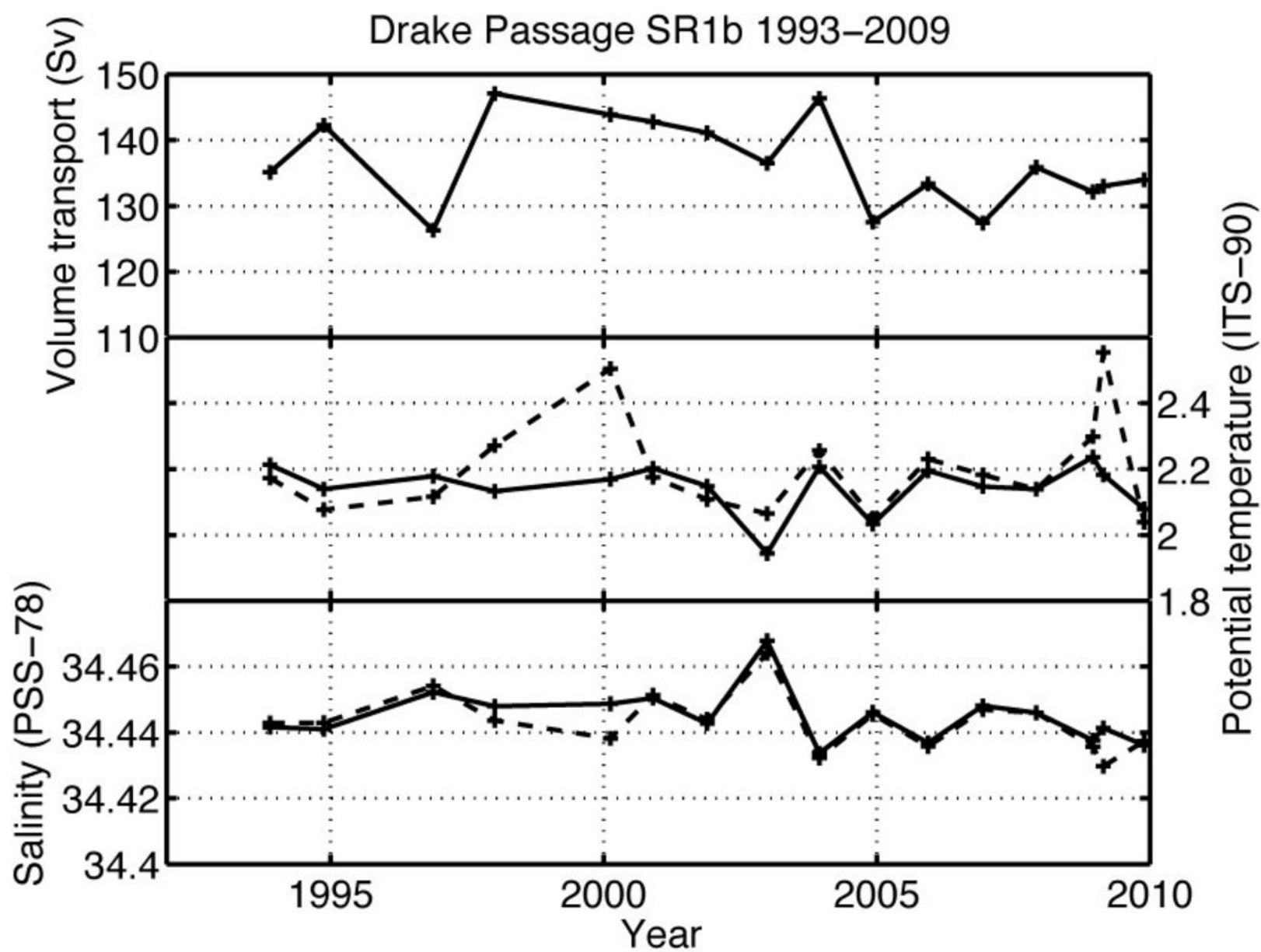
### Monthly trends in SAM, 1990–1999

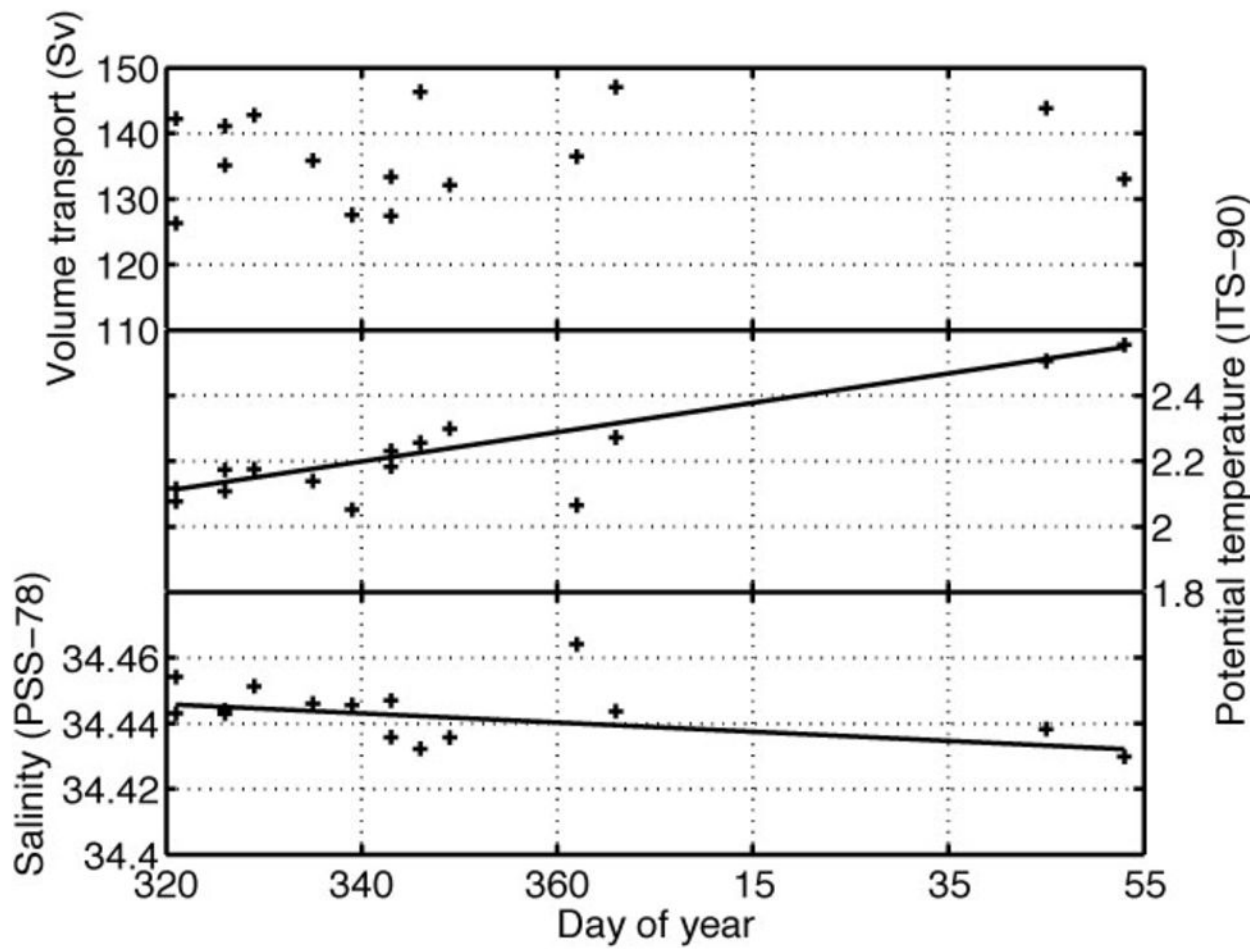


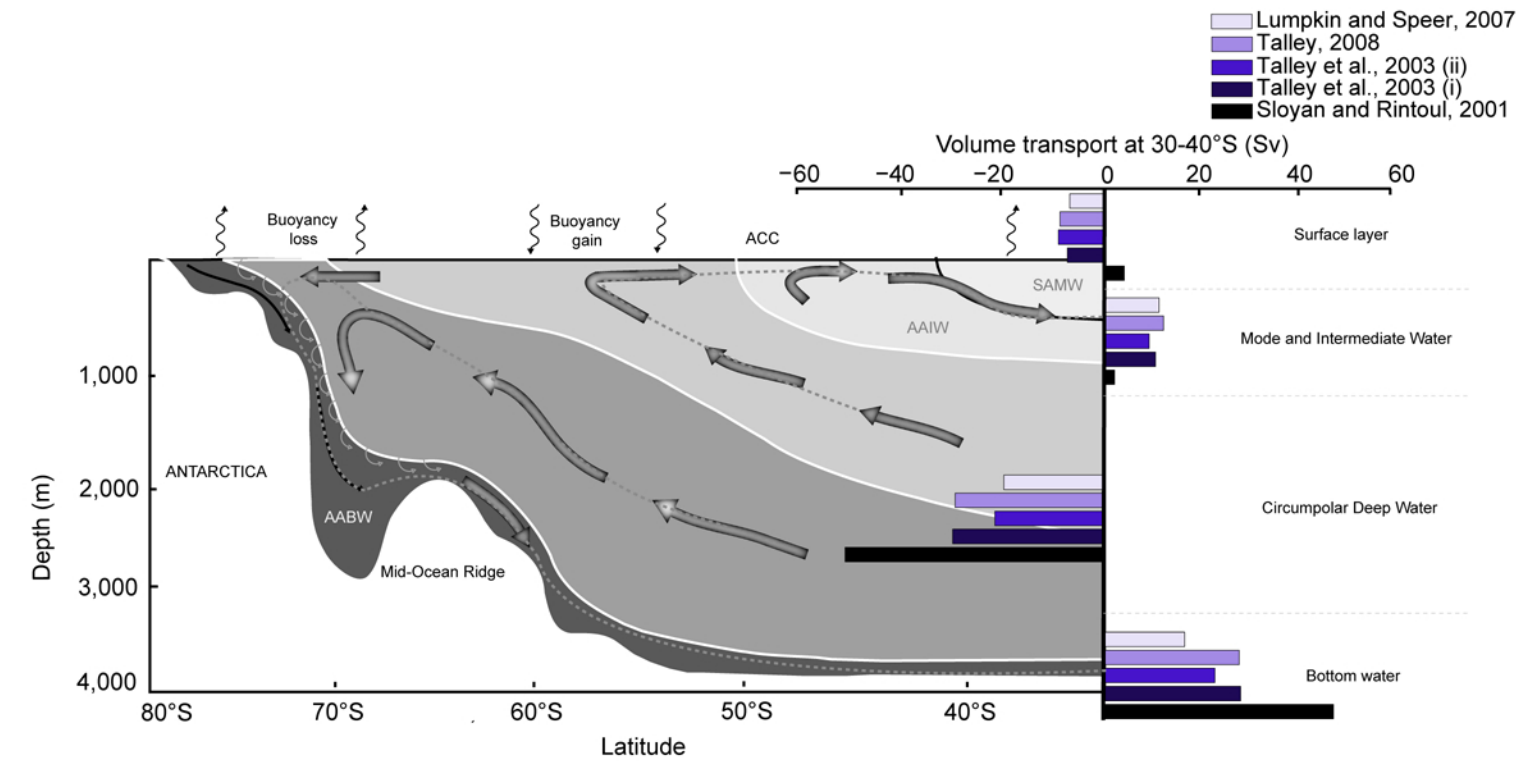


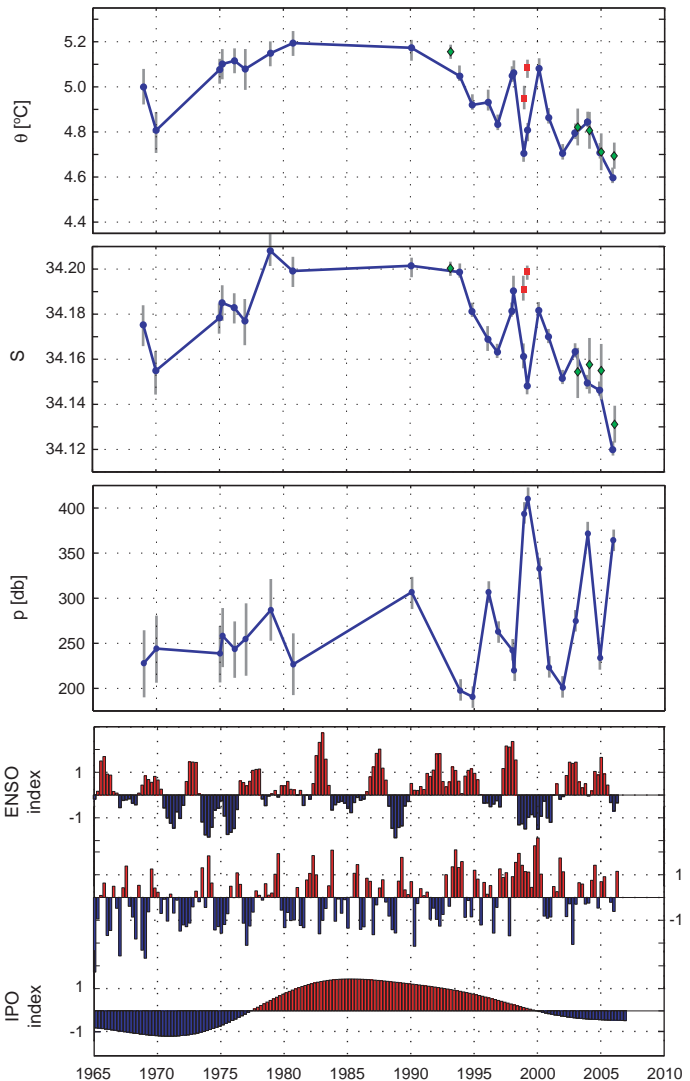
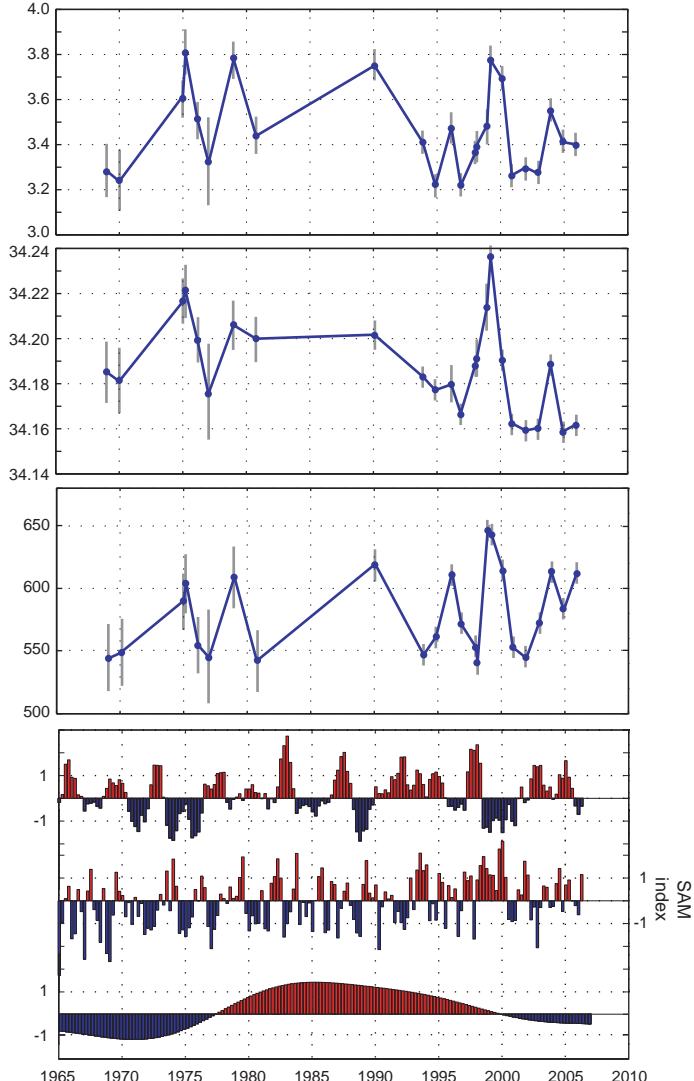
Drake Passage Cumulative Transport at SR1b 1993–2009  
Relative to zero velocity at deepest common level



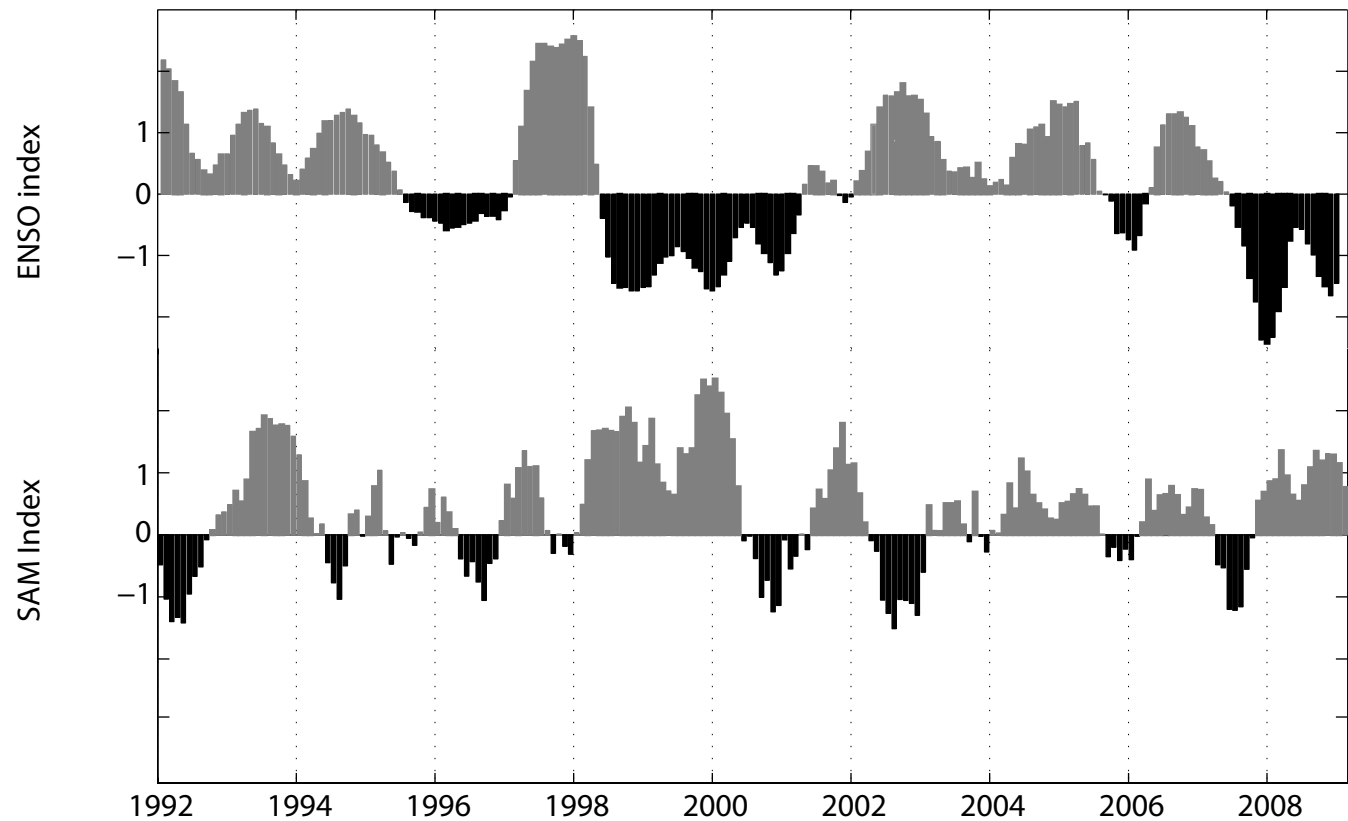
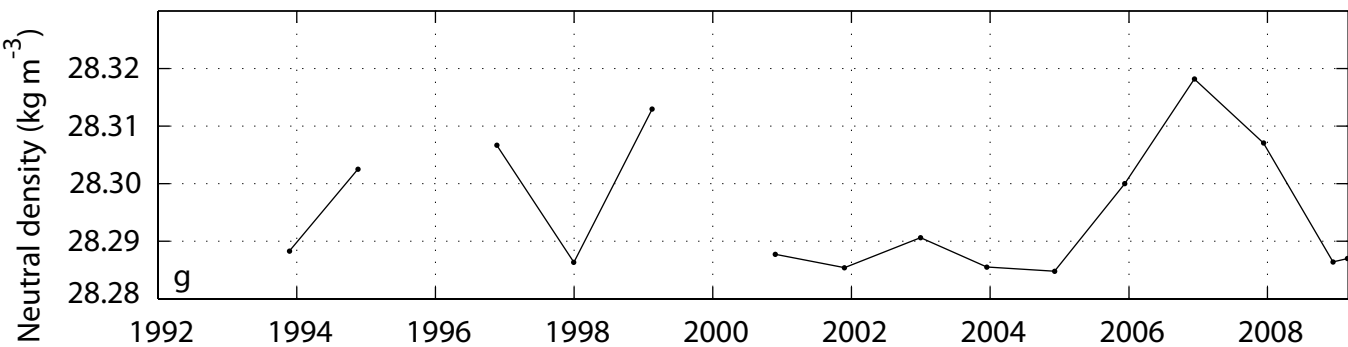
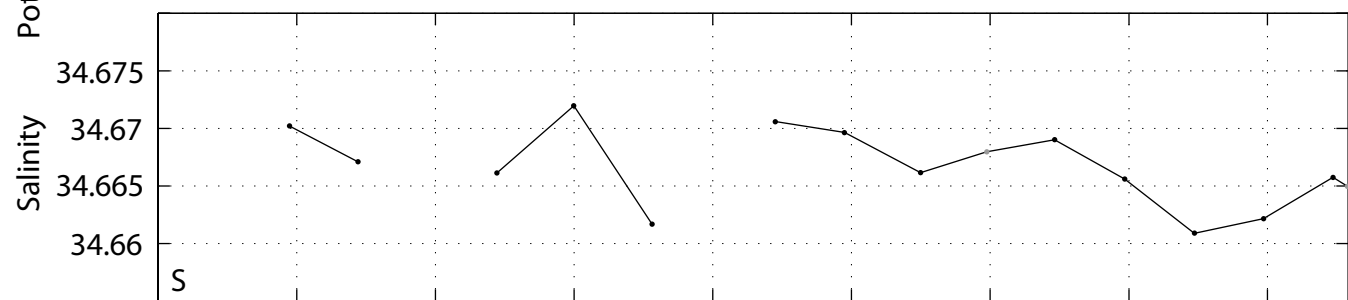
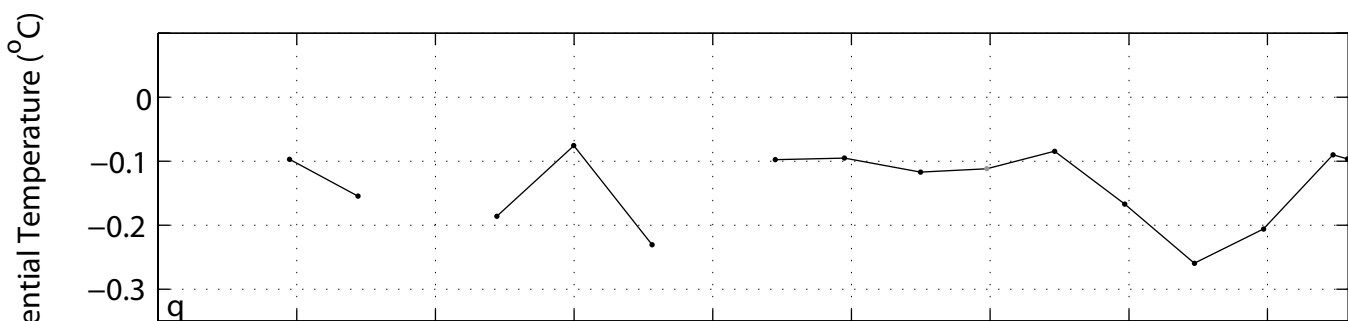






**SAMW****AAIW**

SAMW



Correlation temperature - zonal wind stress

